Investigate the possible reduction of mine water ingress by introducing tree plantations

S Smit

22754164

Dissertation submitted in fulfillment of the requirements for the degree *Magister Scientiae* in Environmental Sciences (specialising in Hydrology and Geohydrology) at the Potchefstroom Campus of the North-West University

Supervisor: Dr SR Dennis

May 2017

ACKNOWLEDGEMENTS

I would first like to thank my supervisor, Dr. Rainier Dennis, for his patience and time to assist in research and writing, his guidance to steer me in the right direction when needed, and expert scientific input into this thesis.

I wish to also thank Dr. Berner (Natural Science Faculty) for his valuable input as a second reader of the plant physiological aspects of this thesis, and for his permission to utilize porometers and other equipment during field visits.

I would like to thank Drian van Schalkwyk and Nicolaus van Zweel for their advice and assistance regarding GIS and technical aspects of this thesis. I would like to thank Pieter Holtzhausen for his assistance during site visits and field work.

I would like to express my profound gratitude to family and friends for providing me with unfailing support and continuous encouragement throughout the last two years of studying and the process of researching and writing of this thesis.

Finally, I would like to thank the Heavenly Father for the privilege and opportunity to study.

ABSTRACT

Continuous influx of groundwater into underground mine workings requires significant financial investment in terms of high pumping costs associated with the pumping of large volumes of water ingress, that could eventually render a mine unprofitable. An innovative alternative to pumping methods with the purpose to reduce water volumes, is the establishment of deep rooted, high water-use vegetation covers to act as “artificial pumps”. Hydraulic control is one of the leading applications of plant-based strategies for remediating and managing groundwater systems by introducing plantations in selected areas with high ingress potential. This study investigated the impact of plantation introduction on the reduction of effective groundwater recharge. A temperature-based field model was formulated to determine daily Evapotranspiration (ET) from measured and observed leaf and air temperature. Results were compared to the FAO Penman-Monteith reference crop ET model and the Shuttleworth-Wallace model in order to validate the predictions of the field model. The developed field model was then used to predict monthly ET values for the Cooke 4 study area (Gemsbokfontein West compartment) to determine the possible reduction of pumping volume. The area selected for the proposed plantation was selected based on groundwater levels and the agricultural potential. A water balance for the study area was developed through the use of the Saturated Volume Fluctuation (SVF) method and inflows to the study area were modelled as head dependent through the use of a conductance term.

Keywords: Groundwater influx, groundwater recharge, stomatal conductance, evapotranspiration, hydraulic control, plantation, Penman-Monteith, Shuttleworth-Wallace, *Eucalyptus*

SAMEVATTING

Deurlopende invloei van water in ondergrondse myne, vereis hoë finansiële insette in terme van uitgawes verbonde aan die pomp van groot volumes ondergrondsewater na die oppervlak, wat ‘n potensiële risko in terme van winsgewendheid vir myne inhou. ‘n Innoverende alternatief om die volume ondergrondse water, en kostes verbonde aan die pomp van water na die oppervlak te verminder, is die vestiging van plantegroei met diep wortelstelsels en hoë water verbruik, om uiteindelik te dien as “kunsmatige pompe” om ondergrondse water aanvulling te beperk. Die gebruik van plantegroei-gebasseerde stelsels, selektiewe vestiging van plantasie vir remediërings doeleindes en bestuur van grondwater stelsels, het drasties toegeneem in die laaste dekade. Hierdie studie ondersoek die impak en effektiwiteit wat plantasie vestiging sal hê op die vermindering van effektiewe groundwater aanvulling. Vir die doel van hierdie studie, is ‘n temperatuur-gebasseerde model geformuleer om daaglikse evapotranspirasie (ET) te bepaal deur gebruik te maak van waargenome lug-en blaartemperature. Die model resultate is vergelyk met die “FAO Penman-Monteith Crop Reference” (Erpm) asook die Shuttleworth-Wallace (SW) model ten einde die akkuraatheid van die model voorspelling te bepaal. Die geformuleerde model was gebruik om maandelikse ET-waardes te voorspel vir die Cooke 4 studie area (Gemsbokfontein Wes Kompartement), om uiteindelik te bepaal wat die potensiaal van plantasies sal wees om die volume ondegrondse water wat huidiglik uitgepomp moet word, te verminder. Die area vir voorgestelde plantasie stigting was gekies op grond van grondwatervlakke en landboupotensiaal. ‘n Waterbalans is ontwikkel vir die studie area deur gebruik te maak van die “Saturated Volume Fluactuation” (SVF) metode, en invloei na die studie area is gemoduleer met druk as die verandelrike, deur gebruik te maak van ‘n geleidings term.

Sleutelterme: Grondwater invloei, groundwater aanvulling, huidmondjie geleiding, evapotranspirasie, hidroliese beheer, plantasie, Penman-Monteith, Shuttleworth-Wallacel, *Eucalyptus*

TABLE OF CONTENTS

LIST OF FIGURES

LIST OF TABLES

LIST OF ABBREVIATIONS

AMD	Acid Mine Drainage
DWAF	Department of Water Affairs and Forestry
DWS	Department of Water and Sanitation
ET	Evapotranspiration
FAO	Food and Agricultural Organisation
GIS	Geographic Information System
GRAII	Groundwater Resources Assessment Phase II
LAI	Leaf Area Index
MAE	Mean Annual Evaporation
mamsl	meters above mean sea level
MAP	Mean Annual Precipitation
MAR	Mean Annual Runoff
mbgl	meters below ground level
NWA	National Water Act
SVF	Saturated Volume Fluctuation
SWAS	South African Weather Services
TSF	Tailings Storage Facility
WMA	Water Management Area
WR2005	Water Resources 2005
WRC	Water Research Commission
WUE	Water Use Efficiency

1 INTRODUCTION

The following section provides an introduction and overview of the project, extent of mine water liabilities and an insight to the desirability and necessity of finding solutions to these liabilities.

1.1 Research problem

In general, the extraction methods applied to obtain minerals from underground have a significant impact on environmental stability and in most cases future sustainability. The disruption or damage to geological features results in the deterioration of subsurface stability, eventually resulting in a serious risk in terms of increased groundwater influx into underground mine workings. It is inevitable that the continuous influx of groundwater into underground mine workings, increase the quantity of water that is exposed to associated mine waste and chemicals which could lead to potential and probable quality deterioration and pollution of valuable groundwater resources (Jarmain, 2003). In addition to the potential deterioration of water quality, the pumping costs associated with high volumes of water ingress could render a mine unprofitable.

Continuous influx of water into mine voids is generally fed by aquifers and leakage from surface water bodies. Since deep mining generally occurs in hard rock formations; fissures, fractures and geological faults present in these formations act as the main conduits of water flow between geological formations and into the underground voids of the mine operating within these geological formations. The fact that groundwater is becoming a more scarce and valued resource, the reduction of impacts on groundwater and ingress of water into mine, depend heavily on effective and sustainable management measures.

1.2 Background to study area

The Cooke 4 mine is located approximately 7 km southeast of the town of Westonaria within the Gauteng Province, and is accessed via the N12 national road between Johannesburg and Potchefstroom.

The continuous influx of water into the underground workings of the Cooke 4 mine, place serious constraints on the sustainability of operations due to financial and technical risks associated with the impacts of mine water ingress. According to a geotechnical report by Johan Fourie and Associates Consulting (2011), the ingress of extraneous water into the Cooke 4 underground workings is attributed to the dolomitic structures overlaying the mining operations. Water contained within this aquifer is conveyed into the mine through a series of faults. Surface runoff is also intercepted by high ingress areas and water is diverted to the subsurface which could

eventually reach mine workings. Once water reaches the underground workings, it is follows a path of least resistance towards the gravity low of the mine which is situated at level 50 Level (50L) of as shown in Figure 1. The 68 Mℓ/d extraneous water that find its way from the overlaying dolomitic compartment to the underground workings are pumped at 50 Level at 40 Mℓ/d, 41 Level at 25 Mℓ/d and at 33 Level at 2 Mℓ/d.

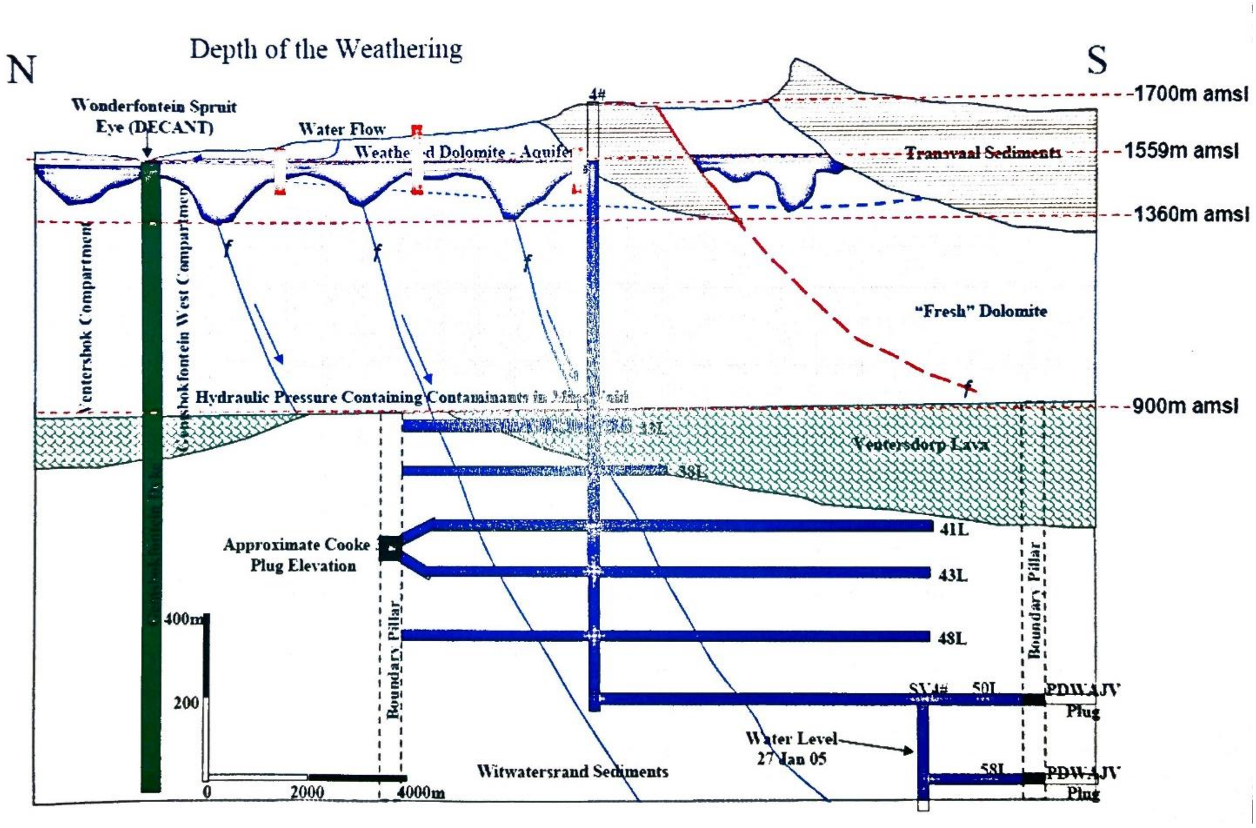

Figure 1: Diagram illustrating the stoping depths (Johan Fourie and Associates Consulting, 2011)

To reduce the ingress volume, dewatering of the overlaying water-bearing dolomitic structure was undertaken. Historically the first ingress of water was encountered during 1972, when water was intersected at 33 Level (±800 mbgl) during an interception of a water-bearing fault on the EC reef stoping horizon (Fourie and Associates, 2011). Soon two other intersections followed again at 33 Level and at 41 Level (± 1000 mbgl) as indicated in Figure 1. In an effort to reduce the volume of water entering underground workings, a pumping framework was established on 33 Level and 50 Level to control underground water volumes (SRK Consulting, 2013). It was soon determined that the mine could not sustain the expenses associated with pumping of water from that depth.

Various programs have been implemented, both on surface and underground, to reduce the ingress of dolomitic water to underground workings. However, these programmes have proved

to be unsuccessful. Consequently, the cost of pumping 68 Mℓ/d from the Cooke 4 underground workings has resulted in the mining operation not to be cost effective anymore.

1.3 Importance of finding solutions to mine water liabilities

The water resources of South Africa are scarce. Whether it is groundwater or surface water sources, the availability and access to water that meets the quality and quantity requirements of people, is a fundamental component of future sustainability. However, factors such as population growth, economic- and industrial development has led to increased constraints on water sources in many areas.

Before the 1970's groundwater was seen as a cheap source of water that required little management, therefore little attention was paid to the potential and proper management of different sectors on surface and groundwater resources (Braune, 2000). Unfortunately, due to lack of management of these resources, especially in the mining industry, groundwater was exploited and significantly impacted. Today the appropriate management of surface and groundwater resources have become a vital component of mining strategies and is managed through the National Water Act (NWA) (Act No. 36 of 1998). The NWA focuses on the sustainable management of water resources through demand management of the available water resources (Braune, 2000).

Rising concern about the impact of contaminants and industrial waste on water has set increased focus on water as a fundamental natural resource and the sustainable management of water resources. Whilst water related issues are considered an increasing global challenge and even though the availability and demand for water differs within geographic regions, water related issues are first and foremost always local problems that can be traced to specific sources impacting on the resource. For this reason, the NWA places the responsibility of water management of surface and groundwater resources on the owners and responsible authorities of the involved industries.

Due to the fact that mining and related industries are seen as some of the most important contributors to water liabilities (Versfeld *et al.,* 1998), strict management reviews are conducted on an annual basis to ensure these industries comply with regulations relating the water management and mine rehabilitation, in accordance with the Environmental Conservation Act 1989, Minerals Act 1991 and the National Water Act 1998. In accordance with the Minerals Act of 1991 (Sections 12, 39 and 54), mines are legally obligated to submit a management and closure plan that identify and evaluate possible pollution risks, and to provide suitable mitigations measures to ensure minimal impairments on the environment and natural resources post-closure. One of the main potential risks generally associated with mining activities include the potential

production of Acid Mine Drainage (AMD) when rock material is exposed to oxygen and water, and the potential decant of polluted water when underground mine workings or voids flood.

Prevention of void decanting and continuous access to mine workings is established by removing water from voids via pumping. This process of pumping water from mine voids to the surface is known as dewatering. Water that is pumped out of underground excavations is then either re-used by mines within operational processes, or pumped to treatment facilities to ensure that this water meets regulatory and environmental requirements before it is released into a receiving water sources. However, many concerns are directed on the negative impact of dewatering on the environment as dewatering processes has the ability to de-stabilise geological formations and reduce groundwater levels. In addition, many concerns arise regarding the impacts of discharged contaminated water and how the quality and quantity of this water will affect the environment. Seepage and movement of contaminated water not only affects water sources in the immediate vicinity, but could extend far beyond their localities.

In order to find solutions to reduce mine water ingress, a clear understanding of the impact of mining on water quantity is necessary. Although a vast range of water related studies have been conducted during the last century, expanding knowledge on this subject will assist in future mine management with regards to managing water resources throughout all phases of mining and associated development.

Historically, insufficient attention was given to the management of water resources of mines that applied intensive mining methods and extracted high volumes of groundwater. Appropriate management of water resources and the significant impact of mining on these resources were not fully understood. Today however, the mining industry is placed under significant pressure to minimise the impact of mining on water resources and to optimise the management of all water resources. The primary objective of water resource management is to protect all water resources in terms of water quality, water quantity and ecosystem health. To achieve this goal, the following objectives should be considered (DWAF, 1998):

- Ensure that water management measures on the surface are taken into account in integrated approaches;
- Separation and management of water of different qualities to prevent contact and deterioration of water quality;
- Minimise contact between water and polluting substances such as waste material;
- Address water pollution issues at the source;
- Avoid discharge of polluted water from mine sites;
- Ensure water management measures are sustainable;

- Ensure that water management measures minimise post-closure impairment of water resources.

Over the past 30 years, significant financial investment has been channelled to environmental research with the purpose to comprehend the impact of mining on the environment and its natural resources, and is currently still a continuous field of research. Results from past and current research are applied and utilised to address current problems, and to prevent future recurrence of these problems. Taking into account results from past and current research, several water management strategies have been developed to control influx of water into mines (Hodgson *et al.,* 2001)

- Re-evaluation of extraction mining methods to reduce impacts on geology and groundwater resources;
- Minimising water influx by not undermining high transmissive aquifers;
- Extensive pumping to holding dams;
- Implementation of barriers and trenches to reduce runoff flow towards faults and ingress points;
- Re-design of mining structures to prevent collapsing and fracturing of strata;
- Construction of evaporation ponds to minimise water balances;
- Sealing of ingress points and fractures;
- Limiting the size of mining.

1.4 Potential solution that is proposed in this study area

An innovative, “green” alternative to extensive pumping methods with the purpose to reduce water volumes, is the establishment of deep rooted, high water-use vegetation covers to act as “artificial pumps”. This bio-drainage strategy is part of a range of phyto-technologies considered as a suitable alternative to conventional engineered-based drainage techniques. The establishment of tree plantations as bio-drainage promoters, can aid in hydraulic control by reducing the effective recharge to shallow groundwater systems. Consequently, the volume of water that is subject to ingress and seepage is reduced. Hydraulic control is one of the leading applications of plant-based strategies for remediating and managing groundwater systems. The reduction of effective recharge to groundwater systems can be achieved through the introduction of plantations in selected areas with high ingress potential (Ferro *et al.,* 2006.

An important consideration that should be taken into account when considering a bio-drainage approach is the depth to available groundwater compared to rooting depth of trees. Many tree species have naturally deep-rooted systems that enables trees to tap into the deep soil layers

reaching deeply situated water resources. The establishment of deep rooted trees in such systems function as artificial pumps, thus removing a substantial amount of water from the saturated zone through natural processes including transpiration, plant uptake and precipitation interception of canopy covers. This is achieved by enhancing the transpiration capacity of a landscape by introducing vegetation types with high water use characteristics to large enough areas in order to maintain a balance between recharge and discharge processes below root zones (Schnoor *et al.,* 1995). This strategy may include the removal and replacement of natural vegetation with vegetation characterised by increased water consumption and abilities to transpire tremendous quantities of water (Schnoor, 1997).

Hydrological studies from across the world demonstrated that trees use more water annually than grasslands and shorter vegetation (Farley *et al.,* 2005). Higher water use characteristics of trees are attributed to (a) high aerodynamic roughness of plantations that results in increased annual transpiration rates – twice as much as the rate of short vegetation; (b) the so-called clothesline effect of prevailing trees in rows, substituting for a conventional drain pipe; (c) deep root systems enabling trees to extract water from considerable depths in comparison to short vegetation with shallow root systems and (d) dense canopies with evergreen properties enabling trees to transpire throughout the entire years, in comparison to grasses with seasonal dormant stages (Burgess *et al.,* 2000). A paper from Sikka *et al.* (2013), based on studies conducted in south India under humid conditions with an average rainfall of 1 379 mm/a, supported the suggestion of trees being more efficient water users than grasslands. This study indicated that the conversion of grasslands into *Eucalyptus* plantations in particular, have reduced annual water yield by 16% during first rotations, and 25.6% during second rotations.

South Africa is classified as a subtropical country with warm temperate conditions. Due to the country's relatively low mean rainfall, the natural vegetation is dominated by non-woody plants. The lack of natural sources of fast growing timber stimulated the introduction and establishment of exotic tree species. Subsequent to years of investment and development, South Africa has become one of the largest cultivated forestry resources worldwide. With a total area of over 1.5million hectares occupied by plantations, South Africa is categorised as the third largest plantation resource in the southern hemisphere. The majority of South African plantations are comprised of non-native *Eucalyptus* and *Pinus* species, comprising 39% and 40% respectively of South African timber plantations (Global Agricultural Information Network, 2014).

Eucalyptus and *Pinus* species are considered among tree species with the highest water use characteristics, predominantly driven by high leaf area indexes. Desirable traits such as high value timber, growth potential, high water consumption, biomass accumulation and physical parameters of *Eucalyptus* and *Pinus* species, has led to increased focus being set on the potential of these

commercial hardwood species to be used as efficient bio-drainage species. Catchment-based studies provide evidence of afforestation and deforestation effects on catchment hydrology and stream flow. Forestry can have a major impact on the water balance in an area, leading to a 30-40mm stream flow reduction per 10% of catchment planted, at peak water use ages (Farley *et al.,* 2005). The impact of afforestation in South Africa is thought to be primarily due to high transpiration rates and productivity of trees, and to a lesser extend due to increased interception losses. Noticeable changes in annual evapotranspiration rates have been reported with the ageing of tree plantations. Due to the fact that plantation productivity peak at different ages among different species, it can be concluded that the age at which stands will have maximum water use will differ among tree species. Roberts *et al. (*2001) conducted a study on *Eucalyptus sieberi* stands in a south-eastern Australian catchment, which indicated increased daily transpiration rates of 2.2 mm in 14-year regenerating stands, in comparison to a lowered daily transpiration rate of only 0.8 mm in stands in excess of 160 years. An international review from Bosch and Hewlett (1982) indicated that a 10% change in humid, evergreen canopy covers of eucalypt and pine plantations, resulted in stream flow changes between 30 mm and 40 mm.

This study seeks to investigate the impact of introducing plantations to reduce the effective groundwater recharge, ultimately contributing to a long-term solution for water influx into underground mine workings. An additional benefit which is particularly important in the South African context from a community aspect includes the opportunities for the production of value-added products such as timber with high wood value. The establishment of plantations as a remedial approach will thus provide an effective water management solution while simultaneously stimulating the timber industry. Strategic placement and implementation of vegetation covers with high evapotranspiration could control water ingress into mine voids as a result of their capacity to store rainfall for subsequent evapotranspiration. Storage capacity of vegetation reduces and limits the amount of surface water that can potentially infiltrate underlying aquifers.

Bio-drainage is a slow, but low-risk approach. Enactment of phyto-technologies and establishment of vegetation communities, have become a common component of mining restoration projects for the restoration of impacted land and removal of chemical contaminants from contaminated medias such as soils, water or sediments. The establishment of bio-drainage systems require specific plant species selection, however once established these systems can be maintained with minimal effort and financial investment required (ITRC, 2009). Phyto-technologies are classified as the only remedial measures that confer simultaneous decontamination and rehabilitation.

1.5 Hypothesis of this study

The hypothesis of this study is that the establishment of a plantation comprising of fast growing trees with high water use characteristics, will increase the total transpiration/evaporation potential of the landscape and reduce direct recharge to the shallow regional aquifer (H_0). It is also hypothesised that changing the natural vegetation from native grasslands to a *Eucalyptus* plantation, effective recharge beyond the root-zone will be significantly reduced, subsequently resulting in the potential of effective evaporation to equal the available recharge (H_1)

1.6 Aims and objectives of this study

The objectives of this study are to reduce the influx of water into underground mine workings, in order to minimise pumping costs at Sibanye Cooke 4 Shaft.

Focus as the objectives of this study includes:

- To formulate a calibrated field model to assess the ET potential of *Eucalyptus* species growing in the study area, in order to determine the potential of *Eucalyptus* plantations as bio-drainage alternatives for reducing water influx into underground mine workings;
- To compare the calibrated field model to the reference ET potential as calculated by the Penman–Monteith model;
- To compare the calibrated field model to the Shuttleworth-Wallace ET model to predict ET potential for other types of landcovers;
- To determine the effect of ET associated with *Eucalyptus* plantations on the volume of mine water ingress.

2 INTERACTION BETWEEN VEGETATION AND RAINFALL

2.1 Plant-water relationships

The movement of water through soil-plant-atmosphere systems, is significantly affected by the way plants function in response to environmental and physiological stimulants. Direct extraction from saturated as well as unsaturated soils, translocation of water between root systems, and storage capacities of plants play a vital role in soil hydrology. Changes in vegetation covers, particularly from small shallow rooted vegetation such as grasslands, to tall deep rooted vegetation such as tree plantations, have a significant impact on groundwater reserves (Le Maitre *et al.* 1999). In strong contrast to grassland with shallow root systems and seasonal dormant stages, trees with deep root systems are capable of extracting water from considerable depths under water-stressed conditions.

An understanding of the interaction between vegetation and groundwater is an essential component of groundwater use and the potential hydrological impacts of groundwater extraction on ecosystems. For research purposes of ecological reserve estimations and potential effects of stream flow activity, the National Water Act (Act 36 of 1998) demand an understanding of the relationships between vegetation and all water resources, as to ensure that all natural resources (including water) are utilised in a sustainable manner (DWAF, 1998). These water demands have stimulated a growing interest in the current trend towards integrated management of natural resources and the necessity to ensure reserves are not depleted, particularly in ecosystems dependent on groundwater. Since trees are more dependent on groundwater they are able to consume large quantities of groundwater and are sensitive to fluctuating water tables, thus stressing the importance of integrating management approaches of forest-and water resources (Calder, 1992). A limited number of studies in South Africa focus on the interaction between groundwater and trees, subsequently a larger body of related literature included in this study are based on research conducted in similar environments such as Australia and Spain.

An arrangement of events occurring in the interaction of trees and precipitation is depicted in Figure 2.

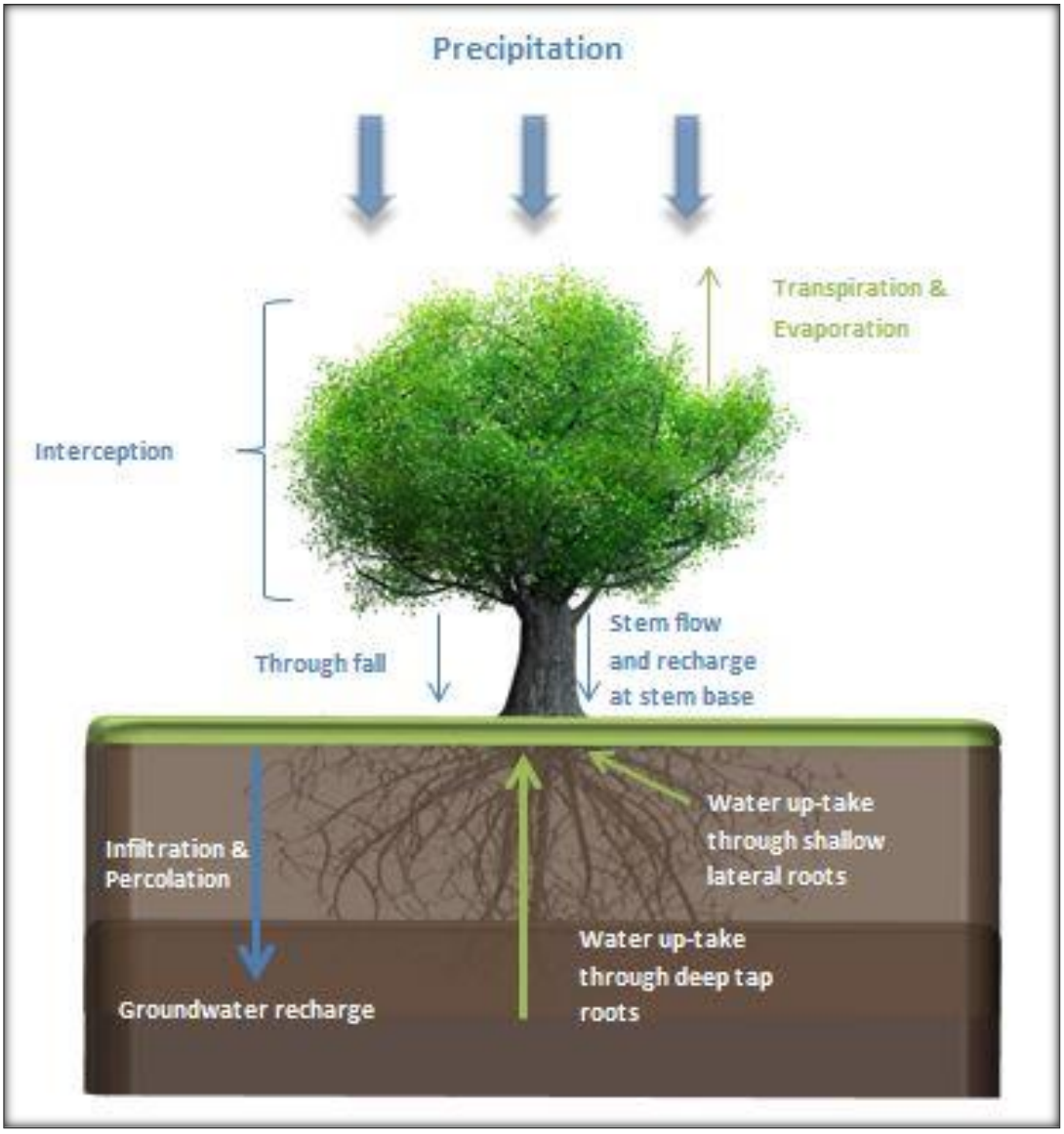

Figure 2: Events occurring during the interaction between recharge and vegetation (Le Maitre et al., 1999)

2.1.1 Interception

Subsequent to precipitation, the distribution pattern and the amount of water reaching the soil surface is influenced by vegetation type, plantation condition and the extent of vegetative coverage. The term, interception, describes the proportion of precipitation that is retained or absorbed by plant tissue subsequent to rain events (Le Maitre *et al.,* 1999). Generally, the most accurate interception estimates are quantified from precipitation losses for single rainfall events rather than seasonal events. Modification in vegetation coverage can significantly affect the amount of rainfall interception and ultimately effective groundwater recharge. The amount of precipitation that is lost to interception depends mainly on the duration and intensity of rainfall

events, and also morphological characteristics of plant surfaces which relates to the retention or absorption of water (Larcher, 1983).

Morphological characteristics such as the roughness of plant surfaces and the size of leaf areas have a significant effect on the ability of water to cling to plant surfaces, and eventually the amount of water lost to interception (Larcher, 1983). Given a rainfall event of high intensity and long-duration over landscapes with open canopies and smooth surfaces, the amount of water lost to interception will be very low. Coniferous plantations with dense canopies, high leaf areas and rough bark constitute ideal characteristics to permit a large amount of interception of up to 60% under low rainfall conditions, and 20% to 24% under intense rain events as was measured by Farrington and Bartle (1991). Research conducted in temperate forests demonstrated that the rapid loss of intercepted water from tree canopies to evaporation, accounted for 20% to 40% of annual rainfall in coniferous forests, and 10% to 20% for *Eucalyptus* forests (Zinke, 1967). As trees mature and exhibit larger leaf areas, interception potential increases until a maximum is reached - generally when canopy covers have completely closed allowing no exposure to bare soils. Interception losses for different forest and/or plantation species are listed in Table 1.

Table 1: Percentage interception losses over a range of vegetation types (Le Maitre et al, 1999)

Vegetation type	% Interception Loss	Source
***Eucalyptus* forests**	1 - 20%	Sharma et al. (1987a)
***Acacia* woodlands**	5 -13%	Langkamp et al. (1982)
***Acacia mearnsii* stands**	25% 6.6%	Calder (1992) Beets and Oliver (2006)
***Pinus radiata* stands**	10 - 20% 12.2%	Pienaar (1964) Versfeld (1988)
***Pinus patula* stands**	13% 10% 12.1%	Beard (1956) Dye (1996c) Beets and Oliver (2006)
***Eucalyptus grandis* stands**	4.1% 5% 8.5%	Beard (1956) Dye (1996a) Beets and Oliver (2006)
Savanna grassland	15 - 20%	De Villiers and De Jager (1981)
Protea and Fynbos shrubland	6 - 18%	Scholes and Walker (1993)
Wattle stands	15 - 20%	Beard (1956)

2.1.2 Throughfall

Throughfall is defined as the proportion of precipitation that is not retained by plant surfaces, and that is shed from wet leaves onto the soil surface. Similar to interception, the amount of throughfall depend on the structure and size of canopy covers, the size of leaves, the number of vegetation layers and the intensity of rainfall events. The shape and structure of plantation canopies, particularly leaf and branch angles, have a significant effect on the spatial distribution of precipitation. These characteristics play an important role in concentrating water in drip points, resulting in larger drop sizes than drop sizes from precipitation in open areas. This in turn affects the nutrient cycles underneath tree covers, as larger drop sizes accounts for higher solute concentrations and mass fluxes of canopy leachates under tree stands than in open areas (Zimmermann *et al.,* 2007).

2.1.3 Stemflow

As mentioned before, the morphological characteristics such as surfaces roughness play a crucial role in the quantity of intercepted rainfall that will cling to vegetation surfaces. As soon as branch and stem surfaces reach a point of maximum saturation, water will flow down the branches and stems to eventually infiltrate soil surfaces around the stem base – this process is called stem flow (Navar and Ryan, 1990). Stemflow can average about 5% of annual rainfall. The uneven distribution of soil-water fluxes will be of much higher importance in landscapes that are exposed to limited rainfall recharge, but will be of less importance in high rainfall landscapes where rainfall is more evenly distributed across a wider area. Table 2 below presents a summary of the partitioning of rainwater into throughfall and stemflow for selected forest and/or plantation species, obtained from various sources.

Table 2: Rainfall partitioning into throughfall and stemflow in selected species (Navar and Ryan, 1999; Zimmerman et al., 2007).

Tree Species	MAP (mm/a)	% Throughfall	% Stemflow	Source
Eucalyptus globulus	599	87.5	1.7	Valente *et al.,* (1999)
Pinus pinaster	529	82.6	0.3	Rowe and Hendrix (1951)
Quercus sp.	725	82.2	3.7	Bryant *et al.,* (2005)
Eucalyptus grandis	1417	84.0	5.0	Tèson *et al.,* (2014)
Fagus orientalis	309	67.0	2.5	Ahmadi *et al.,* (2009)
Fagus sylvatica	840	80.0	5.0	Neal *et al.,* (1993)
Quercus castaneifolia	652	75.0	0.4	Bahmani *et al.,* (2012)

2.1.4 Infiltration and percolation

When rainfall water reach the soil surface subsequent to throughfall and stemflow, water infiltrates the soil matrix and percolates through soil profiles into weathered strata to eventually replenish the undelaying groundwater supplies (Le Maitre *et al.,* 1999). Vegetation covers have a significant impact on the amount of water that infiltrates and contributes to groundwater recharge. Studies conducted on South African *Eucalyptus* plantations have indicated changes in the physical and hydraulic properties of soils after afforestation, subsequently resulting in enhanced deep drainage through macropores (Musto, 1994). Providing litter cover, organic material produced from decomposing litter, binds to soil particles subsequently changing soil characteristics and increasing soil porosity (Valentini *et al.,* 1991). As shown in Table 3, soils with higher porosity demonstrate increased infiltration rates and water-holding capacities. Research conducted by O'Connor (1985) demonstrated the relationship between litter cover and infiltration rates. From this research, it was illustrated that soils with litter cover had a faster infiltration rate, approximately 9 times faster infiltration than bare soils.

Table 3: Relative infiltration rates in relation to soil textures and presence of vegetation covers (Breman and Kessler, 1995)

Soil Type	Vegetation Characteristics	% Infiltration Rates
Sandy	Closed canopy	100
	Open canopy	84
	Open grassland	55
Variable	Complete litter cover	100
	Partial litter cover	33
	No litter cover	12
Loamy	Under *A. tortilis* canopy	100
	Open field adjacent to *A. tortilis*	25
	Under shrubs	100
	Open field next to shrubs	5

Vegetation with deep root-systems also provide preferential flow paths for water through soil profiles, subsequently increasing the percolation rate (Sharma *et al.,* 1987b). Figure 3 illustrates the relationship between soil moisture profiles and plant-available water capacity for soils under different vegetation covers. Preferential flow varies among soil textures, and percolation through

root channels depends mainly on root depth and coarseness of root systems. Johnston (1987) provided evidence of the significantly contribution preferential flow has to groundwater recharge, illustrating increases in vertical water fluxes from 7.5 mm/a to 100 mm/a. In a similar study conducted in Western Australia, root channels under *Eucalyptus* stands provided flow paths for the percolation of rain water to a depth of 12 m over a period of 20 years (Allison and Hughes, 1983). Soils beneath *Eucalyptus* stands in particular, may be water repellent, thus inhibiting infiltration and channelling water to preferential flow paths instead (Burch *et al.,* 1989). For this reason, deep drainage is anticipated in soils underneath Eucalypt covers, as illustrated in Figure 3 where the solid lines resemble the maximum and minimum soil water store limits.

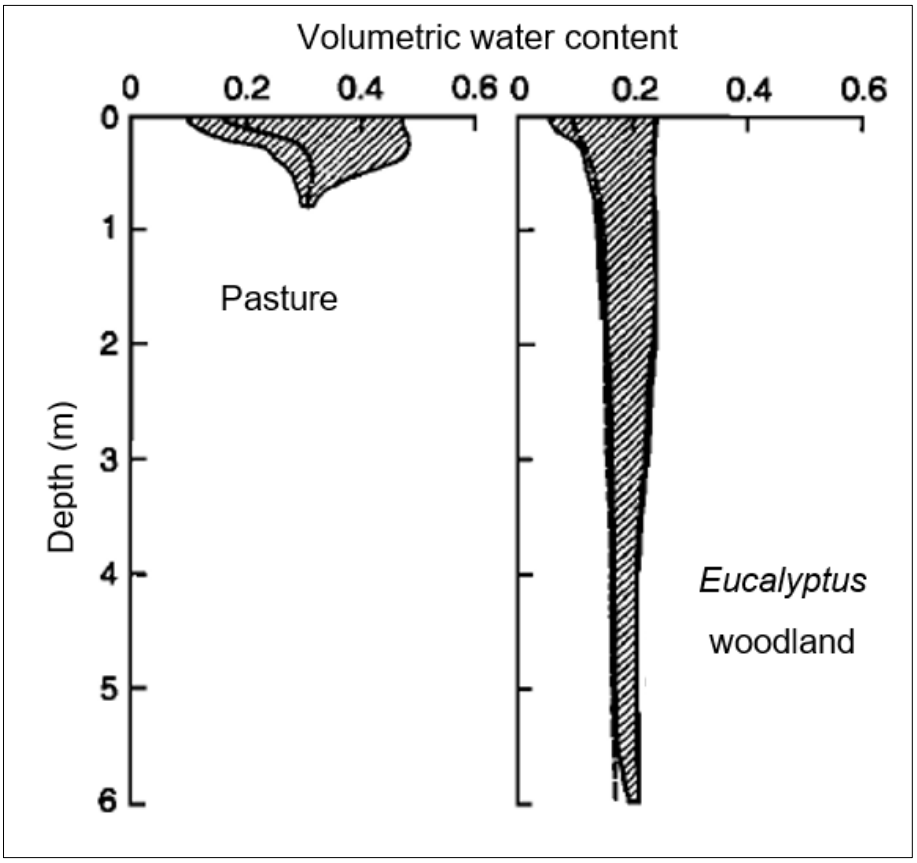

Figure 3: Relationship between soil moisture profiles and plant-available water capacity (Le Maitre et al., 1999)

2.1.5 Groundwater extraction via root uptake

Plant-available water capacity is mainly determined by the depth to which root systems are able to extend, and the hydraulic properties of soils (Zhang *et al.,* 2001). During high rainfall periods, plants mainly extract moisture from shallow soil layers, where root densities are at their highest. As seasons progress and the soil moisture content progressively deteriorates, trees obtain moisture from deeper soil layers in order to ensure continual occurrence of transpiration (Delzon & Loustau, 2005). Root system structures have a significant impact on water-use patterns and

soil water utilisation by trees. Phreatophytic plants, withdrawing water from near the water table via deep root systems, are generally associated with rapid growth potential in order to establish early contact with groundwater sources. Under conditions where the rate of groundwater depth gradually increases, plant roots can maintain contact with declining groundwater if the rate of decline does not exceed root growth potential (Mahoney and Rood, 1998). Research conducted by Horton and Clark (2001) illustrated root proliferation of 1 mm/d to 13 mm/d in *Populus* trees, as a response to gradual groundwater level decline of up to 20 mm/d. Similarly, Kramer (1969) recorded maximum root growth potential of 15 mm/d in arid-shrub species.

Groundwater extraction varies significantly between vegetation types, and is driven mainly by transpiration and evaporation processes, which in turn is driven primarily by limatic conditions. Under water-stressed conditions where plants are extracting water from soils with low moisture content, transpiration rates can be as low as 5% of the annual rainfall in order to conserve water. However, under circumstances where available groundwater is adequate, transpiration could range between 45% - 80% of annual rainfall (Larcher, 1983). For this reason, it has been contemplated that transpiration may be the primary loss of water in vegetated areas.

The depth to which root systems are able to extend vary significantly between woody plants, averaging to depths of 7 m for trees and 5 m for shrubs as documented by Canadell *et al.,* (1996). High rainfall regions are generally associated with evergreen trees that depend on a constant and adequate supply of water. However, research by Nepstad *et al*. (1994) have illustrated the ability of evergreen trees to extract water from depths more than 8 m, which enables them to tap deep water sources to survive periodic droughts. Plants adapted to extract water from deep groundwater sources, generally exhibit rapid root development to ensure early establishment of contact with groundwater. Stone and Kalitz (1991) documented rapid root growth of up to 2.7 m over a 4-year period in *Pinus radiata* stands, and 3.7 m in *Robinia pseudacacia* five years after germination. Similar studies have indicated that root-systems of many savannah trees such as *Acacia* and *Prosopis* are able to reach depths of 3 m to 20 m. Eucalypt species are another species also able to extract water from considerable depths. Research conducted on a three-year-old *Eucalyptus grandis* stand illustrated water abstraction from as deep as 8 m, while a ten-year-old stand growing under low rainfall conditions mainly abstracted water from 10 m depths (Dye, 1996b). From this study, it can be concluded that *Eucalyptus* species are adapted to establish deep root systems while still relatively young, even though the upper profile could have adequate water supplies to sustain these trees.

In addition to deep tap root development, the lateral distribution extent to which tree roots are able to extend can be significant. Sudmeyer *et al.,* (2004) quantified the lateral extent and distribution of four of the most common species growing in Australia; *Eucalyptus globulus, E.*

kochii, Pinus pinaster and *P. radiata*. Result showed considerable differences in the density of shallow root systems, and the lateral extent to which these roots can penetrate soils, ranging between 10 m to 44 m. It was demonstrated that *P. pinaster* generally have the highest density of roots occurring in the upper 0.1 m to 1.4 m of soil profiles, whereas *E. globulus* had the lowest root density. Root distribution is a function of the environment to which different species are adapted to (Loheide *et al.,* 2005). For example, a greater distribution of shallow root systems is anticipated in areas prone to high rainfall events where trees mainly depend on soil water in upper soil layers as opposed to trees growing under water stressed conditions and dependent on groundwater, will have well developed deep root systems and less lateral roots.

2.1.6 Evaporation

A continuous cycling of water exists between land surfaces, vegetation surfaces and the overlying atmosphere. The balance between water exchanged among land surfaces and the atmosphere is referred to as the hydrological cycle (Hopkins and Hüner, 2008).

Rainwater reaching the earth through precipitation is returned to the atmosphere in the form of water vapour. Evaporation processes demand both available kinetic energy and suitable conditions to allow the flow of water vapour away from evaporating surfaces. The energy input to evaporating surfaces initiates the migration of water molecules from the surfaces, resulting in a change of state from liquid water to water vapour. The flow of water vapour from an evaporating surface to the atmosphere is initially a diffusion process in which water molecules diffuse from the evaporating surface with a high concentration towards the atmosphere with a lower concentration. As evaporation advances, the atmosphere gradually becomes more saturated, subsequently slowing the process down (Hopkins and Hüner, 2008). For evaporation to occur, the vapour pressure at the evaporating surface must exceed the vapour pressure in the atmosphere. Therefore, it can be said that the vapour pressure gradient between evaporating surfaces and the atmosphere is the driving force behind the movement of water molecules.

For the process of evaporation to take place from vegetated surfaces, water molecules must first diffuse from the boundary layer. The boundary layer is defined as the thin layer (± 1 mm) around a leaf surface - adjacent to evaporating and transpirating surfaces through which sensible heat exchange takes place (Zhang *et al.,* 2001). The boundary layer thickness is influenced by wind and air turbulence; however, no air turbulence occurs within the boundary layer itself. Once water molecules move out of the boundary layer zone into the atmosphere, further movement of water molecules is driven by mass transport. During mass transport, saturated air-particles flow in response to atmospheric pressure gradients (Hopkins and Hüner, 2008). In contrast to water molecules flowing away from evaporating leaf surfaces, water molecules can also return to

evaporating surfaces by means of diffusion and mass transport. If the amount of water vapour arriving at the leaf surface equals the amount of water vapour leaving the surface, a steady state has been achieved and no evaporation will take place. However, if the amount of water vapour arriving exceeds the amount leaving, a net gain of water vapour has taken place, referring to the process as condensation (Brooks *et al.,* 2013).

Trees with evergreen properties are able to maintain a relative constant evaporation rate over time (Zhang *et al.,* 2001). Unlike trees, grasses and herbaceous vegetation with dormant periods and shallow root systems, tend to have reduced evapotranspiration rates during periods when adequate moisture is not available (Sikka *et al.,* 2003). Hence, in regions with drier climate, plant-available water capacities are expected to be the principle reason for alternating evapotranspiration rates between trees and shallow-rooted vegetation covers.

2.1.7 Transpiration

Foliar canopies are the most distinguished parts of plants, mediating the transport and exchange of gasses and water vapour to the atmosphere through small openings on the leaves called stomata. Under conditions where groundwater availability is adequate, water flow through the soil is relatively passive until intercepted by plant roots (Hopkins and Hüner, 2008). Once groundwater has been absorbed by plant roots, the flow of water through the plant is driven by water potential and water potential gradients. In plant cells, fluctuating concentrations of solutes influence available energy in cellular water. As solutes are added to cellular water, the osmotic potential in the cells are lowered. In response, the water potential gradient between surrounding cells becomes steeper, stimulating the movement of water from plant cell to plant cell (Hopkins and Hüner, 2008). Once stomata open, water escapes to the atmosphere and the water potential in the plant leaf decreases, resulting in a steeper water potential gradient from plant roots to the leaves. In response to the steeper water potential gradient, water moves through plant cells to the leaves where evaporation takes place through open stomata. Water vapour then diffuses through the boundary layer into the atmosphere. Plants restrict the amount of water that is transpired through stomatal regulation, structural and physiological adaptations and root characteristics.

Water loss to transpiration processes are influenced by the type of vegetation, density and coverage expanse. Transpiration rates among different plant species and plant communities are attributed to physical and physiological characteristics including root and foliage characteristics, stomatal responses and overall albedo of plant surfaces (Brooks *et al.,* 2013). Annual transpiration is also affected by seasonal change and duration of growing seasons. Woody shrubs and forests with longer growing seasons have a much longer active transpiration season

than herbaceous vegetation such as grasses. Similarly, deciduous forests (shedding leaves during winter months) naturally transpire in shorter seasons than conifers. For this reason, transpiration rates of evergreen trees are usually higher than any other vegetation (Brooks *et al.,* 2013). Table 4 presents average annual transpiration and evaporation rates for different vegetation types.

Table 4: Average transpiration and evaporation rates for different vegetation covers (Forestry Commission, 2005)

Vegetation type	Annual transpiration (mm)	Annual evaporation (mm)
Conifers	300-350	550-800
Broadleaves	300-390	400-640
Grasslands	400-600	400-600

Noticeable changes have been recorded in transpiration trends as plantations mature, usually reaching a peak during the first few years when biomass production is high, and then reduces as trees reach a particular age and biomass production declines (Forrester *et al.,* 2010; Roberts *et al.,* 2001). Two of the main aspects examined in particular, include leaf area index and sapwood area. Leaf area index has a direct influence on the energy absorption and interception of rainfall, whereas sapwood area influences sap flux and transpiration. Roberts *et al.,* (2001) conducted a study on the transpiration patterns of *E. sieberi* stands aged between 14 and 160 years of age. This study demonstrated that stand transpiration patterns reaches a peak at some time; usually during early ages when biomass production is at its highest, subsequently declining with age as biomass production declines. This provides evidence of increased water yields as plantations mature and biomass production decreases.

Forrester *et al.,* (2010) examined the transpiration, growth rate and leaf area along the *Eucalyptus globulus* plantations aged between 2 and 8 years. Results from this study showed an increase in transpiration from 0.4 mm/d at age 2 years to a peak of 1.6 to 1.9 mm/d in stands aged 5 to 7 years (Figure 4). Age induced changes in transpiration rates were also associated with similar trends in stand LAI and biomass production, which peaked between 4 and 6 years of age, and started decreasing at 8 years of age.

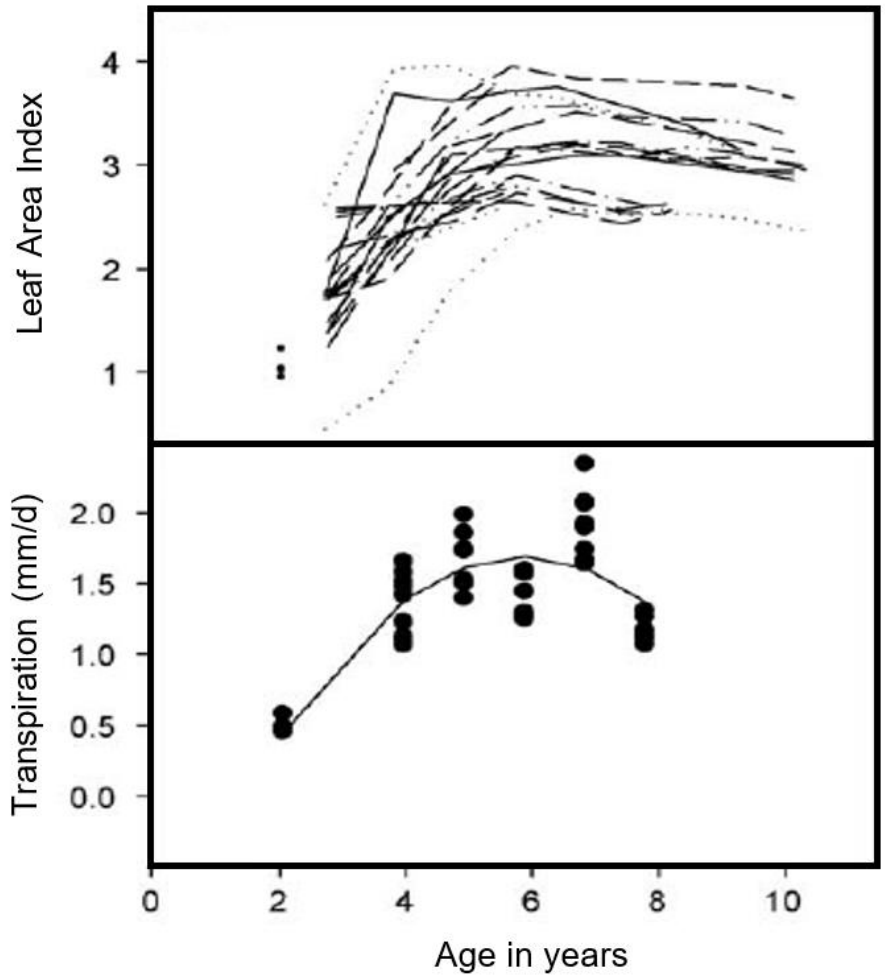

Figure 4: Transpiration rates and LAI with time of Eucalyptus globulus stands (Forrester et al., 2010).

2.1.8 Evapotranspiration

The term evapotranspiration (ET) is used to describe the two most prominent processes of water loss from vegetated surface to the atmosphere namely; transpiration and evaporation (Hopkins and Hüner, 2008). Evaporation is defined as the movement of water from sources such as soil, tree canopies and waterbodies into the atmosphere, whereas transpiration is defined as the movement of water within a plant and the subsequent loss of water vapor through stomtata on leaves. Because these two processes occur simultaneously, the amount of moisture loss from these two independent processes cannot be distinguished, hence the term evapotranspiration.

Similarly, to many most other plant responses, evapotranspiration is influenced by climatic conditions. As the seasons progress and soils gradually becomes drier, the rate of water movement through dry soils gradually decreases and limits the rate of evaporation from soil surfaces. When comparing transpiration from bare soils and vegetated surfaces, the movement

of water to evaporating surfaces of vegetation continues for longer periods due to the fact that roots extract water from greater depths, allowing evaporation of water that would otherwise not evaporate from bare soils (Brooks et al., 2013). As graphically illustrated in Figure 5 below, it is clearly illustrated that the potential soil water depletion under forests with deep roots are very high, and more water is required to recharge soils under forests than soils under herbaceous cover and bare soils. As a result, evapotranspiration affects water yield and the proportion of precipitation input to an aquifer that eventually becomes stream flow (Brooks et al., 2013). Thus, the proportion of precipitation that will eventually become stream flow will be greater for bare soils and areas with herbaceous covers than for afforested areas.

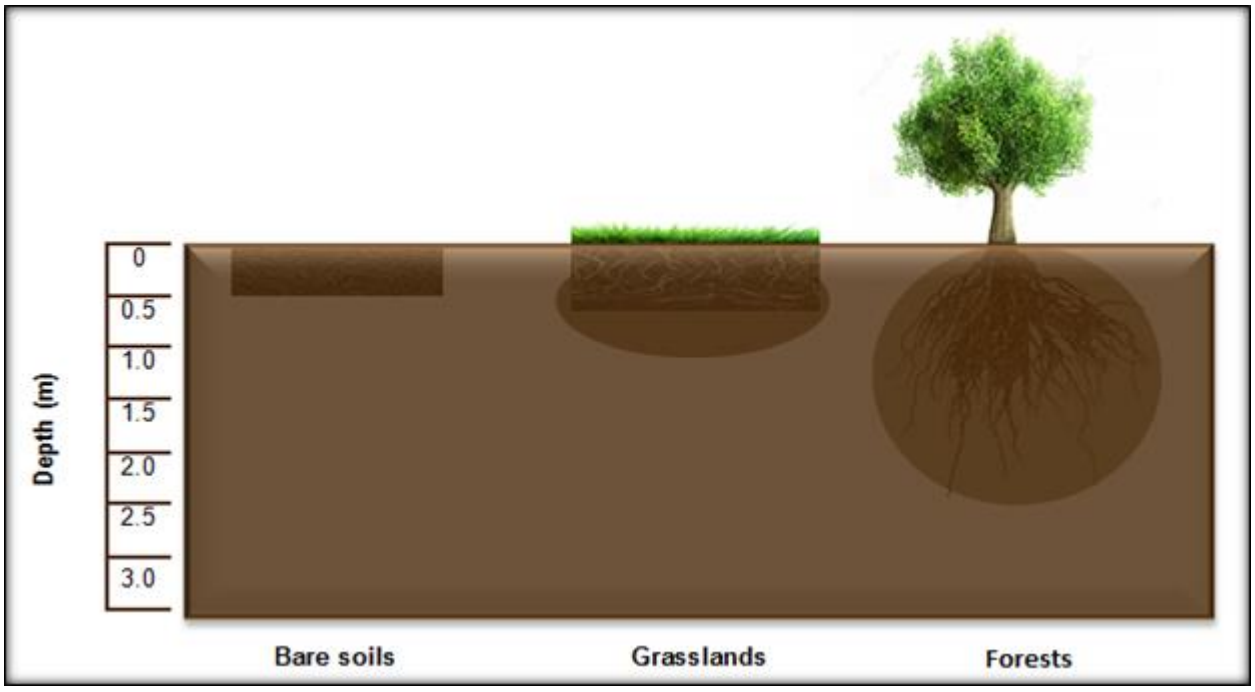

Figure 5: The effect of different vegetation covers on evaporation rates (Brooks et al., 2013).

2.2 Plant responses to water deficiency

The study of plant responses to environmental stress is a fundamental research topic necessary to explain the geographic distribution of vegetation communities, and their performance along environmental gradients associated with distribution patterns. Plant responses to environmental stress induce physiological transitions from functioning under optimal environmental conditions to suboptimal conditions associated with environmental deficits. Depending on the species, plants have different stress avoidance and tolerance strategies in order to reduce the impact of environmental stress (White *et al.,* 1998).

Plants growing under low rainfall conditions are often subjected to soil and atmospheric deficits due to a rapid drop in atmospheric moisture or increase in temperatures, subsequently limiting the capability of plants to acquire adequate water sources crucial for physiological processes (Cohen *et al.,* 1997). Owing to climate change, the prevalence of this phenomenon is becoming more frequent even outside arid and semi-arid regions. Plant responses to water deficits are complex, often requiring adaptive changes in plant biochemistry and physiological characteristics (Scott *et al.,* 1999b). Early responses to water stress supports plant survival and enhances plant function under stressed conditions. Different survival and growth strategies among species are attributed to different capacities for water acquisition and transport within plants under a given water status. Deep groundwater sources are vital for plants especially in low rainfall regions where plants depend on soil moisture for survival. Areas with shallow groundwater tables are able to supply adequate water supply for transpiration and growth and generally support a greater density of vegetation communities than areas with deep water tables (Rood *et al.,* 2002).

Direct deep groundwater uptake has been documented for various species, despite available soil moisture in shallow soil layers. The amount of water up-take varies as a function of vegetation type and species, soil structure, groundwater quality and depth to groundwater sources (Benyon *et al.,* 2002). Vegetation types with shallow root systems are dependent on surface water and shallow groundwater sources, often associated with high rainfall regions with adequate water supply through the year as opposed to shallow-rooted vegetation, trees growing in regions with insufficient precipitation for long-term survival which depend on a supply of water from deep groundwater sources. These plants generally have deep tap root systems in order to maintain contact with groundwater sources; such plants are referred to as phreatophytes (Loheide *et al.,* 2005). Phreatophytes are able to tolerate water stress better and may not require groundwater for long-term survival. Understanding the relationship between vegetation and groundwater is crucial for the management of ecosystems and sustainable use of water resources.

In disturbed areas subject to large quantities of groundwater abstraction due to urbanisation and industrialisation, rapid fluctuations and extended decline of the groundwater table is anticipated. Declining water tables decrease the accessibility of permanent groundwater resources within rooting zones, subsequently inducing water stressed conditions (Scott *et al.,* 1999a). Vegetation growing under water deficits is often subjected to numerous physiological changes, generally influencing tree-water use relationships in response to conserve water. As mentioned earlier, during transpirational processes water is drawn from the soil into plant roots and through conduits in plant cells. As water is transported into cells, turgor pressure and water potential gradually increases and dictates water transport to adjacent cells, driving the transpiration process. Under unfavourable conditions where available groundwater is insufficient, plants are only able to tolerate a decrease in water potential to a tissue and species-specific threshold (Tyree and Ewers,

1991). Beyond this threshold, air pockets are trapped in xylem cavities, blocking water transport through plants. Subsequently, water transport to leaves are decreased causing stomatal closure and a reduction in photosynthesis, often resulting in crown mortality (Cooper *et al.,* 2003). A partial loss of leaves and branches under drought conditions are often a survival strategy reducing plant water needs (Davies *et al.,* 2002).

2.2.1 Alternative water sources: Hydraulic redistribution

Vegetation communities are able to adjust to declining groundwater levels by utilising water from different sources. Under regimes where shallow soil moisture is abundant, plants will preferentially abstract water from these supplies by retaining active roots in shallow upper soil layers, allowing water up-take after rainfall recharge (Caldwell *et al.,* 1998). However, with depletion of shallow groundwater sources, trees are able to adapt their water up-take mechanisms by switching to deep tap root systems in order to tap water from deep groundwater sources (Chimner and Cooper, 2004).

Plant roots exude as well as absorb water in response to gradients in water potentials between roots and soils. Hence, root systems that spans to soil layers of different water potentials, have the ability to act as conduits for the redistribution of soil water from wet soils to dry soils, in order to provide supplemental moisture for roots situated in dry soils (Naumberg, 2005). The driving force behind this mechanism is to prevent lateral roots from dying when not supplied with sufficient moisture. During dry periods when surface soil moisture dries out to the extent that lateral roots discharge all moisture contained in root tissue, lateral root tissue will die unless the moisture is replaced (Hopkins and Hüner, 2008). Similarly, during extremely wet conditions when lateral roots are exposed to excessive water, oxygen deprivation causes roots to die. Tap roots and lateral roots are interlinked by xylem pathways that mediate the transportation of water between these two root systems, predominantly driven by pressure potential. The direction of water movement can be either upward or downward depending on the availability of water reserved in different soil layers. This phenomenon is common in vegetation with established root systems in both wet soils and dry soils, facilitating water up-take through deep tap-roots or shallow lateral roots depending on the water status at the time (Bilal *et al.,* 2014).

Hydraulic redistribution usually occurs nocturnally when transpiration ceases and the water potential of roots in dry soils rise above soil water potential (Richards and Caldwell, 1987). Hydraulic redistribution has illustrated to improve access to limited soil water resources by acting as conduits for the redistribution of groundwater from relatively moist to dry soils (Burgess *et al.,* 2000). The ability of trees to relocate water between soil profiles have been well documented, particularly wherever plants experienced gradients in soil moisture within root zones. The

occurrence of this phenomenon is explained by a number of theories including; to promote a uniform distribution of water through the water column subsequent rainfall periods (Ryel *et al.,* 2004), for the mobilisation of nutrients (Caldwell *et al.,* 1998), improving access to groundwater by relocating water closer to the subsurface (Caldwell *et al.,* 1998), and to maintain turgor pressure within surface root-cells.

Patterns of water use and hydraulic redistribution vary among species and their adaptation to water resource scarcity. Eucalypt root systems in particular consists of lateral roots restricted to shallow soil layers, as well as deep tap roots able to penetrated deep soil layers in order to access deep water resources; therefore, making this species well suited to facilitate hydraulic redistribution (Bilal *et al.,* 2014). Brooksbank et al. (2011) conducted a study on the impact of seasonal variability on tree water use in *Eucalyptus kochii subsp.* borealis growing under a Mediterranean climate with a MAR of 382 mm/a and variable groundwater depths. Results from this study indicated the ability of this species to permit hydraulic redistribution across a range of soil moisture patterns, increasing as soil moisture gradients increased within the rizosphere. However, increasing groundwater depth significantly affected the ability of trees to maintain transpiration rates as dry season progressed.

2.2.2 Natural confining factors

Water stress severity depends on environmental factors including: (a) amount of rainfall, (b) soil types and soil parameters, (c) depth and rate of water decline, (d) stability of water tables and its responses to water abstractions (Shafroth *et al.,* 2000). Given a soil profile consisting of coarse textured soils such as sands and gravel, the impact of declining groundwater will have a severe effect on vegetation due to low water-holding capacities. Conversely, clay and silt profiles with small pore sizes and low infiltration capacities, reduces the rate at which water seeps to deeper soil layers, increasing available water after recharge (Scott *et al.,* 1999a). The height of the capillary fringe in the subsurface layer from which groundwater seeps, strongly depend on soil type decreasing in height from clay, silt, sand and gravel soils (Dragun, 1988).

3 Bio-drainage as an alternative to Artificial Subsurface Drainage

3.1 Artificial subsurface drainage

Under conditions where groundwater fluctuations become problematic, water management options generally resort to artificial drainage methods, consisting of boreholes and pipe-networks for groundwater pumping and translocation (Heuperman *et al.,* 2002). Management of surplus groundwater is especially important, and in many cases comprehensive in the mining-industry, as a preventative measure to minimise the threat of underground excavation-flooding and underground mine-workings being jeopardised.

Groundwater is a common problem in the mining-industry, which, if not managed and controlled correctly, can have detrimental safety, efficiency and economic impacts on mining operations. Subsurface drainage systems are applied by conveying excess groundwater to surface treatment facilities via a range of dewatering techniques (Heuperman *et al.,* 2002):

- In-pit pumping used to pump water from sump areas within pits.
- Dewatering wells used to intercept lateral groundwater flow into voids, to lower groundwater levels prior to mining activities.
- Slope depressurisation drains consisting of inclined and horizontal drainage-systems used to provide flow paths for slow draining groundwater into pits, where water is then pumped to surface
- Cut-of-walls used to seal of preferential flow along permeable rock and soil material.
- Ground freezing reducing the permeability of soils prior to shaft sinking and excavation development.

3.2 Bio-drainage as an alternative

The above-mentioned artificial subsurface drainage methods have all been extensively applied due to satisfying performance; however, these methods require expensive financial investment and intensive management of extracted water (FAO, 1989). At present, the option receiving increasing attention lately for management of groundwater liabilities and in-situ treatment of contaminated soils, is the establishment tree plantations as “bio-drainage covers” (George *et al.,* 1999). Bio-drainage is based on the approach of vegetation introduction and tree establishment in large areas of cleared land, to more closely resemble the natural water balance and increase the transpiration potential of a landscape (George *et al.,* 1999). This approach is considered as an effective, affordable and sustainable alternative management option to manage groundwater fluxes, groundwater seepage and deep drainage (Schnoor *et al.,* 1995). In addition, bio-drainage approaches require minimal initial investment for site development, with potential benefit and

profit return from bio-crop harvesting and timber-production. Table 5 illustrates the differences between artificial subsurface drainage methods and bio-drainage.

Table 5: Difference between artificial subsurface drainage methods vs. bio-drainage (Heuperman et al., 2002)

Variable	Artificial subsurface drainage	Bio-drainage
Financial investment	• High financial investment	• Relatively low financial investment
Drainage efficiency	• Extensively applied • Concerns regarding quality of effluent/extracted water	• Relatively new approach tried and tested at various locations • No effluent, water is used within plant processes or evaporated.
Operation and Maintenance	• Regular maintenance of pipe-networks • Salt harvesting from evaporation dams are required.	• Plantation thinning • Harvesting • Disease control
Water quality required	• Systems are designed to translocate low-quality water	• Dependant on water of relatively good quality during establishment phase
Size of area required	• No area required for sub-surface drainage systems	• Relatively large areas are needed for the establishment of plantations
Advantages	• Improvement of waterlogged areas • Water table control • Salinity control in cases where effluent is effectively disposed • Additional water available for re-use in operational processes	• Improvement of waterlogged areas • Water table control • Provides shelter belts against wind erosion • Bio-crop return from timber production • Contributes to biodiversity
Environmental impacts	• Extracted water may be of low quality, containing high concentration salts, chemicals and drained nutrients • Challenges regarding disposal and treatment of polluted water	• Dewatering, translocation and disposal of polluted groundwater happens simultaneously

In natural environments under natural conditions, elements of the hydrological system such as rainfall, evaporation, transpiration, groundwater storage and changes in groundwater drainage are usually in balance. However, under regimes of increased groundwater recharge, the levels of drainage flow, water tables and soil moisture storage capacities are anticipated to increase. As established in a vast range of research, plant function-and physiology plays a vital role in evapotranspiration potential and water storage capacity of soils. Hence, the natural balance between groundwater recharge and discharge is significantly influenced by the establishment or removal of vegetation in an environment (Hopkins and Hüner, 2008).

Extensive research has been done on the potential of trees as bio-drainage "pumps". Studies of re-vegetation and establishment of tree blocks for recharge management have focused on the adaptation of selected species (Pepper and Craig, 1986), monitoring and measurement of yield responses (McKenzie *et al.,* 1997) and small-scale observations of the impact trees have on groundwater and water table responses (Smith *et al.,* 1998). Evidence from research done in Australia in particular, have proved that tree establishment have the potential to significantly lower water table levels under a broad spectrum of landscape conditions (Greenwood *et al.,* 1985). Conclusions made by Raper (1998) suggest that a significant correlation exists between the proportion of vegetated area and the response in water tables.

The establishment of trees in blocks or belt across areas with high seepage potential have the ability to exert hydraulic control, contain groundwater seepage and reduce the movement of pollutants dissolved in water (Allison and Hughes, 1983). These outcomes are particularly beneficial and suited for environmental requirements constructed for mine management-efforts, to minimize the interaction between groundwater and mine-impacted water that has been chemically affected by mine waste rock, mineral processing and seepage from tailings. The overall objective of this approach is to prevent and minimise adverse long-term environmental, physical and economic impacts of mine water, and to create and maintain a stable landform suitable for current mining operations, or subsequent land-use (Mulvey *et al.,* 1995). Although a bio-drainage approach is not strictly categorised as a phyto-remediation approach, it does comply to the requirements of phyto-remediation strategies, ensuring that the construction of land covers minimise the long-term environmental impacts, fits within topography of the surrounding landscape and ensures that the final landform will perform and evolve predictably with the purpose to limit exposure of mine-influenced waste and natural resources (Mulvey *et al.,* 1995).

Minimising environmental impacts and liabilities using sustainable green covers, requires appropriate cover-design which considers a range of criteria (Weiersbye *et al.,* 2002):

- Ability of selected vegetation to establish easily and stabilise the landscape

- Rapid growth rate to promote early contact with groundwater
- Deep root systems for the extraction on groundwater from considerable depths
- Increased transpiration potential
- Tolerance to high electrical conductivity levels, heavy metals and low nutrient levels often associated with mine-impacted environments
- Low invasive potential according to the CARA categorisation
- Reasonable wood properties and qualities
- Indication of hardiness and good survivorship under mine-influenced conditions
- Ability to reduce infiltration and groundwater recharge
- Capable of pollutant sequestration

Taking the above-mentioned criteria into consideration, research undertaken in the Sustainable Vegetation of Gold Slimes Dam Project (Weiersbye *et al.,* 2002) identified only a few species appropriate for establishment, growth and survival in the harsh conditions generally associated with mining environments. Since tree species have deeper root systems and continue to transpire throughout the year, in contrast to seasonally dormant grasslands with shallow root systems, it is anticipated that the selective establishment of tree blocks or belts should reduce effective recharge to deep groundwater reserves.

3.3 South African timber industry

South Africa's forests cover approximately 1.5 million hectares of the country's total land area of 122 million hectares. The benefits of this industry in terms of production, income generation and provision of jobs are undisputable (Chamberlain *et al.,* 2005). According to DWAF (1998), South Africa has the highest percentage of proportional area of certified plantations in the world, and about 82% of commercial plantations areas in South Africa have achieved the global Forest Stewardship Council certificate. The history of forestry in South Africa was driven by the protection of a very small indigenous resource, while creating a substitute plantation resources that has satisfied the ever-growing demand of a growing population, and establishing an export-orientated and competitive industry. The local commercial forestry industry is one of the leading contributors to the country's economy, acting as a stimulant for socio-economic growth and development. The largest proportion of the country's timber plantations are spread over the higher-rainfall regions, in the Limpopo, Mpumalanga, KwaZulu-Natal, Eastern and Western Cape, covering an estimate of 1.5 million hectares (Scott *et al.,* 1999b). Refer to Figure 6 for a vegetation map illustrating forestry regions, and Table 6 for the percentage plantation area per province.

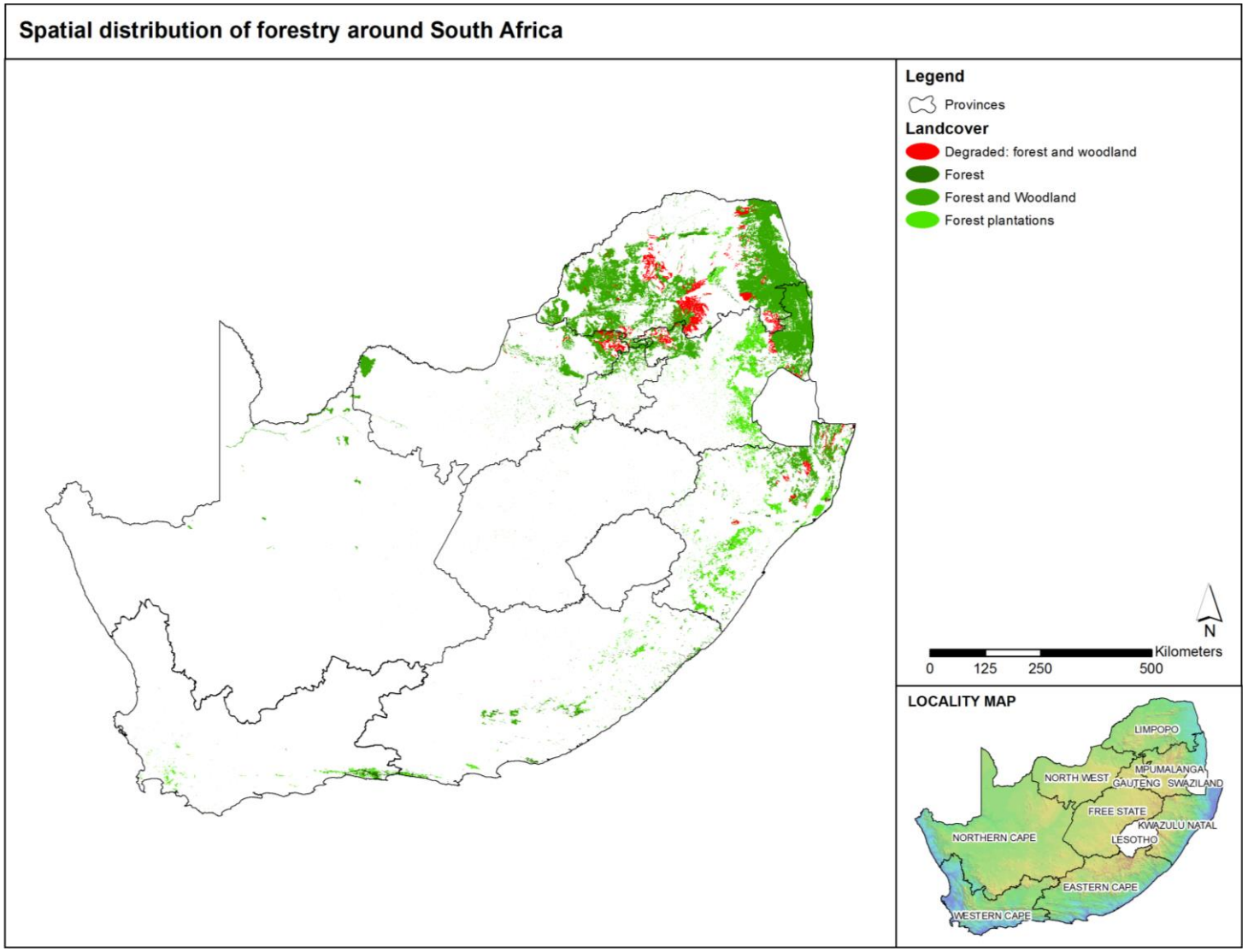

Figure 6: Spatial distribution of forestry in South Africa

Table 6: Plantation area by Province (DWAF, 1998)

Province	Total area (ha)	% Privately owned	% Publicly owned
Mpumalanga	519 210	75.2%	24.8%
KwaZulu-Natal	501 808	93.7%	6.3%
Eastern Cape	142 175	80.3%	19.4%
Western Cape	54 361	98.4%	1.6%
Limpopo	47 953	54.1%	45.9%
North West	304	0%	0%
Northern Cape	0	0%	0%
Gauteng	0	0%	0%
Free Stet	0	0%	0%

Commercial forestry in South Africa are primarily based on the cultivation of Pine, Eucalypt and Wattle species (Figure 7). The introduction of exotic species with high wood quality in conjunction with faster growth rates in comparison to indigenous species, brought a major advantage to the industry. Following the introduction of several exotic tree species and a number of trials conducted by various research organisations over a substantial period of time, the current list of commercialized hardwood species in South African breeding programmes include: *Eucalyptus, Pinus* and *Acacia* (Wattle). Refer to Table 7 for general characteristics of some commercial species in South Africa.

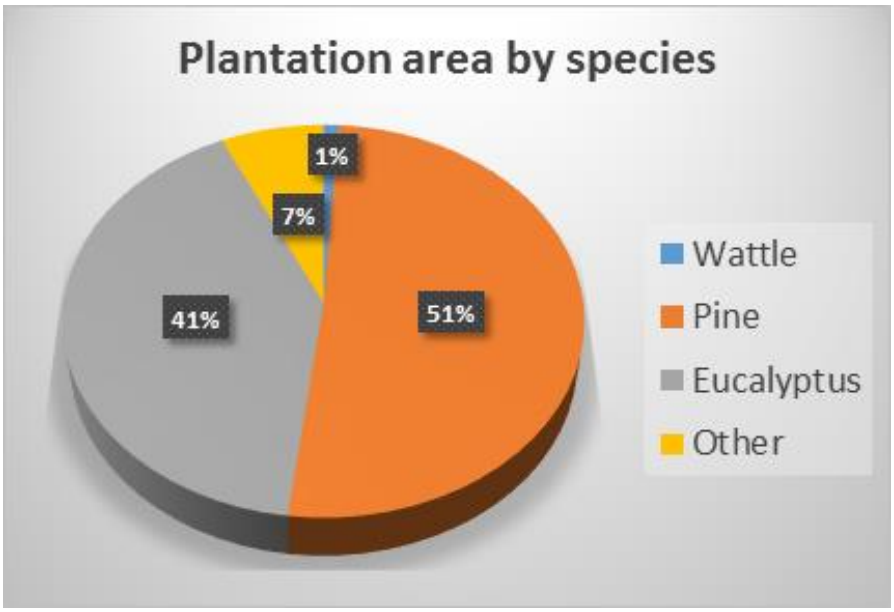

Figure 7: Plantation area per species (DWAF, 1998)

Table 7: Characteristics and traits of various commercial species (Sappi, 1994)

Genus	Rotation length (years)	Preferable sylvicultural zone	Improved genetic stock	Tolerance		Growth rate
				Cold	*Drought*	
Pinus:						
P. patula	± 17-20	Cool temperate	High	Moderate	Moderate	High
P. radiata			High	Moderate	Moderate	High
P. elliotti			Moderate	Low	Low	High
Eucalyptus:	± 6-7 for pulp ± 12-15 for solid wood	Warm temperate				
E. grandis			High	Moderate	High	High
E. globulus			Moderate	Moderate	High	High
E. camaldulensis			Moderate	Low	Moderate	Moderate
E. nitens			Moderate	Moderate	Moderate	High
Acacia: ***A. mearnsii***	± 8-10	Warm temperate	Low	Moderate	Low	Moderate

3.4 Water-use potential of introduced species

Eucalyptus and *Pinus* species are considered among tree species with the highest water use characteristics, predominantly driven by high leaf area indexes (Table 8). Desirable traits including increased above-ground biomass production, increased evapotranspiration rates, rapid growth potential, luxurious water consumption and physical parameters allowing easy establishment of *Eucalyptus* and *Pinus* species, has led to increased attention set on the potential of these commercial species to be used as efficient bio-drainage species.

Numerous research studies assessing the impact of introduced plantations on South African hydrology, suggests that indigenous tree species exhibit lower water-use efficiencies and water-use rates than introduced species such as Pines and Eucalypts. This suggestion has been tested and supported by many, including Gush *et al.,* (2011), who showed that the water use efficiency (WUE) of indigenous *Podocarpus henkelii* (Yellowwood) were below that of introduced *Pinus patula* (Mexican Pine) plantation, both growing in the same area under similar conditions. Figure 8 illustrates a comparison of water use efficiencies between introduced species (more productive systems) and indigenous species (less productive systems).

Table 8: Maximum daily whole-plant use rates (Wullschleger et al., 1997)

Species	Height (m)	Leaf Area (m^2)	Water use (l/d)	Source
Eucalyptus camaldulensis	-	-	29	Greenwood *et al.* 1985
Eucalyptus globulus	-	17	37	Greenwood and Beresford (1997)
Eucalyptus grandis	56	219	174	Olbrich (1996)
	23	73	94	Dye *et al.,* (1992)
	34	71	141	Dye (1996a)
Eucalyptus regnans	58	303	285	Vertessy *et al.,* (1997)
Pinus caribaea	7	-	100	Sansigolo and Ferraz (1982)
Pinus pinaster	20	-	161	Granier et al. (1990)
	26	-	125	Loustau et al. (1996)
Pinus radiata	16	-	179	Greenwood *et al.* (1995)
	6	265	150	Edwards (1986)
	25	300	349	Teskey and Sheriff (1996)
Poplus deltoids	15	15	51	Hinckley et al. (1994)
Quercus robur	-	-	12	Brèda et al. (1993)
Quercus sessilis	-	-	129	Kuèera et al. (1977)

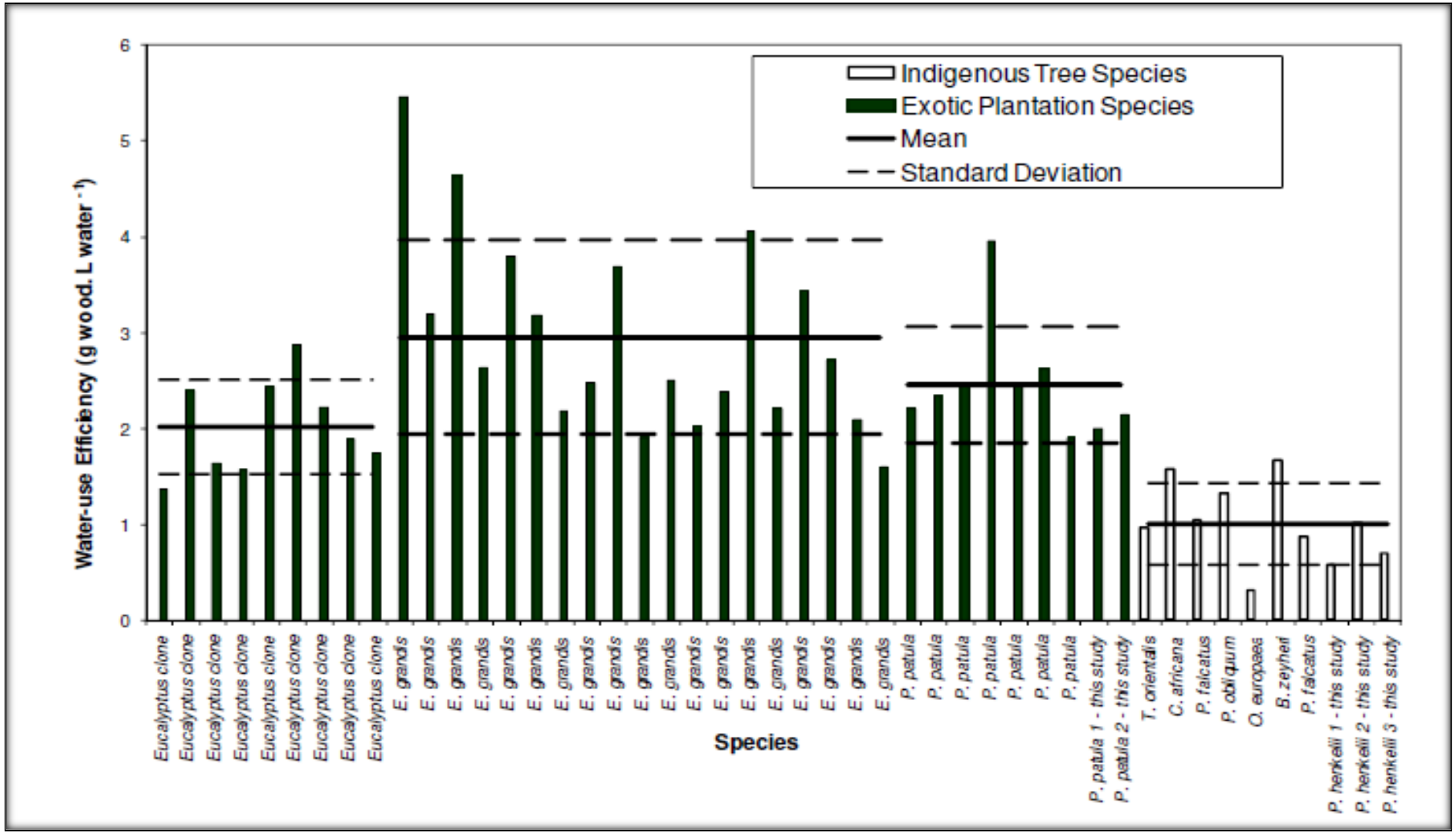

Figure 8: Water use efficiency for different species (Gush et al. 2011)

3.5 Hydrological studies on introduced species

3.5.1 Eucalyptus species

Many concerns have been raised about the expansion of land-use for the establishment of *Eucalyptus* plantations. A large body of research complimented by intensive hydrological monitoring of *Eucalyptus* plantations supports the suggestions that *Eucalyptus* species have the potential to cause recessions of water tables (Engel *et al.,* 2005; Salama *et al.,* 1994; Bacon *et al.,* 1993), reductions in stream flow (Scott and Lesch, 1997; Van Lill *et al.,* 1980; Bosch & Hewlett, 1982; and complete drying out of soils (Soares and Almeida, 2001; Srivastava *et al.,* 2003).

Decreased recharge after plantation establishment of *Eucalyptus* spp. is presented by Allison and Hughes (1983) in a study conducted in a semi-arid region in southern Australia, with an average rainfall of 250 mm/a to 320 mm/a.

Similar findings have been reported by Engel *et al.* (2005) who explored the hydrological impact of *Eucalyptus camaldulensis* establishment adjacent to grasslands in Argentina. Sap flow measurements from this study indicated transpiration rates ranging between 2 mm/d to 3.7 mm/d, lowering water table levels with more than 0.5 m/a in contrast to surrounding grasslands. Due to increased rainfall interception and transpiration potential of the landscape, the hydraulic gradient caused by lower water tables under the Eucalypt plantation, induced groundwater flow from the grasslands into the plantation resulting in a rising of water table levels during the night. The differences between measured daily sap flow and the estimated groundwater use were proportional to fluctuations in soil moisture, thus indicating that *E. camaldulensis* utilised both groundwater sources as well as moisture sources from the vadose zone. The outcome of this study suggested that groundwater sources represented 67% of the total annual water use in *E. camaldulensis* plantations. A similar study was conducted by Joshi and Palanisami (2011) to document and quantify the impact of continuous *Eucalyptus* cultivation on water table depths over a period of 20 years. Results documented in this study indicated an increase in water table depth to 260 m, compared to the mean water levels of 177 m in monitoring boreholes in the study area.

Soares and Almeida (2001) demonstrated a recession of 2.5 m in the water table levels under the E. grandis plantation. The assumption that *Eucalyptus* species utilize several hundred litres of water per day is quoted in numerous studies. However, Dye (1996a) suggested that the most realistic average water use ranges between 40 l/d to 50 l/d in conditions with high water availability. Due to the potential of Eucalypts to extract groundwater from considerable depths (± 8 m to 12 m), these species are extremely tolerant to drought periods. This is supported by Crombie (1992) who proved that stomatal conductance, transpiration and water potentials of

deeply rooted Eucalypts (± 8 m to 10 m), remained higher than the less deeply rooted shrubs and trees in the same area, exposed to a 1 to 2-month summer drought period receiving no rain.

Figure 9 to Figure 12 presents general characteristics of *Eucalyptus* species.

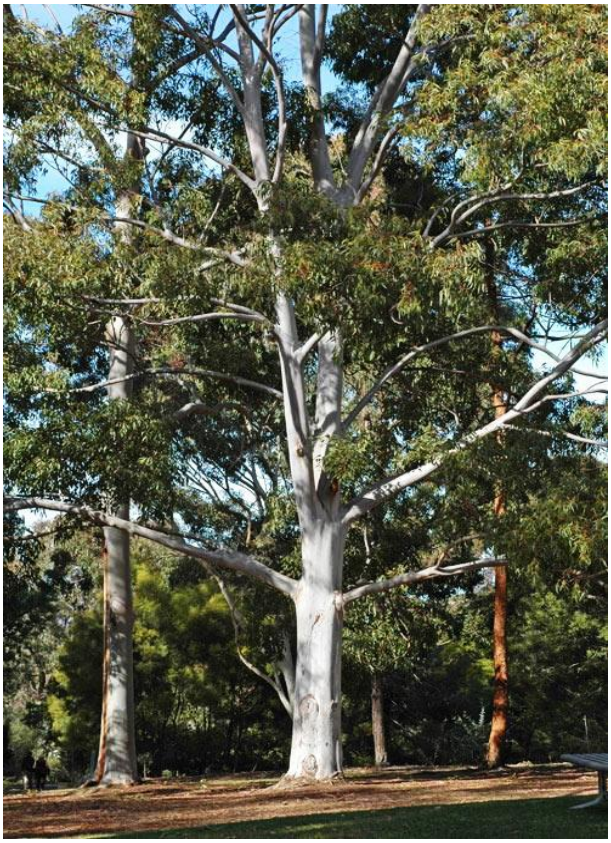

Figure 9: Eucalyptus natural stand with branched canopy and noticeable light stem (SANBI, 2016)

Figure 10: Lanceolate foliage bundle and inflorescence characteristic of Eucalyptus species (SANBI, 2016)

Figure 11: Eucalyptus timber plantation, easily distinguished by tall straight stems and high canopies (SANBI, 2016)

Figure 12: Eucalyptus stem and bark as by SANBI (2016)

3.5.2 Pinus species

Of all the associated environmental effects, the hydrological impact of commercial timber plantations is probably the most extensively and intensely investigated topic, supported by a vast range of research and literature providing insight to the influence of plantations on aquifers. Typical examples include research conducted by Bosch (1979) reporting a 82% reduction in streamflow 20 years after the establishment of *Pinus patula* afforestation in Kwa-Zulu Natal. Similarly, multiple catchment experiments conducted by Van Wyk (1987) a reported 55% streamflow reduction in a Western Cape fynbos catchments 23 years after the establishment of a *Pinus radiata* plantation.

A case study by Van Lill *et a*l. (1980) assessed the hydrological impact of complete replacement of grasslands with a *Pinus patula* plantation in the Mokobulaan research catchment in Mpumalanga. Results from this study showed total drying up of streams in the area 6 to12 years of afforestation. Similar research was conducted by Huber *et al.* (2007) assessing the impact of 12 to 17-year-old *Pinus radiata* plantations on the water balance in Chile. The results were compared to areas covered with perennial grasses and shrubs at the same sites, indicating average canopy interception of 36% to 40% of the annual rainfall. The same study also reported a 32% increase in evapotranspiration over the landscape. Related research by Duncan (1995) indicated a 63 mm/a to 167 mm/a decrease in water yields between 3 to 7 years after the establishment of *Pinus radiata* plantations on land area previously cultivated with crops.

Figure 13 to Figure 16 presents general characterises of Pine species.

Figure 13: Needle-like leaves and cone of Pine tree (Sappi, 1994)

Figure 14: Natural Pine stand (Sappi, 1994)

Figure 15: Pine tree bark and stem (Sappi, 1994)

Figure 16: Pine timber plantation (Sappi, 1994)

3.5.3 Acacia mearnsii

Acacia mearnsii is one of the most important invasive and widespread species in South Africa, causing serious infestations in the higher rainfall regions where they are often associated with replacing seasonal dormant grasslands and fynbos. It is widely accepted that the removal of *A. mearnsii* stands leads to improved catchment water yields (Dye and Jarmain, 2004).

Acacia mearnsii generally grow in dense evergreen stands, maintaining a high leaf area, and consequently a high transpiration rate throughout the year. Several studies assessing the water-use of *A. mearnsii* have reported high evaporation rates occurring in riparian zone where trees are not exposed to water deficits. Dye and Jarmaln (2004) assessed the water-use patterns of *A.mearnsii* stands growing in the Western Cape and Kwa-Zulu Natal. After a one-year period, results from the Western Cape stand indicated transpiration of 1318 mm/a, and estimated evaporation yield of 1503 mm/a. The Kwa-Zulu Natal experiments were conducted over a 4-year

period, with annual precipitation records of 874 mm/a, 616 mm/a, 1016 mm/a and 860 mm/a measured during the experimental period. Sap flow result from the study indicated peak evaporation between 7 mm/d and 8 mm/d, and evaporation yields of 1240 mm/a, 1364 mm/a, 1239 mm/a and 1048 mm/a, respectively.

Similarly, Dye *et al.* (2001) conducted a comparative study of annual ET between indigenous riparian plant communities and riparian *Acacia mearnsii* stands at four sites in the Western Cape and KwaZulu-Natal. The results from this study concluded that the removal of riparian *A. mearnsii* and its replacement by indigenous herbaceous plants may indeed result in significant reductions in annual evapotranspiration, and could very likely lead to streamflow enhancement. Dye and Jarmain (2004) also assessed the daily transpiration rates of *A. mearnsii* stands in response to seasonal variability. Transpiration patterns indicated peak rates between 5 mm/d and 6 mm/d during months when rainfall was at its highest. As rainfall decreased with seasons, and soil moisture reserves started tending towards depletion, transpiration rates progressively declined to about 3 mm/d. The results from this study provide clear evidence that *A. mearnsii* stands depend on available soil water, and do not have the ability to tolerate drought-stress.

Figure 17 to Figure 20 presents *Acacia mearnsii* characteristics.

Figure 17: Acacia mearnsii natural stand (a) (SANBI, 2016)

Figure 18: A. mearnssi leaves (SANBI, 2016)

Figure 19: A. mearnsii inflorescence and foliage (SANBI, 2016)

Figure 20: A mearnsii natural stand (b) (SANBI, 2016)

3.6 Bio-drainage management

As emphasised in the aforementioned sections, tree plantations are known to have the potential to reduce effective groundwater recharge and decrease surface runoff (Benyon *et al*., 2002; Bosch and Hewlett, 1982; Van Dijk *et al.,* 2007), particularly in low rainfall regions and high evapotranspiration regions where high transpiration demands make trees significant water users (Benyon *et al.,* 2002; Jackson *et al.,* 2005). These impacts are frequently regarded as a negative aspect of tree plantations; however, tree plantation establishment may have a positive outcome if the aim of the forestry project is to reduce groundwater recharge and in turn, groundwater levels (Dean *et al.,* 2016). Effective groundwater recharge in low rainfall regions is also affected by various other factors, in particular topography, soil characteristics and geology, that cause spatial variability (Winter, 2001; Schilling *et al*, 2008; Webb *et al.,* 2008). However, conclusions made from recharge studies have not been combined with the results of tree plantation studies, and have been directly applied to water resource management problems accompanying the establishment of tree plantations (Farley *et al.,* 2005)

Since the earliest studies on groundwater systems, it has been concluded that groundwater recharge is controlled predominantly by the topography of a landscape; where the majority of groundwater recharge occurs at topographic heights, and discharge generally occurs in topographic lows where upward hydraulic gradient prevent recharge from occurring (Schilling *et al*., 2008). However, in arid and semi-arid regions, groundwater recharge subsequent to rainfall events, often occurs mainly in local depressions and along perennial streams, due to concentrated overland flow in these areas (Dean *et al.,* 2016). Water tables under perennial streams are generally below streambed, except under extended periods of high rainfall, therefore upwards groundwater gradients do not occur most of the time. Recharge infiltrations beneath these area, may sometimes be encouraged by the preferential flow paths, along which infiltrating water may reach the underlying water table (Winter, 2001; Delin *et al.,* 2000).

As mentioned earlier, vegetation establishment can significantly impact groundwater recharge due to transpiration, rainfall interception and limiting surface runoff. For this reason, it is anticipated that changing the land-use of a landscape, will therefore affect groundwater recharge patterns. This statement has been supported by various researchers. For example, the replacement of native Eucalyptus forests with pasture and crops in south-eastern Australia, has led to increased recharge which raised water tables. Rising water tables resulted in saline groundwater to move closer to the surface and discharging saline water with high mineral contents, into surface water features – eventually resulting in salinization (Allison and Hughes*,* 1983, Bennets *et al.,* 2006). In contrast, afforestation in cleared landscapes is likely to decrease groundwater recharge, as a result of high transpiration, interception of surface runoff and increased evaporation from canopies (Benyon *et al.,* 2002). Various studies indicated that evergreen tree species, *Eucalyptus* species in particular, take-up and transpire significantly more water than pasture, intercept more rainfall, and have greater root depths than grass species, which is indicative that Eucalypts are able to extract water over a larger volume of the soil column (Bosch and Hewlett, 1982). For this reason, it is suggested that tree plantations are considered for the management of groundwater systems (Bennetts *et al.,* 2006).

3.6.1 Recharge management

As mentioned before, plant functions responses to environmental and physiological stimulants, have a great influence on water resources, and is therefore a fundamental element to be taken into consideration in hydrological management. Water fluxes flowing beneath the root zones of vegetation communities, are laterally discharged through subsurface aquifer systems (Heuperman *et al.,* 2002). Thus, the clearing of natural vegetation for land development disturbs the natural maintenance of the hydrological balance under rain fed conditions. Despite evidence of groundwater recharge generally concentrated in topographic lows, groundwater management

strategies operate on the assumption that recharge occurs primarily in the upper parts of a catchment, particularly along ridgelines (Dean *et al.,* 2016). For this reason, the establishment of consumptive water-use tree plantations at higher landscapes or on break-of-slopes (slope changing from convex to concave), is becoming a popular technique to intercept rainfall recharge occurring upslope, and subsequently reduce the volume of rainfall that is subjected to overland flow, infiltration and deep groundwater recharge at low laying areas. Figure 21 and Figure 22 below illustrates how upslope and break-of-slope plantation establishment changes the patterns of groundwater flow (Benyon *et al.,* 2002).

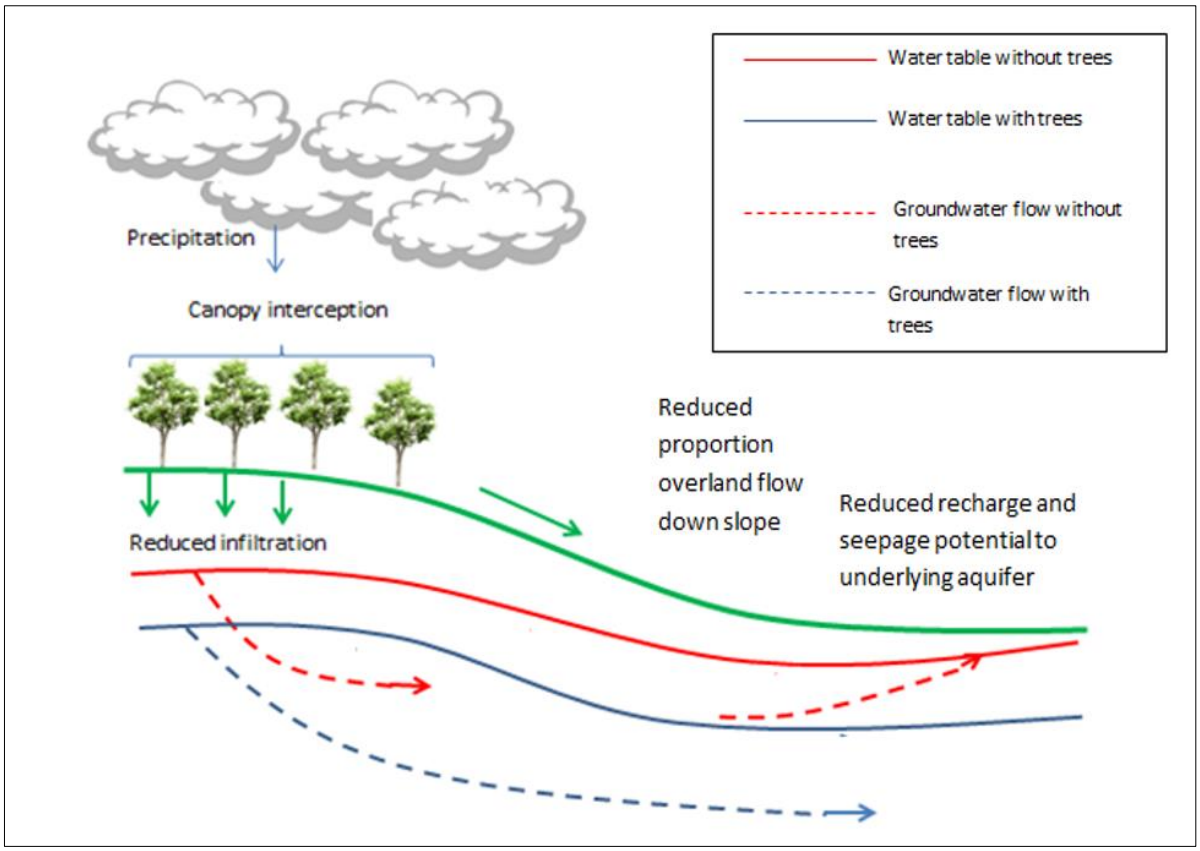

Figure 21: Illustration of recharge control upslope (Heuperman et al., 2002)

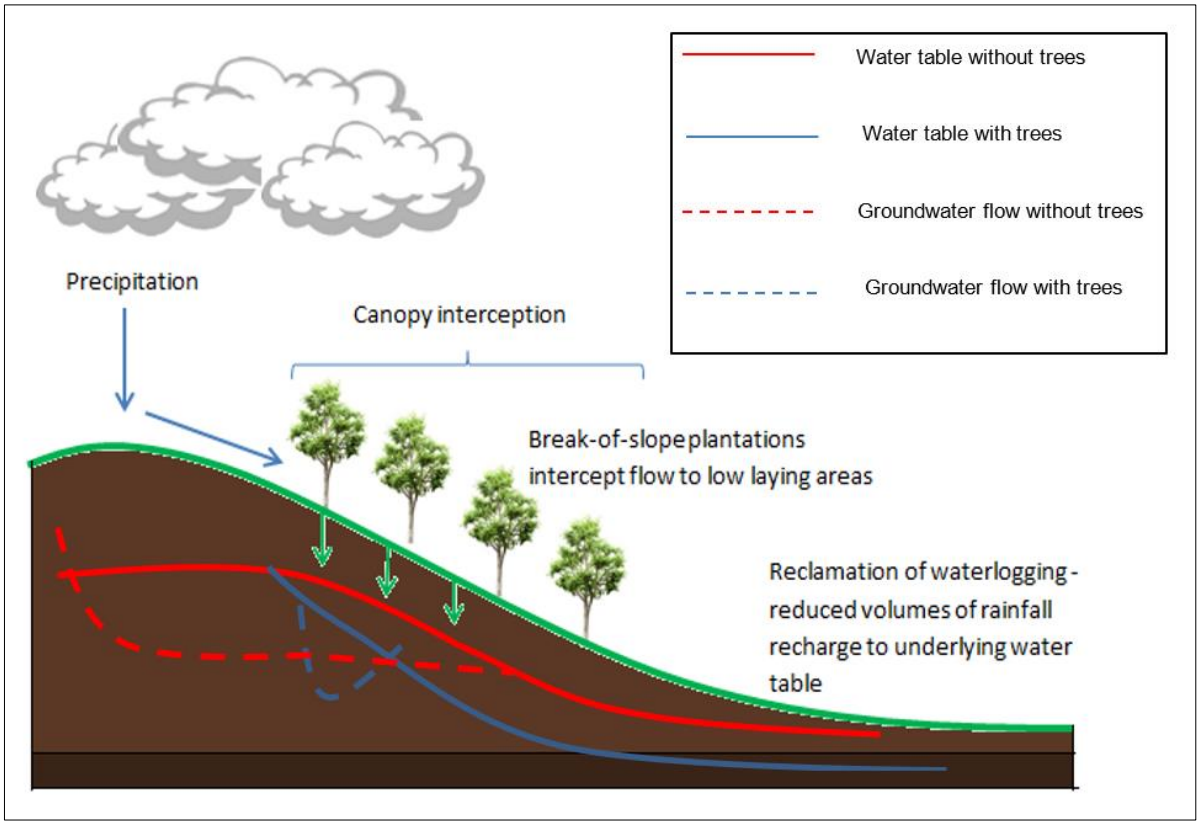

Figure 22: Illustration of break-of-slope plantations (Heuperman et al., 2002)

Break-of-slope (mid-slope) plantations are believed to be well suited to landscapes with unconfined flow of groundwater through colluvial deposits overlaying low-permeable strata (McJannet *et al.,* 2000). The work done by McJannet *et al.,* have proved this approach to be beneficial in recharge control. Research by George *et al. (1999)* supports the suggestion that a positive correlation exists between the proportion area planted and the response in water levels, reporting a 0.4 m regression in water level for every 10% area planted in recharge areas. Under circumstances where the evaporative capacity of newly established vegetation exceeds the pre-clearing evaporative demand, water sources in close proximity is at risk of completely drying out. This situation is often encountered in catchments where natural vegetation is replaced with fast growing plantations.

The success of these planting approaches is illustrated by research from George *et al.,* (1999), providing evidence of water table regression after the establishment of plantation blocks at up-slope and mid-slope (break-of-slope) positions. In this study, observed water level regressions for mid-slope plantings ranged between 0.9 m to 3.5 m, in contrast to water level regressions for up-slope plantings ranging between 1.5 m to 5.5 m. These results illustrate increased water level responses as trees are positioned further up-slope. The most probable reason for this is the fact that trees are more effective at reducing recharge up-slope where water tables are located at a

relatively greater depth and deep recharge takes longer, than in low landscape with shallow water tables quicker recharge of groundwater.

Further contributing to the potential groundwater recession at different slope positions, is the lateral flow that is driven by steeper hydraulic gradients associated with hillslopes (George *et al.,* 1999).

3.7 Water table control

It is well established that the interaction between physiological functions within plantations correlates well with the hydrology of the landscapes in which plantations are based. The integration of these two intricate fields have led to a better understanding of efficient plantation management, and the potential of utilizing these resources as sustainable bio-drainage options to address groundwater liabilities. Trees growing on shallow water tables have the ability to extract water either through direct extraction from the saturated zone below the water table, extraction from unsaturated capillary fringe above the water table, or from unsaturated upper soil layers after rain fed conditions. Thus, the establishment of plantations in parallel field drainage arrangements may have a similar outcome potential in groundwater control than artificial drainage methods (McJannet *et al.,* 2000).

Discharge areas are generally low-laying areas characterised by shallow water tables, high soil moisture content and high salinity levels. The contribution of rainfall accumulation in low-laying areas accompanied by shallow underlying water tables, frequently result in insufficient drainage and waterlogged depressions. However, the utilising of plantations as bio-drainage options in both recharge and discharge areas, have become a fundamental element in groundwater management (McJannet *et al.,* 2000; George *et al.,* 1999; Smedema, 1997). It has been suggested that shallow groundwater can be exploited by fast-growing tree species that depend on constant water sources, with low tolerance for drought and water-stress, as presented in Figure 23 (McJannet *et al.,* 2000).

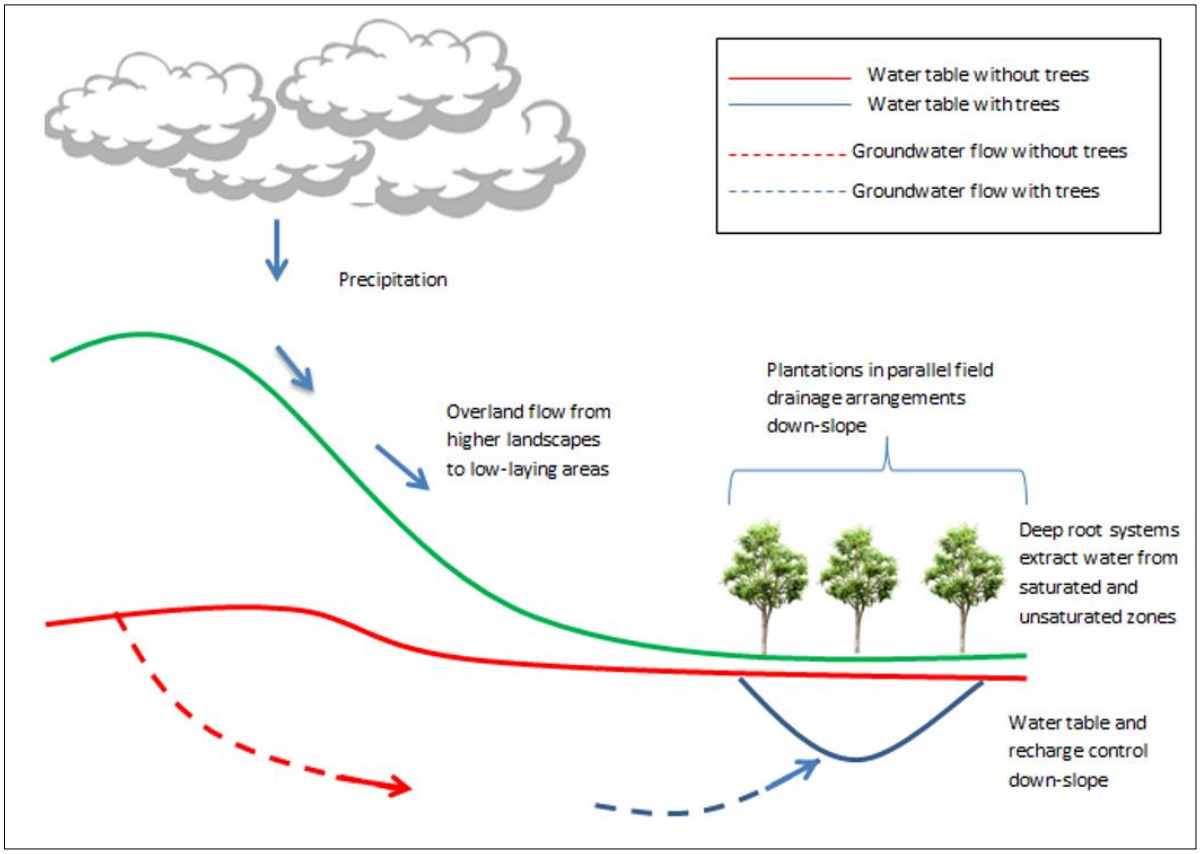

Figure 23: Illustration of down-slope plantation establishment (from Heuperman et al., 2002)

Work done by George *et al.* (1999), have illustrated a 0.4 m regression in water table levels, with every 10% increase in area planted in discharge areas. Long-term observations from down-slope plantings have illustrated water table regressions ranging between 1 m to 2.5 m. However, reductions in water table levels are rarely observed more than 10 m to 30 m from planted areas, thus it can be concluded that plantations established in discharge areas will have greater aquifer impacts on small scale (local or immediate) than on regional scale (Smith *et al.,* 1998).

Despite the general belief that down-slope plantings are most suited for the immediate reclamation of waterlogged areas due to shallow water tables and more access to groundwater, mid-slope plantings have proved to have the highest impact on water table regression discharge areas, ranging between 1.5 m to 4 m. The reason for greater water level regressions from mid-slope plantings than down-slope plantings is suggested to be due to an increased probability of lateral groundwater flow.

With proper planning of landscape utilisation and plantation management, the establishment of plantations is likely to result in beneficial control of groundwater levels. In cases where root penetration is not able to access groundwater or the capillary fringe, trees depend strictly on infiltration from rainfall events, and will not control groundwater levels, but will however, reduce

effective recharge to groundwater. However, groundwater responses to plantation establishment are equally affected by water-use capacity of trees in response to physiological and environmental limits, as to site conditions and area planted. Hence, under conditions where rainfall exceeds plant water demand, leaching of water to deep groundwater sources is still possible, in contrast to a significant decrease in water-use during dry drier periods (Van Hylckama, 1974).

4 STUDY AREA DESCRIPTION

This chapter provides an overview of the study area with respect to the locality, climate, drainage, landcover, geology and geohydrology.

4.1 Locality

The Cooke 4 operations (formerly known as Ezulwini gold mine), is a mature brownfield gold-uranium mine located within the West Rand District Municipal Area in Gauteng Province, South Africa. Dominant residential developments in the area include: Westonaria, Bekkersdal, Hillshaven, Glenharvie, Venterspost, Simunye, Libanon and Waterpan mining towns. The mine is situation approximately 7 km southeast of the town of Westonaria, and is accessed via the N12 national road between Johannesburg and Potchefstroom.

Figure 24 provides an indication of the Cooke 4 mine location. The study area resides on the watershed boundaries of quaternary catchments C22A, C22H, C22J and C23D. The boundaries of the study area itself is governed by geological features and will be discussed in more detail in a later section, but effectively constitute the Gemsbokfontein-Wes compartment.

A Google Earth map of the mine and surrounding residential infrastructure are presented in Figure 25.

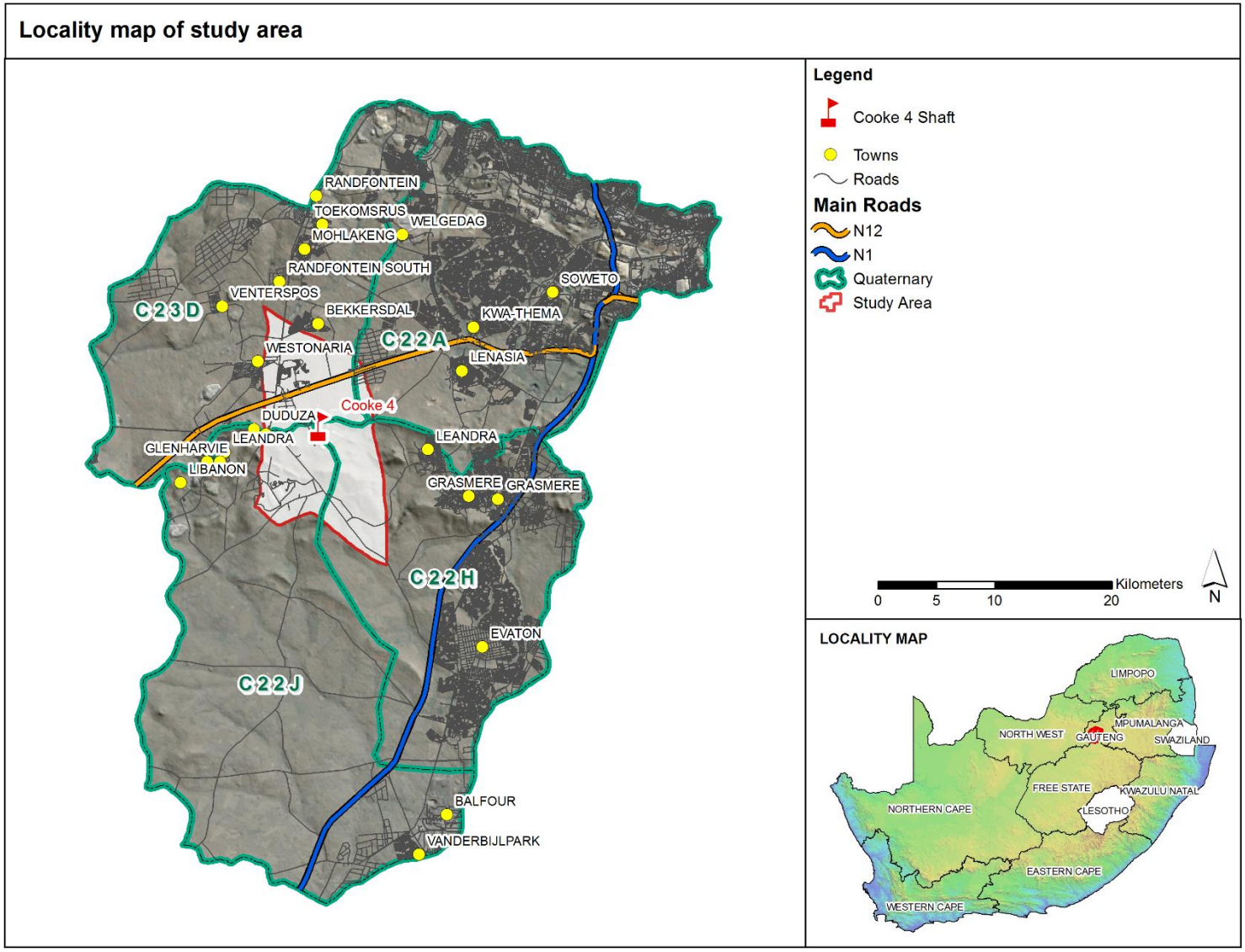

Figure 24: Locality map of the Cooke 4 study area

Figure 25: Google Earth the study area and surrounding residential, mining and road infrastructure.

4.2 Climate

The weather and climate data presented in this section, was sourced from SAWS, DWS Hydrological Services (www.dwaf.gov.za/Hydrology) and Accuweather (www.accuweather.com).

South Africa experiences distinct weather patterns in summer and winter. The project area falls within the interior Highveld region of the country, generally characterised by unstable summer conditions with regular rainfall events, and stable winter conditions caused by a dominant high pressure system resulting in clear skies and pronounce temperature inversions. Generally, climate patterns are cold to mild winters from May to September, and hot to very hot summers from November to March, with moderate or considerable variations in daily temperatures and abundant sunshine. Temperature is closely related to elevation. In general, the mean winter temperatures in Westonaria range between 0°C to 9°C in winter, and 21°C to 30°C during summer months. The maximum relative humidity remains above 60% for the majority of the year, ranging between 57% in November to 72% in March.

Precipitation in this region predominantly occur in the summer months. Figure 26 indicates the variation in monthly average temperatures and precipitation amounts throughout the year. On average the area has approximately 170 sunny/clear sky days, and 120 rainy days per annum (Figure 27). Wind conditions are highly variable, and is affected by topographic characteristics. Wind conditions in the project area generally range between 0.3 m/s to 5.7 m/s, as presented in Figure 28.

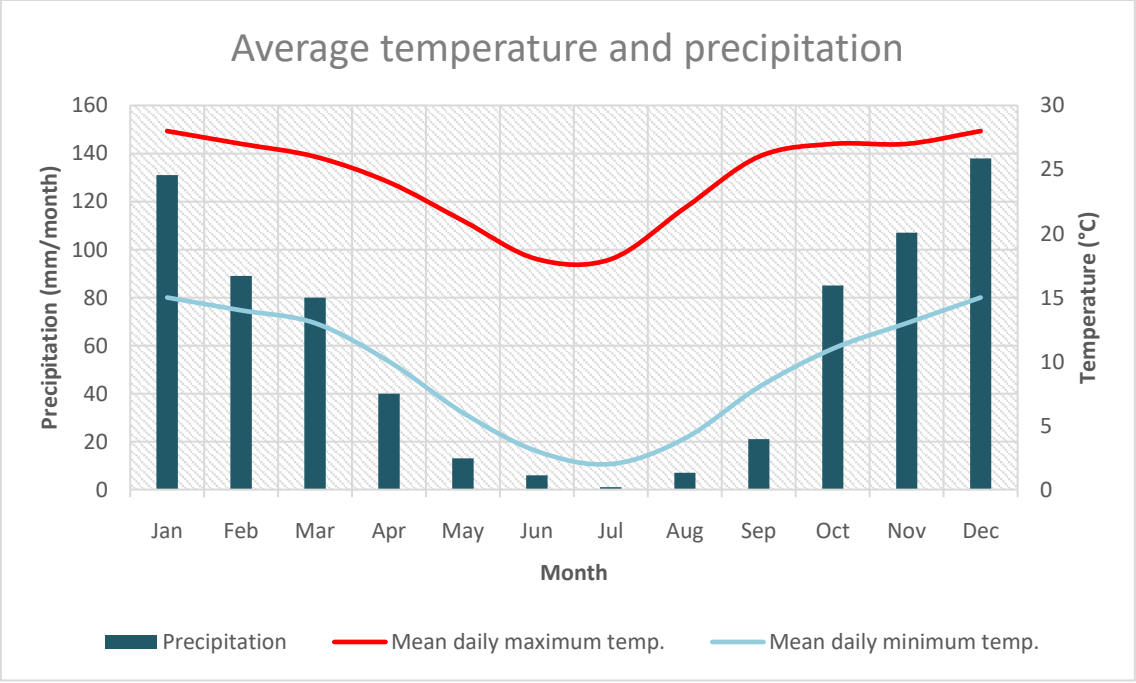

Figure 26: Monthly variations in temperature and precipitation throughout the year

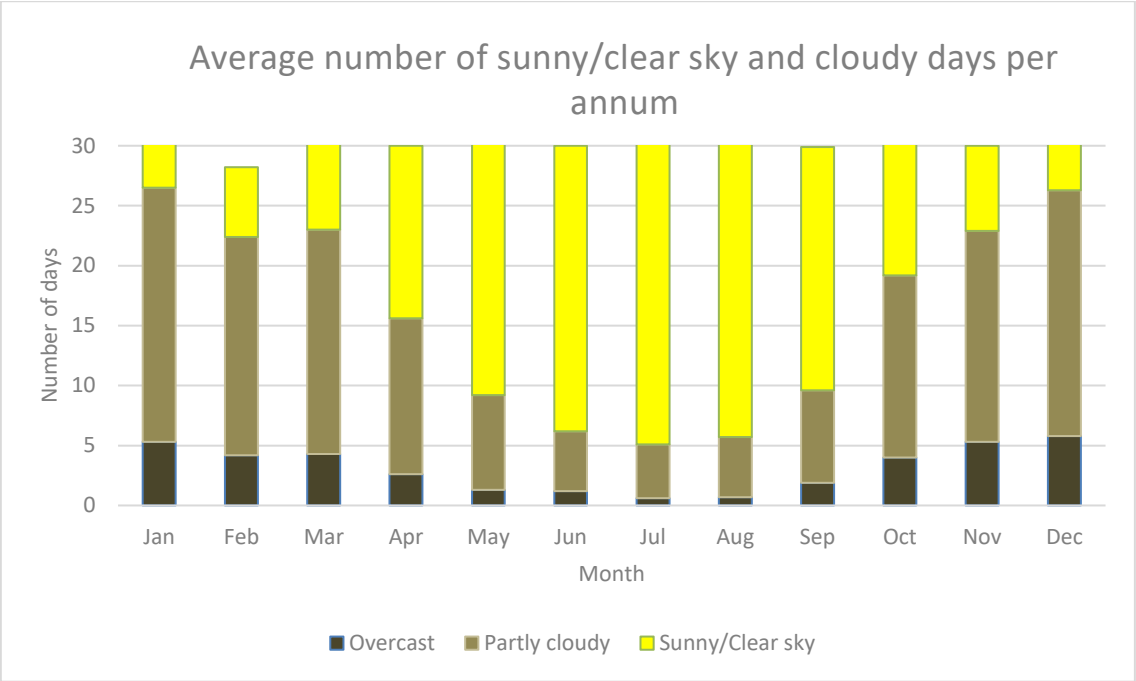

Figure 27: Number of Sunny/Clear sky and Cloudy days per annum.

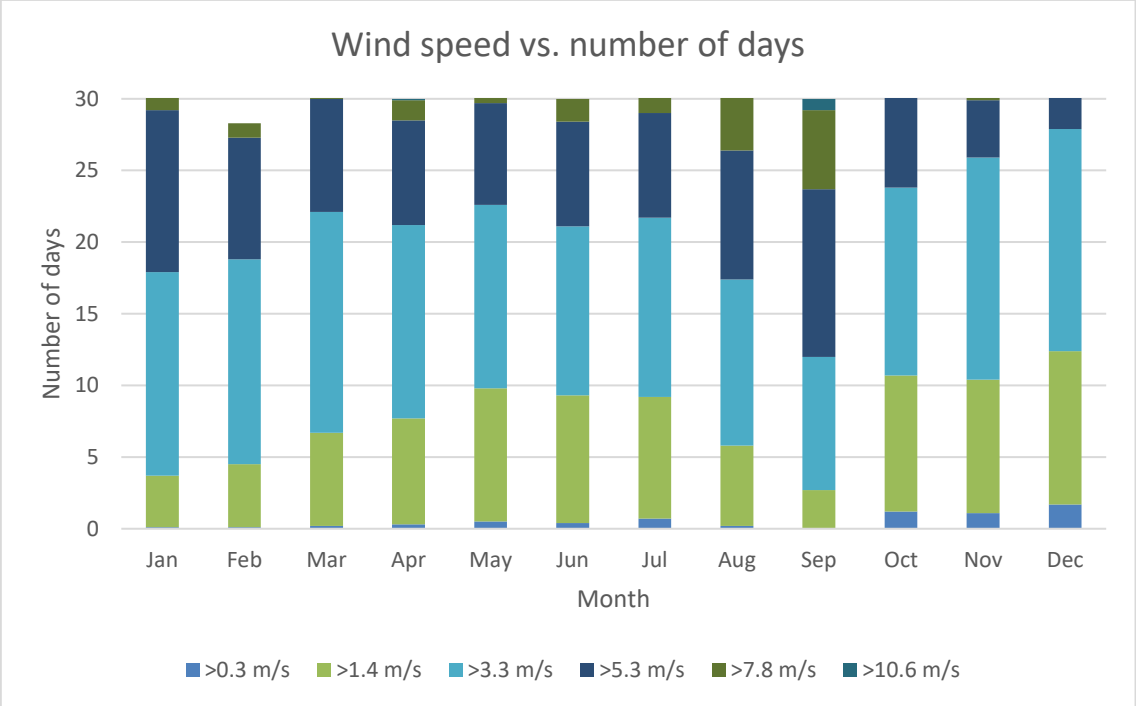

Figure 28: General wind conditions in the study area

Rainfall in the project area is strongly seasonal, occurring primarily as thunderstorms during summer months (October to March), whilst winter months (May to August) are very dry. An estimated 83% of MAP occurs during summer months.

Figure 29 presents the correlation between the average monthly rainfall and evaporation trends for January 2000 to December 2015, obtained from DWS Hydrological Services and measured at the Zuurbekom Pump-Station (C2E007). As illustrated, rainfall generally peaks during December and January, before decreasing towards the end of April.

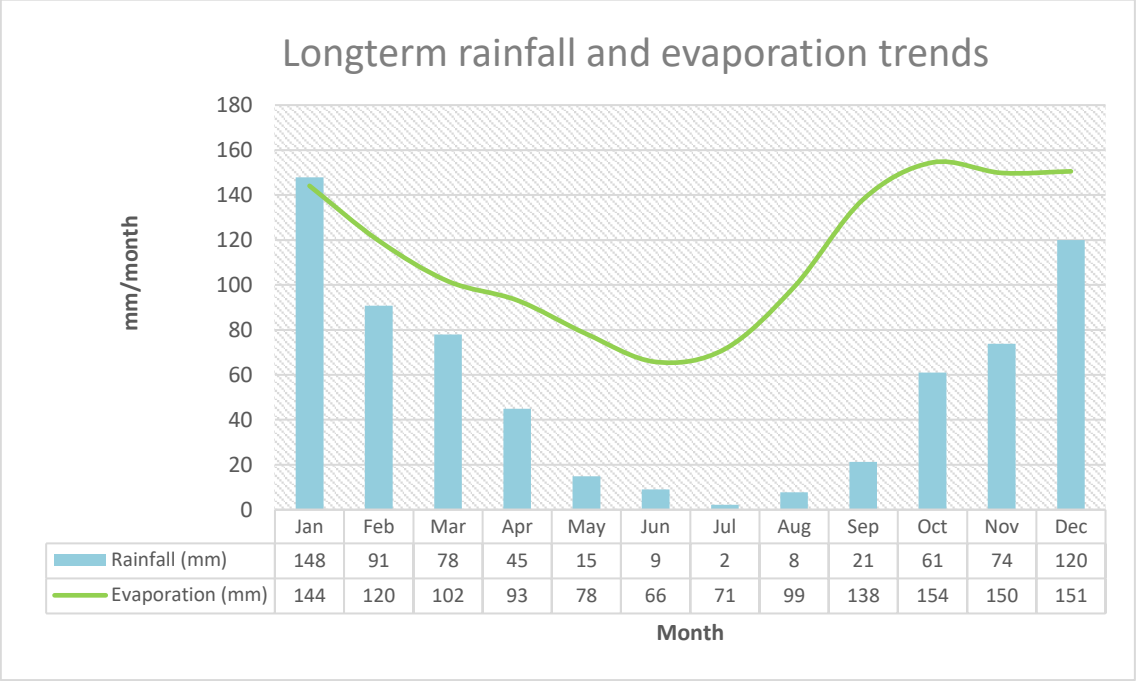

Figure 29: Average long-term rainfall and evaporation trends

4.3 Topography and Drainage

The project area consists of a series of low lands (valleys), hillslopes and plains with a low relief. The Cooke 4 mine is situated at an elevation of 1600-1650 mamsl, on the southern slope of the anticline between two prominent ridges of Gatsrand on the Transvaal Highveld (Figure 30). The most prominent features in the area are formed by the Quartzite ridges of Gatsrand trending to the east-west. Gatsrand divides the area into two sub-areas namely:

- Northern part of the ridge characterised by 7-8km wide slopes which trend downwards towards the Wonderfontinspruit in the north-western corner of the project area, and gently inclines to the northeast and the east, where it reached the Klipriver; and
- Southern part that is characterised by the hogs back ridges of Gatsrand and broad open valleys separated by the ridges in the east with gentle rolling topography intervening the ridges in the west.

The study area is situated in the Upper Vaal WMA which is the uppermost water management area in the Vaal River catchment. The study area resides on the watershed boundaries of quaternary catchments C22A, C22H, C22J and C23D as shown in Figure 30.

The surface water parameters to these catchments as obtained from WR2005 (WRC, 2005) is presented in Table 9.

Table 9: Quaternary catchment parameters (WRC, 2005)

Quaternary	Area (km^2)	MAP (mm/a)	MAE (mm/a)	MAR (mm/a)	Baseflow[1] (Mm^3/a)
C22A	548.5	695.0	1650	31.5	6.08
C22H	454.1	639.5	1650	21.9	4.72
C22J	668.7	632.7	1650	21.0	4.60
C23D	510.1	663.5	1650	29.5	10.37

The Wonderfonteinspruit runs through the northern section of the compartment. The Wonderfonteinspruit has a typical karts topography in the sense that the river disappears and reappears – thus stream water quality will have an impact on the aquifer quality and vice versa (Parsons, 1989). Surface water attributes in the area includes the Kleinwes Rietspruit, Leeuwspruit and the Peter Wright Dam. As Cooke 4 is situated on the southern anticline of the Gatsrand, no significant runoff or discharge occurs to the north of the study area, therefore all surface runoff drain south via the Kleinwes Rietspruit and the Leeuwspruit.

Runoff emanating from quaternary catchment C23D, drains in a south-western direction to the Wonferfonteinspruit, which is the largest river in this quaternary catchment. Runoff emanating from quaternary catchment C22J drains in a southern direction via the Leeuwspruit, which is a non-perennial stream, but flow is maintained through mine water discharge. Runoff emanating from quaternary catchment C22H drain in a southerly direction via the Rietspruit. The intersection of C22A with that of the study area is considered negatable with respect to the runoff generated in this catchment.

The Gemsbokfontein eye which is not flowing due to mine dewatering is situated in the north-west corner of the compartment. It is expected that spring flow will resume once mine dewatering has ceased. Rison Groundwater Consulting (2011) reported historic spring flows of ±9 Mℓ/d for the Gembosbokfontein eye pre-1986.

[1] Baseflow refers to groundwater contribution to baseflow and the values expressed is based on the Pitman model

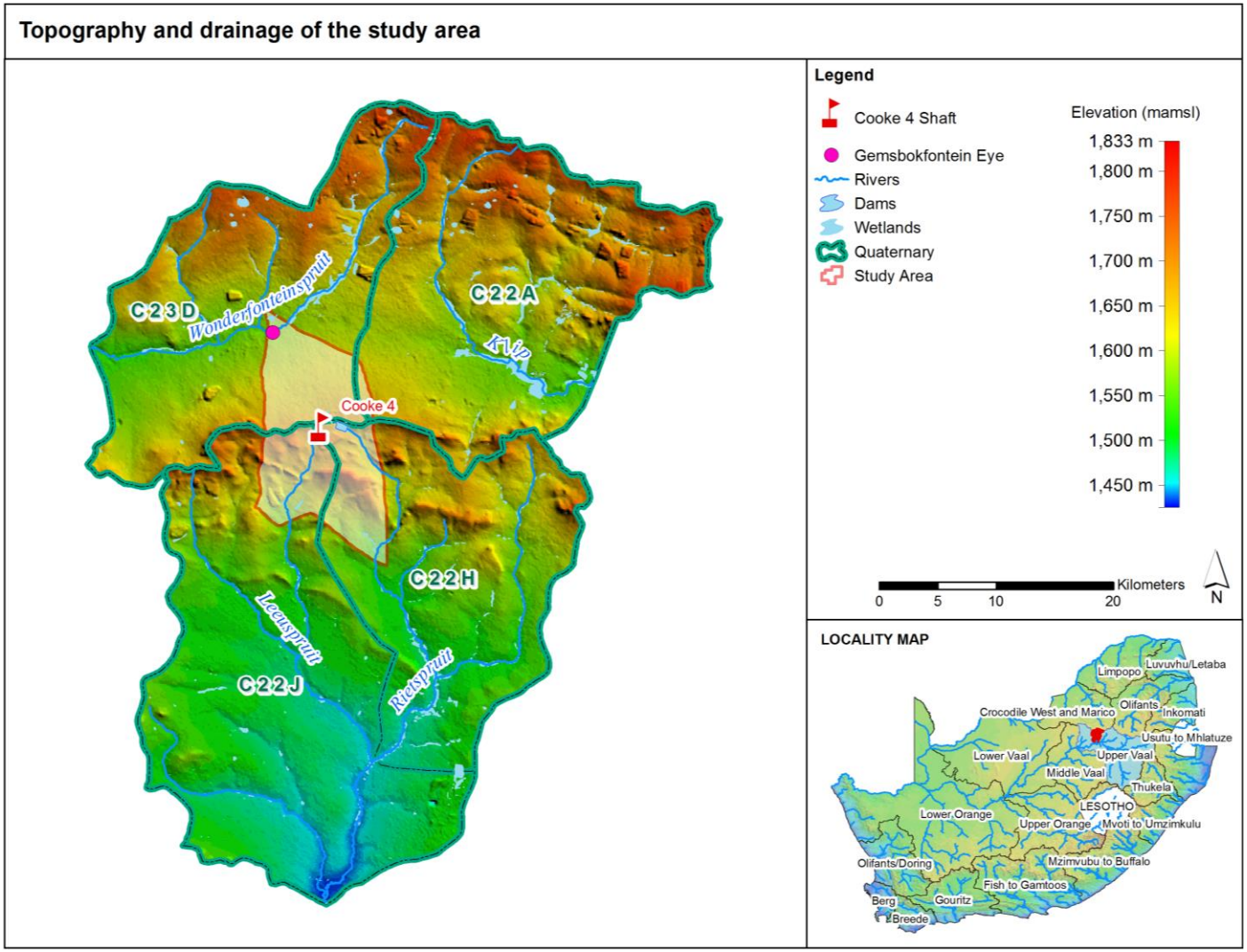

Figure 30: Topography and drainage of the study area

4.4 Landcover

4.4.1 Landcover

The national landcover based on the South African National Biodiversity Institute (2009) datasets, indicates that natural vegetation still dominates over large areas in the region as shown in Figure 31. Pre-mining land capability within the mine lease area consists mainly of grazing and cultivation with monocrops and fruit crops. Surrounding land are being utilised for growing crops and pasture for grazing. A large area of natural vegetation in the region has been transformed during intensification of mining activities and construction of associated mining infrastructure and residential areas (Figure 31).

4.4.2 Land Use

The primary land use in the surrounding area is cultivated agricultural land, predominantly maize and mono crops, with grazing being the main use (Rison Groundwater Consulting, 1992). Residential areas of Westonaria and Simunye are situated in a north-western direction from the Cooke 4 mine.

4.4.3 Vegetation

According to Mucina and Rutherford (2006), the regional vegetation consists of undulating grasslands, which are indicative of Bakenveld type. Remnants of native vegetation, such as open savannah type, shrubby karoo and thorn tree occur on the hilly grounds where minimal disturbance have occurred (Tucker and Viljoen, 1986). Clusters of Eucalyptus trees are present in the area, possibly established as wind breaks during the time mining intensified in the area.

4.4.4 Agricultural Potential

Prior to commencement of mining activities, the land within the mining lease area was utilised for cultivation purposes of monocultures and eventually grazing after cultivation ceased. The dominant soil types in the area have been defined as poor, acid, shallow, sandy and stony soils with low fertility (SRK Consulting, 2013).

As indicated in Figure 32, the study area has pockets of land that has low to high agricultural potential. Land with low agricultural potential are predominantly surrounding the Cooke 4 shaft and associated infrastructure. However, portions of land where little development has taken place, in general have medium to high agricultural potential.

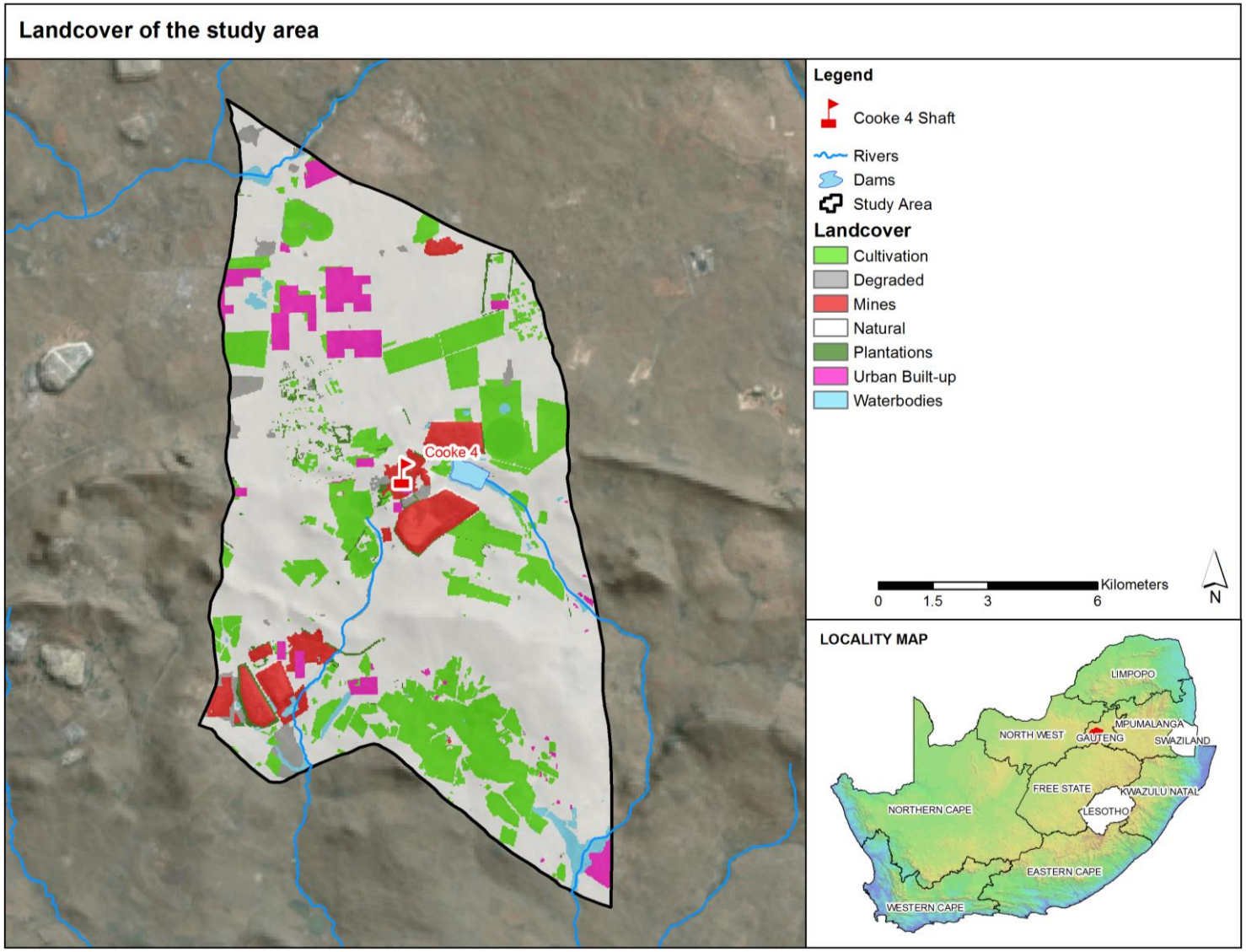

Figure 31: Landcover of the study area (SANBI, 2009)

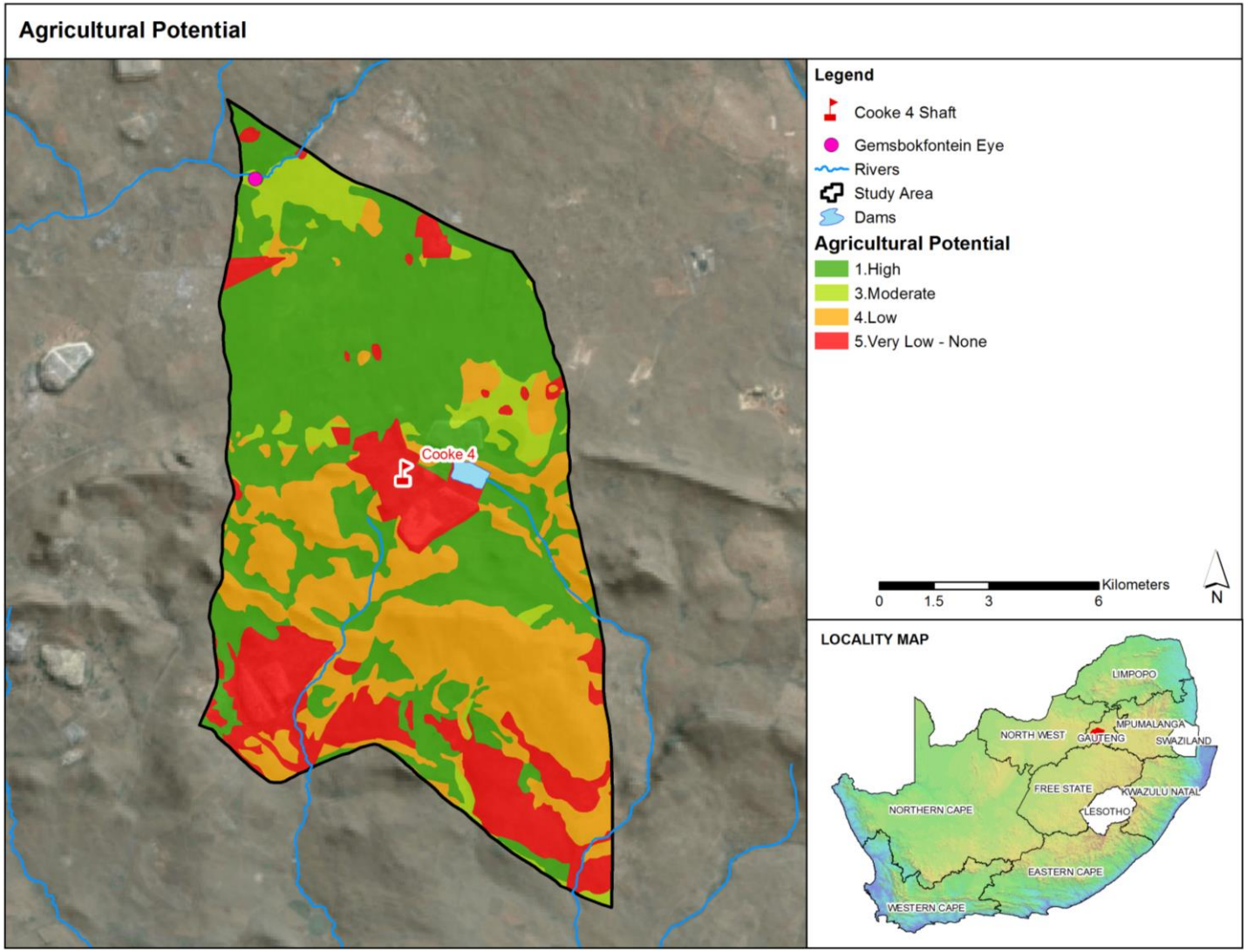

Figure 32:Agricultural potential of the study area

4.5 Geology

4.5.1 Regional geology

The study area is situated within the Witwatersrand Basin. The Witwatersrand Basin is a well-established gold-mining area with an impressive history of established gold producing mines. The Witwatersrand Basin is defined as an Achaean sedimentary, characterised by an elongate surface expression with a longitudinal extension of approximately 300 km northeast-southwest and 100 km northwest-southeast (Tucker and Viljoen, 1986).

The sediments and volcanic rocks within the Witwatersrand basin were deposited on the Dominion Group and Granite-Gneiss Basement (Figure 33). The majority of the rocks in the Basin are overlain by younger sequences. The Granite-Gneiss represents newly cartonized continental lithosphere during the time of development (Tucker and Viljoen, 1986). The Granite-Gneiss basin consist of older greenstone fragments together with granitoid gneisses, and is exposed in the Johannesburg, Westerdam and Hartbeesfontein domal areas.

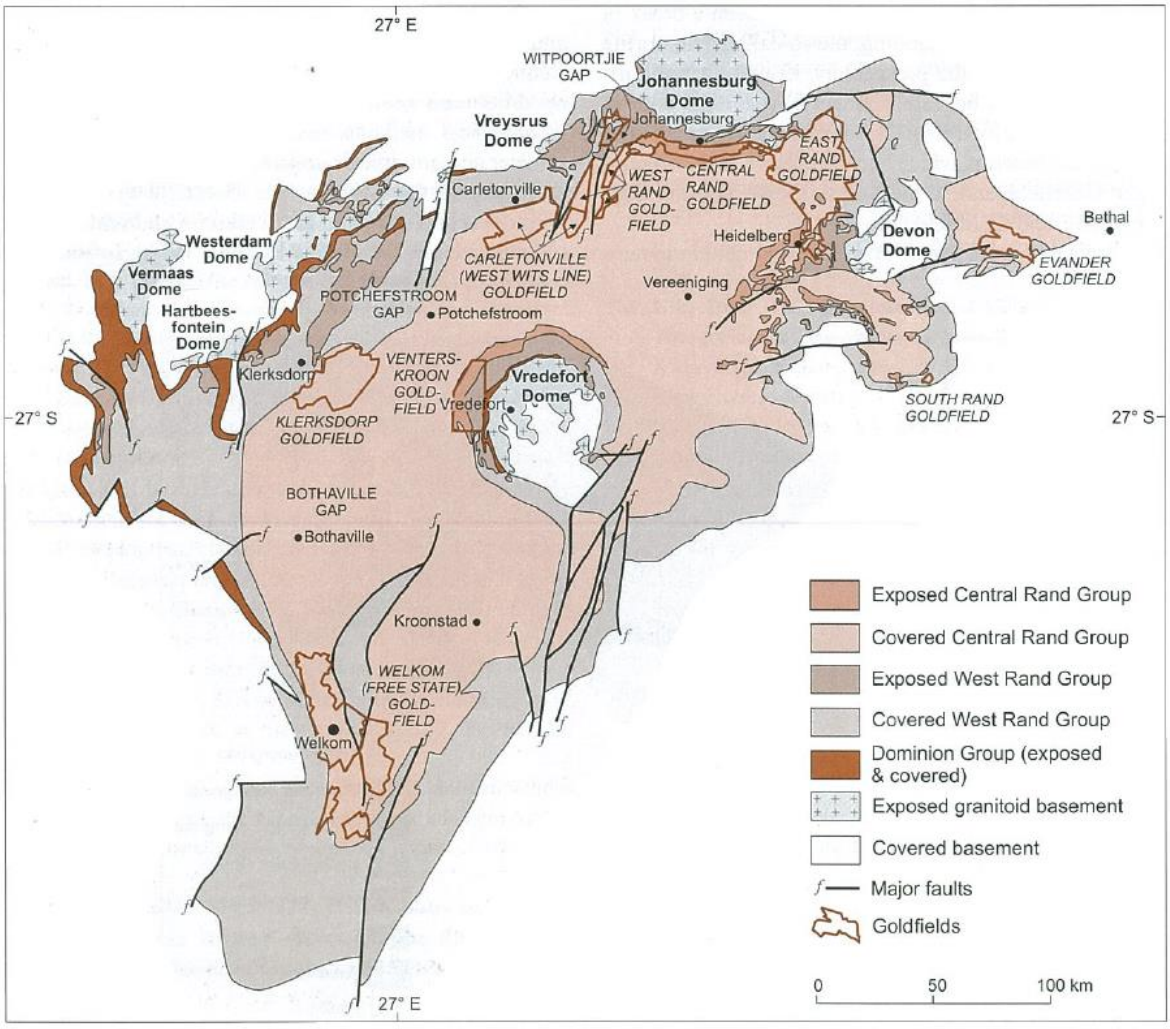

Figure 33: Witwatersrand Basin, with younger geology removed (from McCarthy, 2006)

The succession within which the Witwatersrand Supergroup occurs, is referred to as the Witwatersrand Triad comprising of three prominent geological groups namely:

- Witwatersrand Supergroup
- Transvaal Supergroup
- Ventersdorp Supergroup

4.5.1.1 Witwatersrand Supergroup

As a result of extensive mining in the Witwatersrand Basin, the geology of the Witwatersrand Supergroup has been well exploited and documented. The Witwatersrand Basin consists of a thick sequence of shales, quartzites and conglomerate units. According to Mellor (1917), the Witwatersrand Super Group is divided into two distinct groups; (1) West Rand Group, distinguished by arenaceous and argillaceous sediments; and (2) Central Rand Group, dominated by quartzite with auriferous conglomerate layers. The transition between these two groups is gradational and diachronous, younging in a SE direction. Overall the Witwatersrand Supergroup displays a coarsening-upwards profile (SACS, 2006).

The West Rand Group is divided into three distinct subgroups namely Hospital Hill, Government Reef and Jeppestown. The lithology in these subgroups consists mainly of shales with intermittent units of quartzites, banded ironstones, tillite and lava.

The Central Rand Group is divided into two subgroups namely Johannesburg Subgroup and Turffontein Subgroup. Lithology in these groups is dominated by quartzites with interbedded fragments of conglomerate reefs. An argillaceous zone of shales known as the Booysens Shale, occurs between the two subgroups, separating the Johannesburg Subgroup from the Turfontein Subgroup.

4.5.1.2 Ventersdorp Supergroup

Rock units of the Witwatersrand are overlain by younger layers of the Ventersdorp Supergroup. The Ventersdorp Supergroup is composed mainly of andesitic lavas and related pyroclastics, however acid lavas and sedimentary intercalations also occur. The Ventersdorp Supergroup consists of the Platberg Group and the Klipriviersberg Group. The Klipriviersberg group is most prominent in the study area, and consists of the Alberton and Westonaria formations. Lithology of the Ventersdorp Super Group is exposed to the southeast Panvlakte-Roodepoort fault, extending eastwards Central Rand (Tucker and Viljoen, 1986).

4.5.1.3 Transvaal Supergroup

Sedimentary deposits of the Transvaal Supergroup overlie the Ventersdorp lava units. The Transvaal Super Group sedimentary rocks mainly include the Malmani Dolomite, which dominates the geology at the Cooke Section (Tucker, 1980). The geological formations most prominent in the Transvaal Supergroup include:

- Timeball Hill Formation
- Hekpoort Formation
- Oaktree Formation
- Black Reef Formation
- Monte Christo Formation

Lithology in the Timeball formation consists mainly of quartzite's, shales and siltstone. Over time, weathering of the shale has resulted in reddish to grey silty sand and clay in the area. A large portion of the rock units in the lower layers are covered with younger sedimentary rocks.

The Hekpoort Formation consists mainly of andesite lava units. The landscape in this area is described as uneven, attributed to scattered lava outcrops. The origin of the topographic features present in the area is believed to be a result of quick erosion of soft tuffaceous sediments that are interbedded between the amygdaloidal lava flows. Weathering of the Hekpoort andesite units have resulted in dark to reddish-brown sands containing quartzite fragments (SRK Consulting, 2013).

The Oaktree formation consists of dark-grey dolomitic units interbedded with carbonaceous shales which decrease in thickness from the base of the formation upwards. The Black Reef Formation consists mainly of calcareous argillaceous and arenaceous sediments.

The Monte Christo Formation following on the Oaktree formation consists mainly of dolomitic units with alterabting cherts. The estimated thickness of these dolomites is 700m, with a 1.5m thick chert layer consisting of thin manganese layers towards the base of the formation. According to Parsons and Killick (1985), layers of crystalline dolomite, calcerous shales and fine white dolomites with chert fragments also occur in the sequence.

The Malmani Subgroup dolomite of the Chuniepoort Group has a thickness of 200 m to 1500 m (Parsons and Kallick, 1985). The geological setting is complicated by numerous dykes and faults occurring in this area (Tucker and Viljoen, 1986). The richest gold and urainium deposits in the Central Rand Group occur toward the northwestern parts of the Witpoortjie Horst, which is bounded by two distinct faults namely Witpoortjie and Panvlakte-Roodepoort.

4.5.2 Study area geology

The Cooke 4 mine is located in the West Rand Group. Mineral contents of this group are hosted in the Central Rand Group within the upper Witwatersrand Super Group. The area contains a 6 km broad stratigraphic sequence consisting predominantly of quartzites and shale's - known as the Booysens Shale Formation. This shale formation is alternated with volcanic rock material (Tucker and Viljoen, 1986). The mine is situated on the southern slope of the anticline, located between the two most prominent ridges of Gatsrand on the Transvaal Highveld. The Gatsrand ridge consists primarily of quartzitic ridges, tending roughly east-west to form the most prominent features (SRK Consulting, 2013).

Gold deposits are mainly hosted by the Upper Elsburg and Middle Elsburg reefs of the Mondeor Formation, whilst the majority Uranium is primarily found in the Middle Elsburg Reef (SRK Consulting, 2013). The two primary gold-bearing ore bodies, the Upper Elsburg and Middle Elsburg reef, are approximately 400 m apart (SRK Consulting, 2013). Figure 34 shown a conceptual model of the local geology and structures at the Cooke 4 under ground operations.

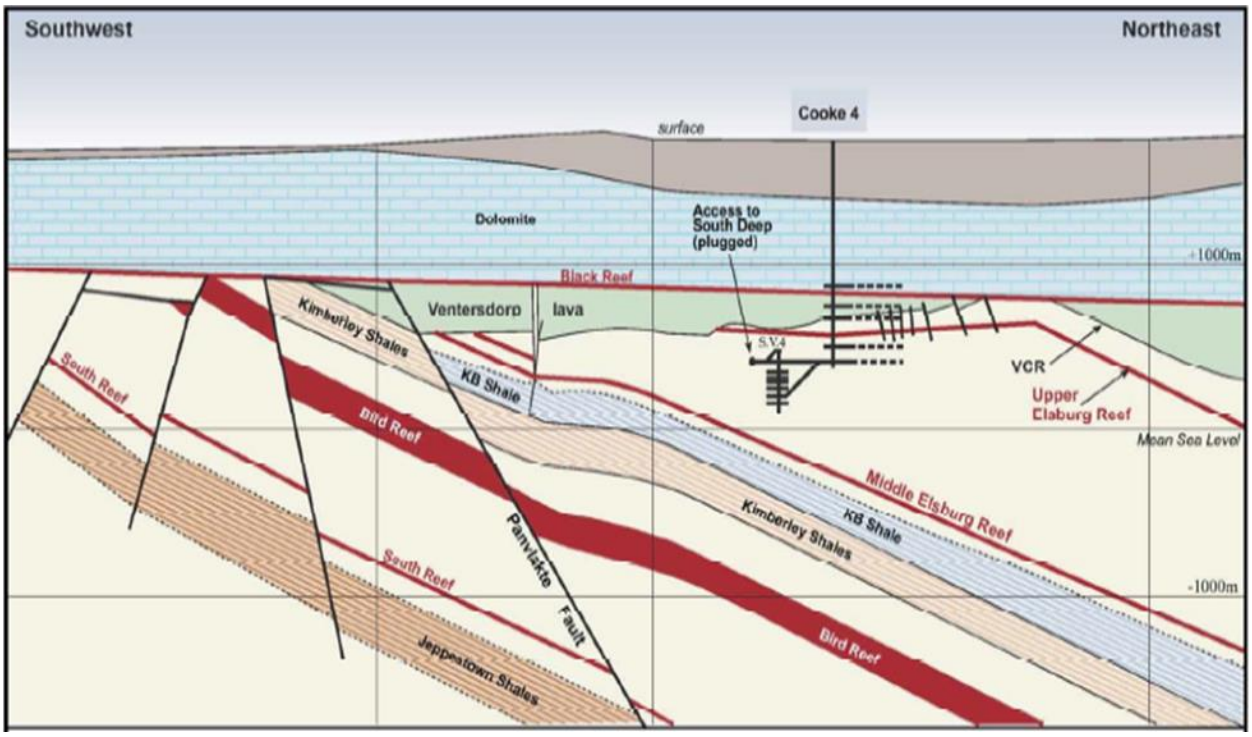

Figure 34: Local geology and structures of the Cooke 4 underground operations (SRK Consulting, 2013).

The study area comprises the Gemsbokfontein-West compartment. The western boundary is the Gemsbokfontein dyke and the eastern boundary is the Magazine dyke. The northern boundary is the Panvlakte dyke and is southern boundary was chosen on the geology. Figure 35 and Figure 36 shows the geology and aerial magnetic survey respectively for the study area.

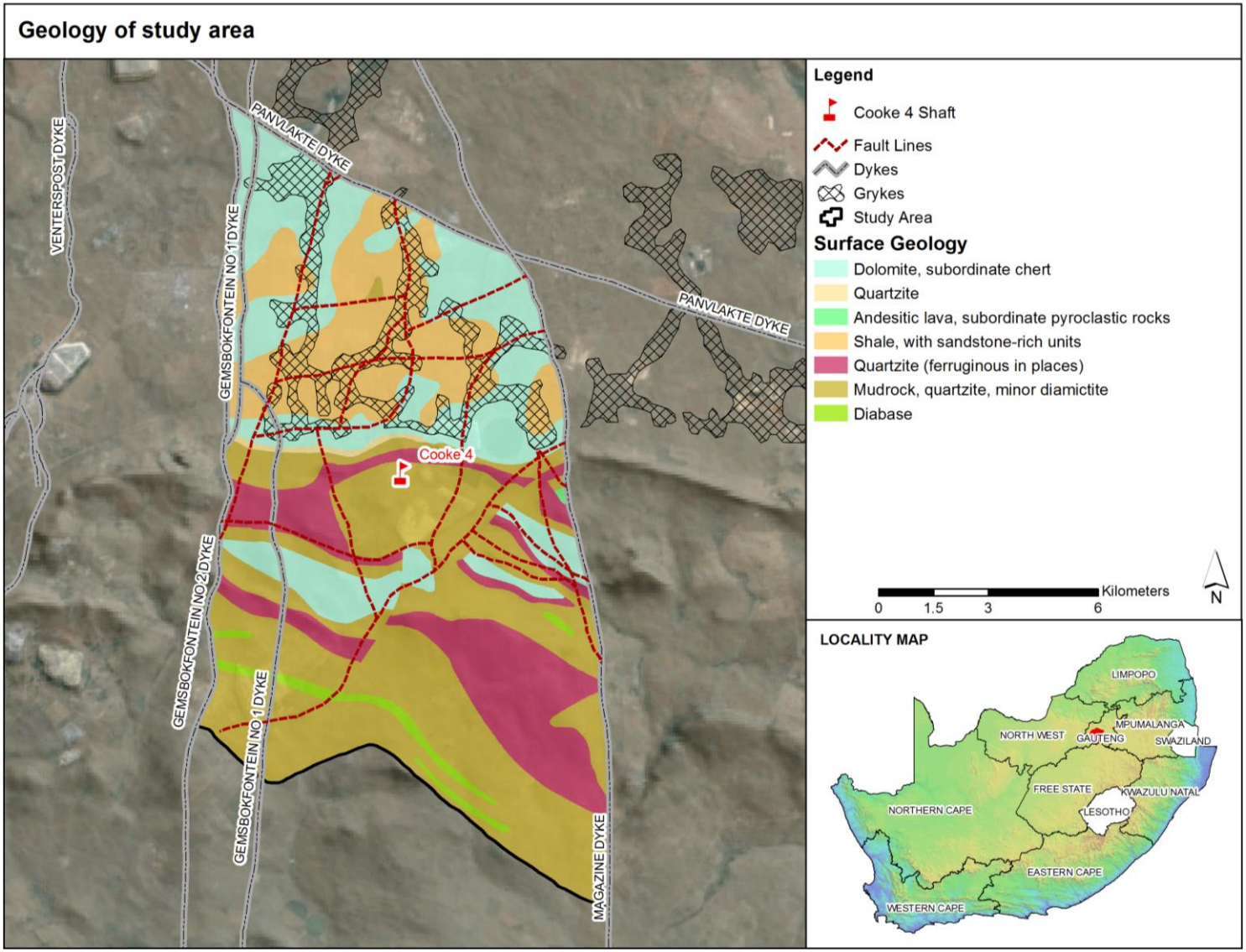

Figure 35: Surface geology of the study area

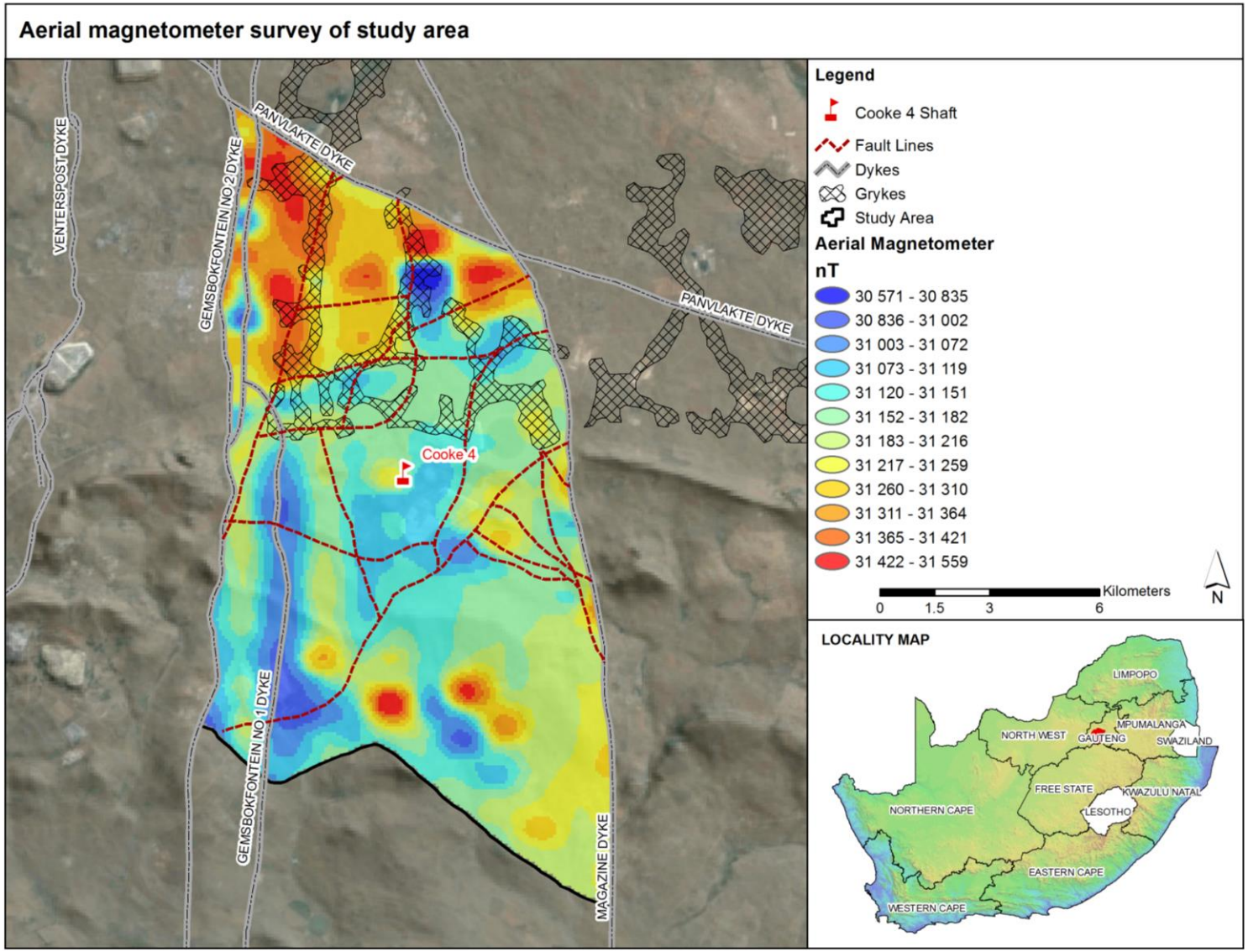

Figure 36: Aerial magnetic survey of the study area

The dolomites are close to surface in the northern part of the study area and then dip beneath the Transvaal Supergroup in a Southern direction as shown in Figure 37.

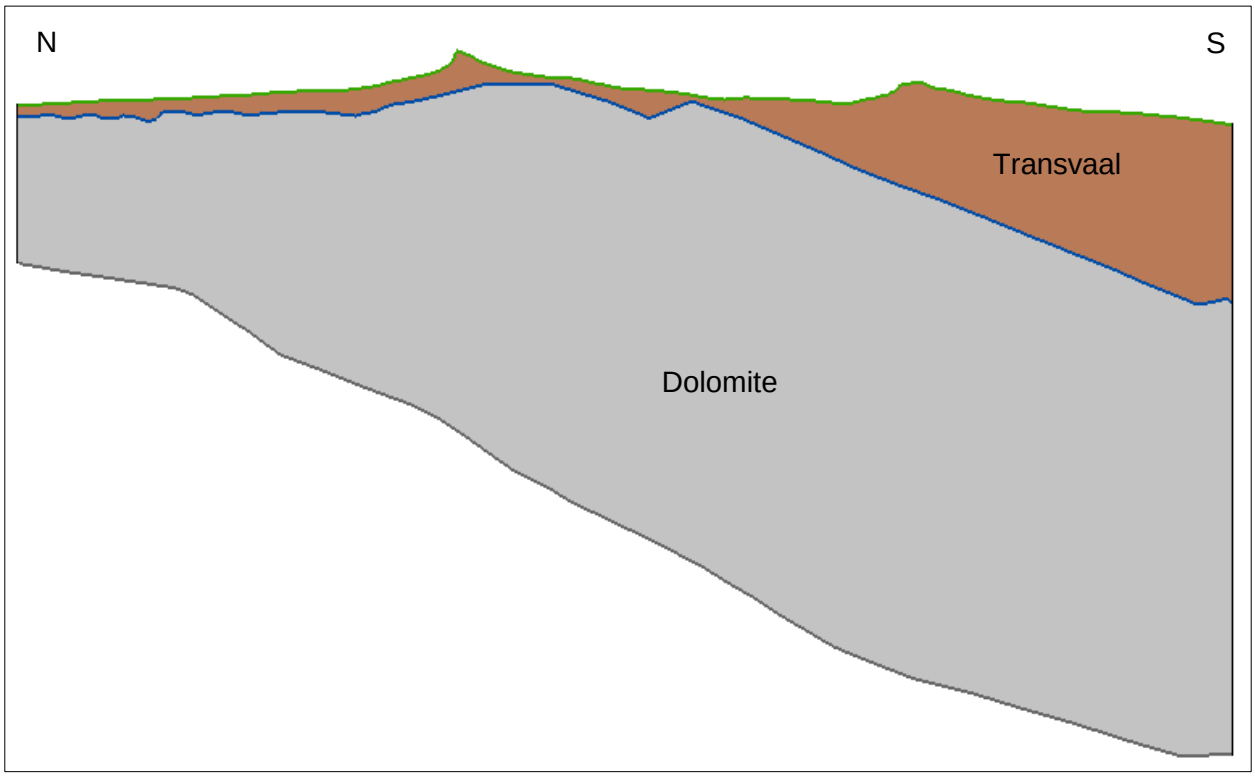

Figure 37: North-south cross section through study area

The Grykes identified in during a gravity survey in the northern part of the study area are areas where the dolomite is very highly weathered and act as preferred flow paths. Based on regional gravity and resistivity surveys that were conducted in 2011, faulting occurs between 0 and 100 m below the top of the dolomites, with some individual fractures between 100 m and 180 m below the top of the dolomites. However, the surveys indicated that the latter are considered to be relatively deep below the surface and it is likely that the weight of overlaying ithologies will eventually close the fractures, effectively decreasing the transmissivity of the dolomitic aquifer to near zero. As a result of fluctuating water levels within the dolomites, a number of sinkholes have formed over the years. Existing sinkholes appear to have been stable since the 1990 (SRK Consulting, 2013).

4.6 Geohydrology

4.6.1 Aquifer description

Groundwater occurrences within the Gemsbokfontein-West compartment are mainly restricted to 3 aquifer types:

i. An upper aquifer associated with weathered sedimentary deposits in the Transvaal Formations;
ii. A lower aquifer associated with less weathered, but fractured sedimentary deposits in the Transvaal Formations; and
iii. Dolomite aquifer

The groundwater occurrence as obtained from the geohydrological map series of South Africa is shown in Figure 38.

4.6.1.1 Upper weathered and lower fractured aquifers

Groundwater occurrence in this aquifer is mainly restricted to the weathered sedimentary deposits of the Timeball Hill and the lava units of the Hekpoort Formations where rock material is exposed to the surface. Although these formations are not considered as sustainable aquifer types, high water yields are expected where fractures intersect. Previous studies conducted by SRK Consulting (2013) suggested that open fractures seldom occur deeper than 60 m as the weight of overlaying material will over time close deeper fractures that will in return decrease transmissivity potential. The aquifer base consists of impermeable quartzite, shale and lava formations, and the top of the aquifer is presented by the surface topography. Although the upper weathered and lower less weather aquifers are hydraulically connected, confining layers of clay and shale often separate the two aquifers, classifying the aquifers as semi-confined.

4.6.1.2 Dolomite aquifer

The dolomite aquifer yields the largest portion of groundwater and is generally associated with sustainable groundwater abstraction. The study area is underlain by the partially dewatered Gemsbokfontein-West groundwater compartment. Rock material in this aquifer is basically impermeable accounting for practically no effective porosity. Historically, the dolomite strata in the aquifer have been exposed to numerous karstification and erosion periods. Potential groundwater exploitation in this aquifer depends mainly on the extent of groundwater drainage and leaching of percolated rainfall into the aquifer, and the ability of the aquifer to yield large quantities of water and sustain abstraction. During dissolution processes, the carbonates are removed from the dolomite, subsequently leaving silica, manganese, and iron oxides behind. This residual material is compressible with a low density and high void volume – consequently creating the potential of cave formation. Fault zones also have a high weathering potential prone to forming ground water conduits. Due to lithostratigraphical control on leaching of dolomites, an extensive cover of residual debris and younger sedimentation occurs within the aquifer, underlain by karstified dolomites. Extensively karstified dolomites occurring near the surface has a large storage potential.

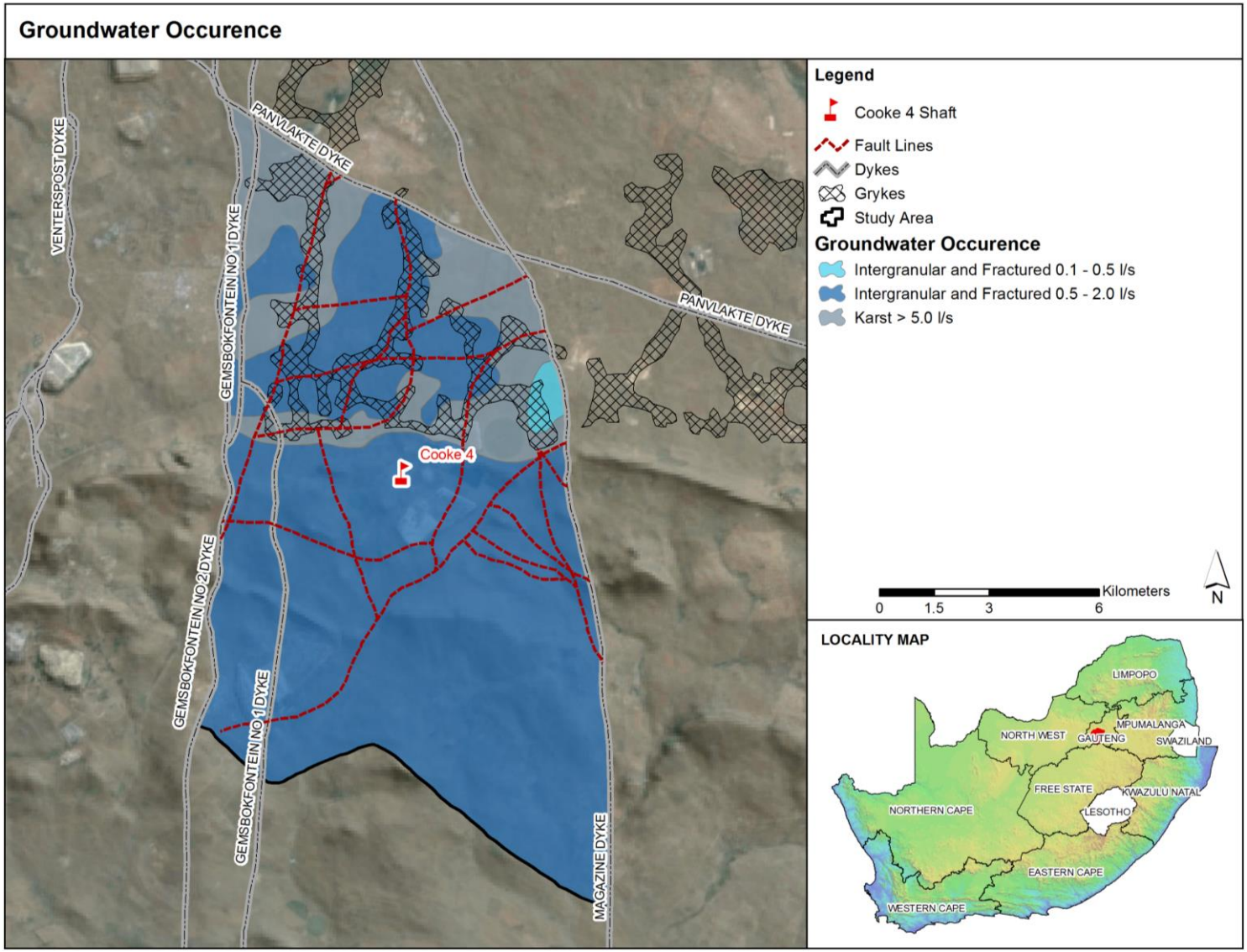

Figure 38: Groundwater occurrence in the study area

4.6.2 Recharge

Parsons (1989) mapped the dolomitic outliers to the south of Gatsrand, indicating that dolomitic outliers are hydraulically connected with the Gemsbokfontein compartment as these dolomites are continuous beneath the overlaying Timball Hill rock formations. The Gemsbokfontein-East sub-compartment has not been dewatered up to date, however the Gemsbokfontein-West sub-compartment has been partially dewatered. Previous studies conducted by Johan Fourie and Associates Consulting (2011) concluded that the Gemsbokfontein Groundwater Compartment is recharged by various sources including:

- Roughly 15 % attributed to MAP;
- Artificial recharge into the aquifer after surface water diversions from Westonaria and Simunye residential areas toward the Wonderfonteinspruit (situated in the north-western corner of the Gemsbokfontein Compartment);
- Artificial recharge from the Kleinwesrietspruit flowing eastwards from the Peter Wright dam, and the Leeuspruit flowing toward the south west;
- Approximately 6 Mℓ/d leakage from the Magazine Dyke; and
- Approximately 9 Mℓ/d leakage from the Panvlakte Dyke.

Areas of subsidence/sinkholes is visible in the direct vicinity of the mining operation which could also contribute to direct recharge of the subsurface as shown in Figure 39.

Figure 39: Subsidence/sinkhole in vicinity of mining operations

Groundwater recharge figures for the Gemsbokfontein groundwater compartment (Hodgson *et al*., 2001) are summarised in Table 10 and are expressed as a percentage of MAP. Brendenkamp has quoted the highest recharge figure and no other literature could be found substantiating it.

Table 10: Recharge estimations for dolomitic Gemsbokfontein compartment

Source	Recharge (%)
Fleisher (1981)	12.8
Wolmerans (1978)	5.3
Bredenkamp *et al.* (1995)	27.0
Enslin & Kriel (1968)	7.5
Average	**13.15**

The GRAII recharge figures for the quaternary catchments comprising the study area are presented in Table 11. The GRAII recharge figures, which are based on the chloride mass balance method, are comparable to that reported by Wolmerans and Enslin & Kriel in Table 10. It is expected that direct recharge on surface dolomite would be represented by the higher values (± 13%) and that of direct recharge on the Transvaal formations would be represented by the lower values (± 7%).

Table 11: Recharge estimations for dolomitic Gemsbokfontein compartment (WRC, 2005)

Quaternary	Recharge (%)
C22A	6.7
C22H	6.2
C22J	6.6
C23D	7.4
Average	**6.73**

4.6.3 Groundwater level

Borehole water levels were obtained for the study area and historic and current water levels were compared with each other as shown in Figure 40.

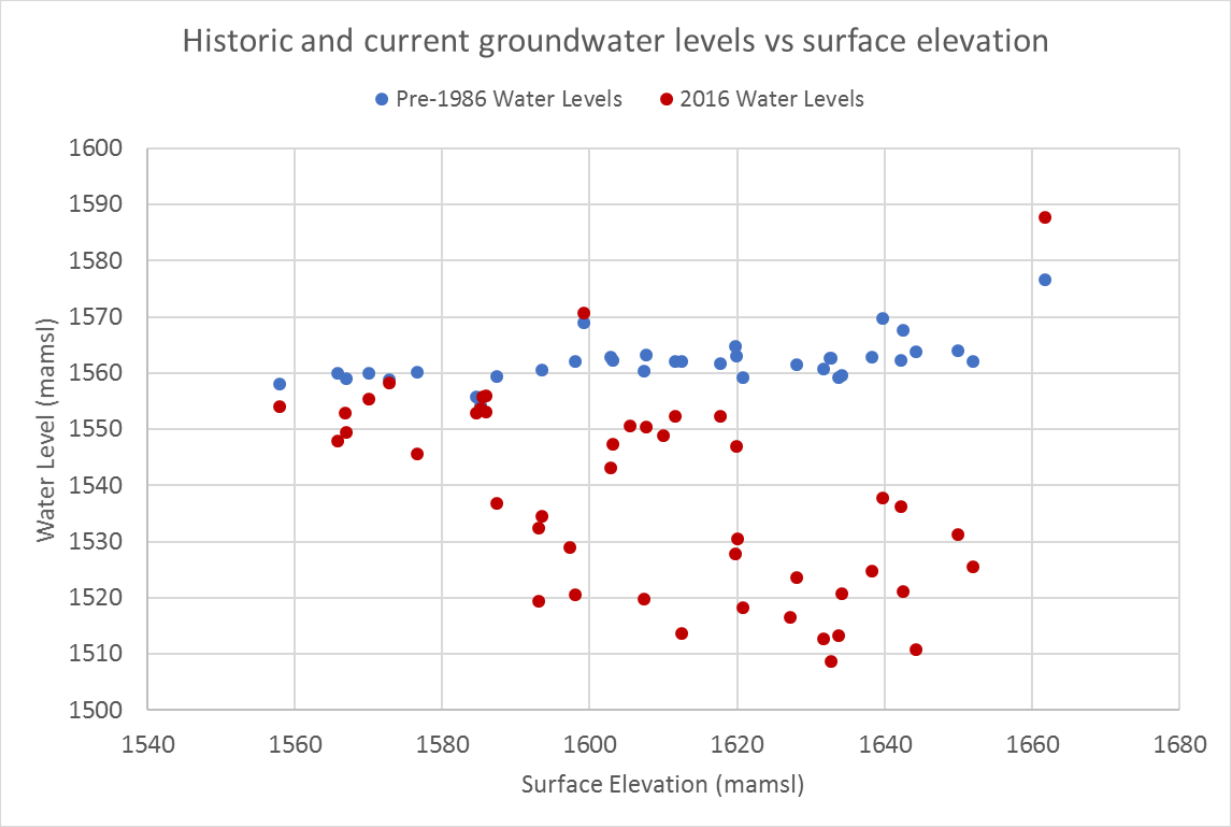

Figure 40: Comparison of historic and historic groundwater levels cross the study area

A distinct drop in water level is observed over time due to the dewatering that is taking place within the compartment (Figure 41). There exists an extremely low correlation between the measured water levels and the surface topography. The historic water levels have a water table that doesn't vary with topography which is typical for what is expected within a dolomite aquifer.

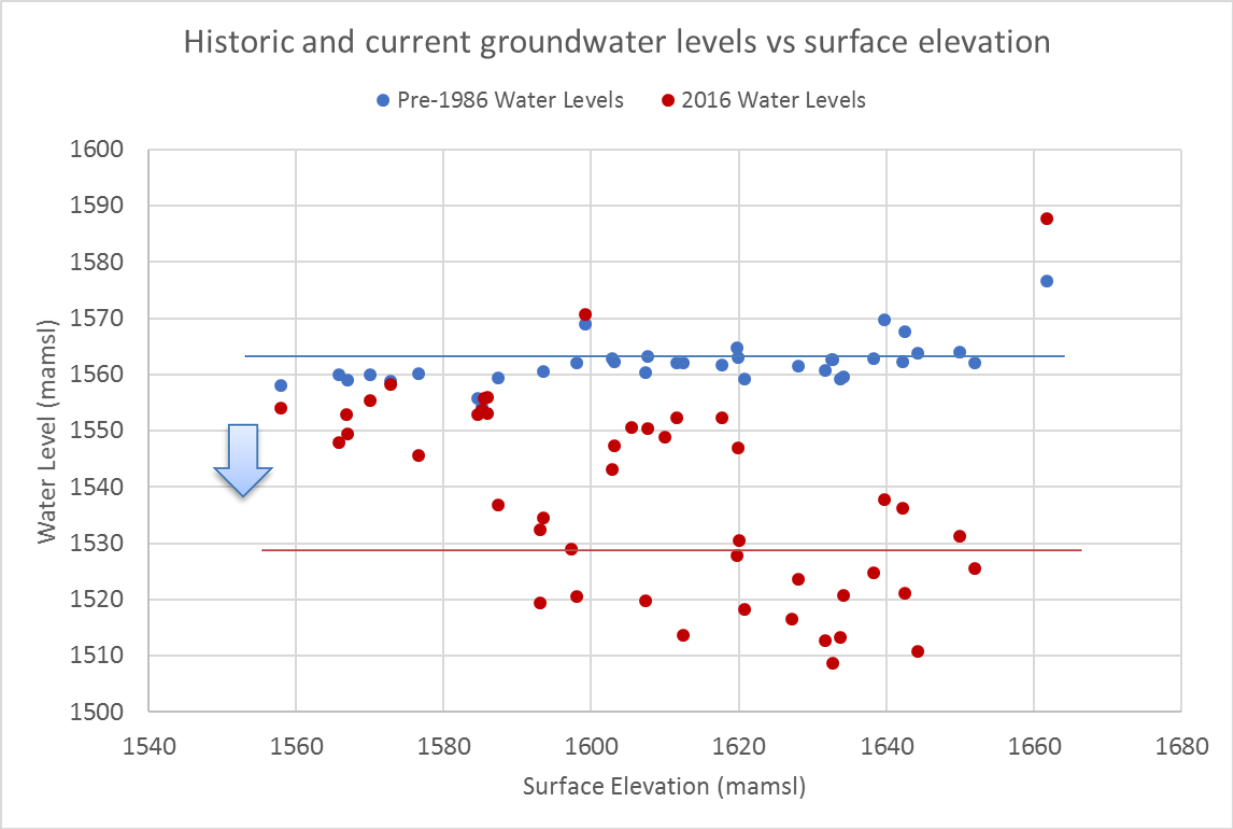

Figure 41: Comparison of historic and current water levels across the study area

Water contained in the shallow upper aquifer is attributed to infiltrating rainfall recharge through weathered material, consequently being delayed by the low permeability of underlying dolomite material. Although the low permeability of underlying unweathered material delays the infiltration of rainfall recharge, a proportion of the water contained in the upper aquifer still migrates through to eventually recharging the lower aquifer.

A significant portion of the groundwater levels were found to lie within the shallow weathered aquifer (SRK Consulting, 2013). The largest volume of water stored in the main dolomitic aquifer occurs in the top 100 m below the water level. The effective base-depth of this aquifer ranges between 150 m and 200 m below the surface. The underlying dolomites has an approximated thickness of 900 – 1100m, however it is unlikely that large amounts of groundwater flow occur below this depth, except along intersecting structural conduits to the underground mine workings (SRK Consulting, 2013).

Making us of Kringing interpolation, a groundwater level map based on the current groundwater levels were constructed and the results are shown in Figure 42. There is a clear cone of depression in the vicinity of the Cooke 4 shaft which is consistent of what is expected with the mine dewatering that is taking place.

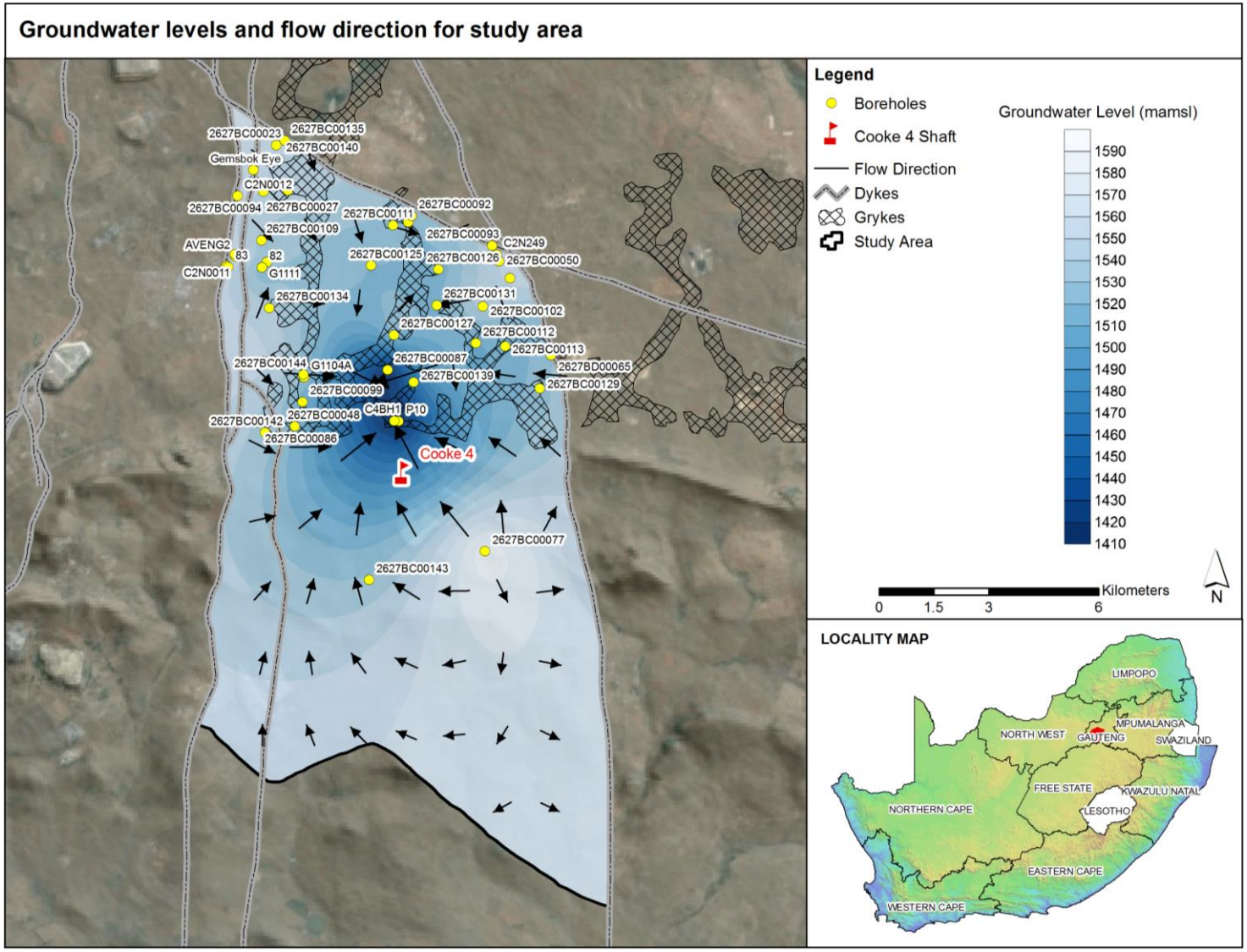

Figure 42: Groundwater level map of study area

5 METHODOLOGY

The methodology consists of the following sections which will be discussed in more detail in the sections that follow:

- Climatic data collection
- Field measurements
- Model development
- Water balance modelling

5.1 Climatic Data Collection

5.1.1 Temperature Data

Hourly temperature data were obtained from the SAWS from the closest weather station to the study area. The historic and recorded temperature during the course of the field measurements are required in the development of an evapotranspiration model.

5.1.2 Radiation and Vapour Data

Regional radiation and vapour data were obtained from the South African Atlas of Agrohydrology and Climatology (Schultze, 2006) in the absence of measured data at the study area. Once again, these variables are required in the development of an evapotranspiration model.

5.2 Field Measurements

5.2.1 Experimental Site Selection

Native vegetation types in the study area consists of open savannah type grasslands, with sparse distribution of shrubby Karoo and thorn trees in areas where minimal mining influence have occurred. However, due to significant mining influence in the area, the dominating vegetation in the area includes indigenous *Eucalyptus* species. Although there are no accurate planting records of trees in the area, it is believed that *Eucalyptus* species were established as wind breaks in the 1970's, during the development of the TSFs. Site selection were based on sites which have *Eucalyptus* species present and representative trees per site were chosen for measurements.

5.2.2 Representative Vegetation Assessment

In order to include a range of trees pertaining similar characteristics, thus anticipated to be of similar age groups, tree height and stem diameter measurements were taken. Measurements

and characteristic surveys were conducted independently over the experimental sites. Representative trees were selected at each site for measurement and assessment purposes.

5.2.2.1 Tree Height, Stem Circumference and Crown Diameter

A non-destructive field method was conducted to log tree characteristics, allowing the data of each site to be combined for analysis. Tree species were identified to ensure homologous data were collected. Following identification, diameter at breast height (DBH)[2], mean height and crown diameter was measured to include trees of comparable size, thus anticipated to include trees of similar age. Measurement of tree diameter and tree height with the use of a reference stick is illustrated in Figure 43.

Figure 43: Measurement of stem diameter and tree height

[2] Diameter at breast height (DBH) is the standard for measuring tree diameter, referring to tree diameter measured at 4.5 feet (± 137 cm) above the ground.

5.2.2.2 Canopy Volume and Crown Projected Area

The canopy volume was determined using the method described by Verma *et al.,* (2014), based on manual measurements of crown diameter and canopy height, assuming an appropriate 3D crown shape. Canopy volume was determined using the following volume formulation:

$$V_C = MH_C D_C \quad (1)$$

where,

V_C = *Volume of canopy (m^3)*
H_C = *Height of canopy (m)*
D_C = *Diameter of crown (m)*
M = *Multiplier determined by crown shape*

The crown projected area was determined using the following equation adapted from Verma *et al.* (2014):

$$A_C = \frac{\pi D_C^2}{4} \quad (2)$$

where,

A_C = *Crown projected area (m^2)*
D_C = *Crown diameter (m)*

5.2.2.3 Leaf Area and Leaf Count

Leaf samples were collected and measured in order to determine an average leaf length and width for the estimation of leaf area. Leaf count were determined by counting the number leaves within a m^3 volume as shown in Figure 44.

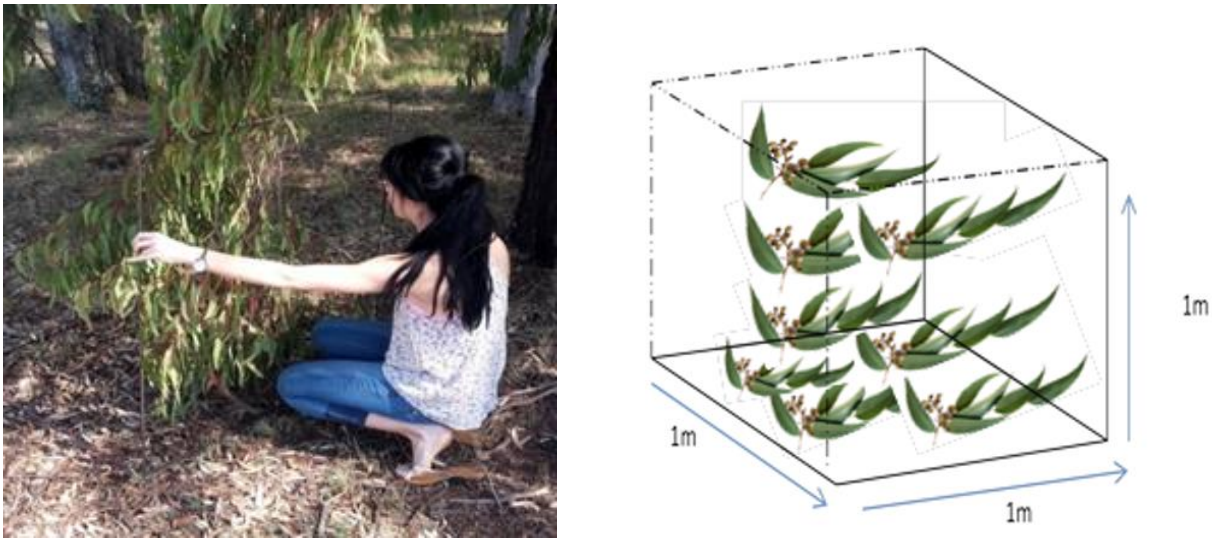

Figure 44: Leaf count making use of quadrant count

5.2.2.4 Effective Leaf Area per Square Meter

The effective leaf area per square meter can be calculated by making use of the following formula:

$$A_{Leff} = \frac{V_C C_L A_L}{A_C} \quad (3)$$

where,

A_{Leff} = *Effective leaf area per m²*
V_C = *Volume of canopy (m³)*
C_L = *Count of leaves per m²*
A_L = *Average area of individual leaves (m²)*
A_C = *Projected crown area (m²)*

5.2.3 Stomatal Conductance Measurements

Stomatal conductance measurements together with leaf temperature were performed on a set of 8 leaves per tree, distributed throughout the outer part of the lower and mid canopy, using a handheld Delta-T AP4 Leaf Porometer as shown in Figure 45. Porometer measurements were run until four readings per leaf were obtained. Conductances were measured at 15-minute intervals within a 3-hour period. The AP4 Leaf Porometer measures the rate of Relative Humidity (RH) increase in a chamber clamped to a leaf surface; as water vapour is released through the stomata during transpiration, the RH in the chamber rises. A rapid rise in the chamber RH is an indication that the stomata are open and provides measurements of water vapour loss from a leaf.

Figure 45: Measuring stomatal conductance through Delta-T AP4 Leaf Porometer

5.3 Evapotranspiration modelling

An ET model was formulated based on the field observations of *Eucalyptus* trees. The formulated field model is based on temperature observations obtained from the closest weather station and was calibrated to field readings of leaf temperature and hourly stomatal conductance. Hourly measurements, for a duration of 12 hours, were conducted to record leaf temperature and stomatal conductance at a control site. The recorded data was used to determine the relationship between leaf temperature and stomatal conductance and this relationship was used to formulate an evapotranspiration model to predict ET based on air temperature.

The model results were then compared to the FAO Penman-Monteith reference crop model and the Shuttleworth-Wallace ET model to ensure that the field data model results are realistic and comparable to that of existing models.

The Penman-Monteith model calculates ET from a hypothetical crop with an assumed crop height of 0.12 m, a fixed canopy resistance of 70 s/m and albedo of 0.23, which closely resemble ET from an extensive surface of green grass cover of uniform height, actively growing, completely shading the ground and not short of water.

The Shuttleworth-Wallace model is a variation of the Penman-Monteith model which allows the specification of landcover types based on the parameters presented in Table 12.

Table 12: Landcover parameters for Shuttleworth-Wallace model (from Zhou et al.,2006)

Code	Type	α_m	LAI_{max}	h_c (m)	w_{max} (m)	F_{cl}	$r_{ST\ min}$ (s m^{-1})	$NDVI_{98\%}$	d_{rz} (m)	z_{0g} (m)
1	Evergreen needleleaf forests	0.16	5.5	17.0–17.0	0.001	1.0	150	0.689	2.5	0.020
2	Evergreen broadleaf forests	0.20	7.0	30.0–30.0	0.05	0.0	150	0.611	2.5	0.020
3	Deciduous needleleaf forests	0.15	3.3	17.0–17.0	0.001	1.0	150	0.689	2.5	0.020
4	Deciduous broadleaf forests	0.18	7.0	25.0–25.0	0.08	0.0	150	0.721	2.5	0.020
5	Mixed forests	0.17	5.7	20.0–20.0	0.04	0.5	150	0.721	2.0	0.020
6	Closed shrublands	0.20	4.6	1.5–1.5	0.01	0.0	150	0.674	1.0	0.020
7	Open shrublands	0.15	3.0	1.0–1.0	0.01	1.0	100	0.674	1.0	0.020
8	Woods savannas	0.20	1.5	0.8–0.8	0.01	0.5	180	0.611	1.0	0.020
9	Savannas	0.25	0.9	0.1–0.8	0.01	0.8	120	0.674	1.0	0.020
10	Grasslands	0.23	1.8	0.05–0.8	0.01	0.0	115	0.674	0.5	0.010
11	Permanent wetlands	0.10	6.0	0.05–1.0	0.01	0.0	65	0.674	1.0	0.010
12	Croplands	0.20	7.0	0.0–0.8	0.01	0.0	90	0.674	0.7	0.005
13	Urban and built-up	0.18	–	–	–	0.0	0	0.674	0.001	0.020
14	Cropland/natural vegetation mosaic	0.20	6.5	0.1–0.8	0.01	0.5	120	0.674	1.0	0.010
15	Permanent snow and ice	0.70	–	–	–	0.0	0	0.674	1.3	0.001
16	Barren or sparsely vegetated	0.15	0.3	0.05–0.8	0.01	1.0	120	0.674	1.0	0.001
17	Water bodies	0.08	–	–	–	0.0	0	0.674	1.3	0.001

Code is IGBP number for vegetation type, α_m is maximum albedo (full cover), LAI_{max} is maximum leaf area index, h_c is vegetation height (a function of LAI), w_{max} is maximum vegetation leaf width, F_{cl} is fraction of clumped vegetation, $r_{ST\,min}$ is minimum stomatal resistance of individual leaf, d_{rz} is root depth, z_{0g} is roughness length of substrate ground.
Perennial vegetations: codes from 1 to 8, and annual vegetations: others; tall vegetations: codes from 1 to 5, and short vegetations: others; root depth for codes 15 and 17 represents the average water depth.

Detail regarding the formulation of the Penman-Monteith and the Shuttleworth-Wallace model is available in Appendix A and Appendix B respectively.

5.3.1 Formulation of the Field Model

The enzymes that catalyze the photosynthetic reactions are all strongly temperature dependent, so leaf temperature can play an important role in determining the assimilation rate for a leaf (Campbell and Norman, 1998). In turn stomatal conductance determine assimilation rate and assimilation rate determine conductance (Campbell and Norman, 1998). It is therefore expected that a correlation can be identified between leaf temperature and stomatal conductance.

Air temperature and leaf temperature are related through some function as shown in Figure 46. Being able to calculate leaf temperature from air temperature facilitates the calculation of stomatal conductance through the relationship established between leaf temperature and stomatal conductance during field observations.

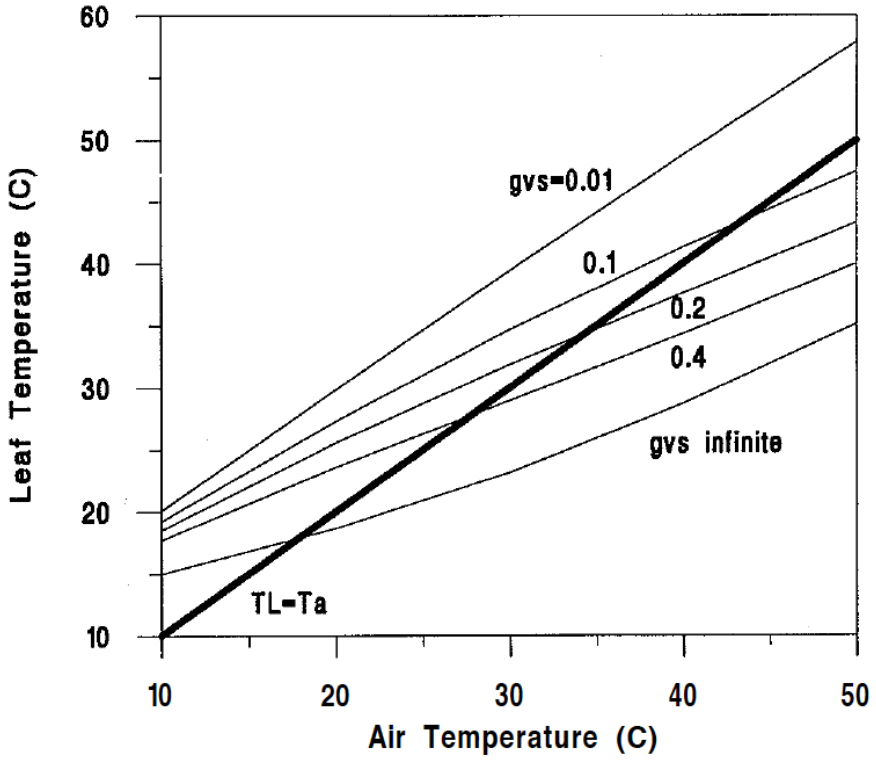

Figure 46: Leaf temperature vs air temperature for different stomatal conductances (Campbell and Norman, 1998)

The estimation of leaf temperature is calculated using a linearization technique adopted from Campbell and Norman (1998):

$$T_L = T_a + \frac{\gamma^*}{\Delta/_{P_a} + \gamma^*}\left[\frac{R_{ni}}{gH_r c_p} - \frac{D}{P_a \gamma^*}\right] \quad (4)$$

$$\gamma^* = \frac{\gamma g H_r}{g_v} \quad (5)$$

$$g_{H_r} = g_{H_a} + g_r \quad (6)$$

$$g_{H_a} = 1.4 \times 0.135\sqrt{\frac{u}{d}} \quad (7)$$

$$g_v = 1.4 \times 0.147\sqrt{\frac{u}{d}} \quad (8)$$

$$g_r = 0.002T_a + 0.1565 \quad (9)$$

$$e_s(T_a) = 0.6385e^{0.0623T_a} \quad (10)$$

$$e_a = 0.611e^{\left(\frac{17.502T_a}{T_a+240.97}\right)} \quad (11)$$

$$D = e_s(T_a) - e_a \quad (12)$$

$$R_{ni} = R_{abs} - \varepsilon_s B \quad (13)$$

where,

T_L	=	*Leaf temperature in (^0C)*
T_a	=	*Air temperature in (^0C)*
D	=	*Vapour deficit of the atmosphere (kPa)*
Δ	=	*Vapour pressure gradient (Pa/^0C)*
ε_s	=	*Surface emissivity*
P_a	=	*Atmospheric pressure = 101.3 kPa*
c_p	=	*Specific heat of air = 29.3 J/mol/^0C*
$e_s(T_a)$	=	*Saturation of vapour pressure (kPa)*
e_a	=	*Vapour pressure of air (kPa)*
g_{Hr}	=	*Net radiation (mol/m^2/s)*
g_{Ha}	=	*Boundary layer conductance (mol/m^2/s)*
g_v	=	*Vapour conductance (mol/m^2/s)*
g_r	=	*Radiative conductance (mol/m^2/s)*
γ	=	*Psychrometric constant: 6.66x10^{-4} $^0C^{-1}$*
d	=	*Characteristic leaf dimension*
u	=	*Wind speed (m/s)*
R_{ni}	=	*Nett radiation (W/m^2)*
R_{abs}	=	*Absorbed radiation (W/m^2)*
B	=	*Black body emittance (W/m^2)*

5.3.2 Converting Stomatal Conductance to ET

Stomatal conductance measured in mmol/m^2/s were converted to evapotranspiration through the use of the ideal gas law, by calculating the volume of vapour and expressing it as mm/m^2/s. Conversion through the use of the ideal gas law is applicable as stomatal conductance relates to the amount of vapour passing though stomata. The formulation for the ideal as law is as follow:

$$V = \frac{nRT}{P} \qquad (14)$$

where,

V = *Volume (m^3)*
n = *Number of moles*
R = *Gas Constant = 0.082057*
T = *Temperature (K)*
P = *Pressure (atm)*

5.4 Water Balance Modelling

5.4.1 Saturated Volume Fluctuation

The impact of the ET on effective recharge can be modelled through the use of a groundwater balance model, where the ET component will be used to reduce the effective recharge. The model used is the SVF model (Van Tonder and Xu, 2000) which translate a change in volume to a change in water level. The SVF model is formulated as follows:

$$h_i = h_{i-1} + \frac{\sum Q_{in} - \sum Q_{out}}{S_y A} \qquad (15)$$

where,

h_i = *Groundwater level in month i (mamsl)*
h_{i-1} = *Groundwater level in month i-1 (mamsl)*
ΣQ_{in} = *Sum of all inflows to the system e.g. recharge (m^3/d)*
ΣQ_{out} = *Sum of all out outflows e.g. pumping and ET (m^3/d)*
S_y = *Specific yield*
A = *Area (m^2)*

The balancing of the system is achieved through proper selection of recharge and specific yield while achieving the best fit of simulated vs. observed water levels.

5.4.2 Conductance of External Inflows

The SVF model considers an enclosed area where inflows and outflows are explicitly specified. Inflows from neighbouring compartments will vary with a change in head and therefore it is required to make use of a conductance term to properly account for these inflows. Conductance is formulated as follows in terms of Darcy's law:

$$Q = kiA = k\frac{\Delta H}{L}A = C\Delta H \qquad (16)$$

$$C = \frac{k}{L}A \qquad (17)$$

where,

Q	=	*Flow (m^3/d)*
k	=	*Hydraulic conductivity (m/d)*
i	=	*Hydraulic gradient (m/m)*
A	=	*Cross sectional area of flow (m^2)*
L	=	*Length of flow (m)*
ΔH	=	*Head loss (m)*
C	=	*Conductance (m^2/d)*

6 RESULTS AND DISCUSSION

6.1 Climatic Data Collection

6.1.1 Temperature Data

Hourly air temperature data were obtained from the Zuurbekom weather station for the study area for the period 1 January 2015 to 31 December 2015. Refer to Figure 51 for a map depicting the weather station. The monthly hourly average is shown in Figure 47 from 06:00 to 18:00. A relative consistent drop in temperature is observed from January to May, after which a sudden drop is observed for the months of June and July. Temperatures for August are comparable to that of May after which a steady rise in temperature is observed up to December which has the hottest hourly average for 2015.

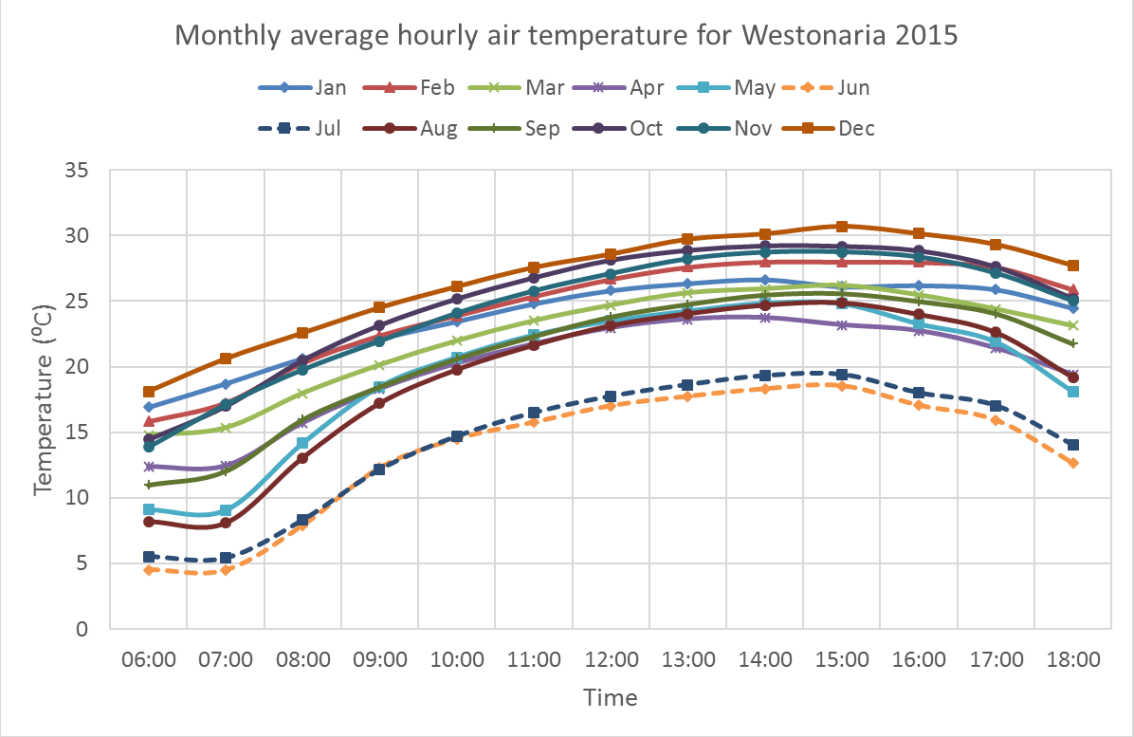

Figure 47: 2015 Monthly air temperature average for Westonaria

6.1.2 Radiation and Vapour Data

The actual vapour pressure and radiation per month for the study area obtained from the South African Atlas of Agrohydrology and Climatology (Schultze, 2006) is shown in Figure 48. It should be noted that the aforementioned atlas offer this type of data only on a large regional scale and is not site specific.

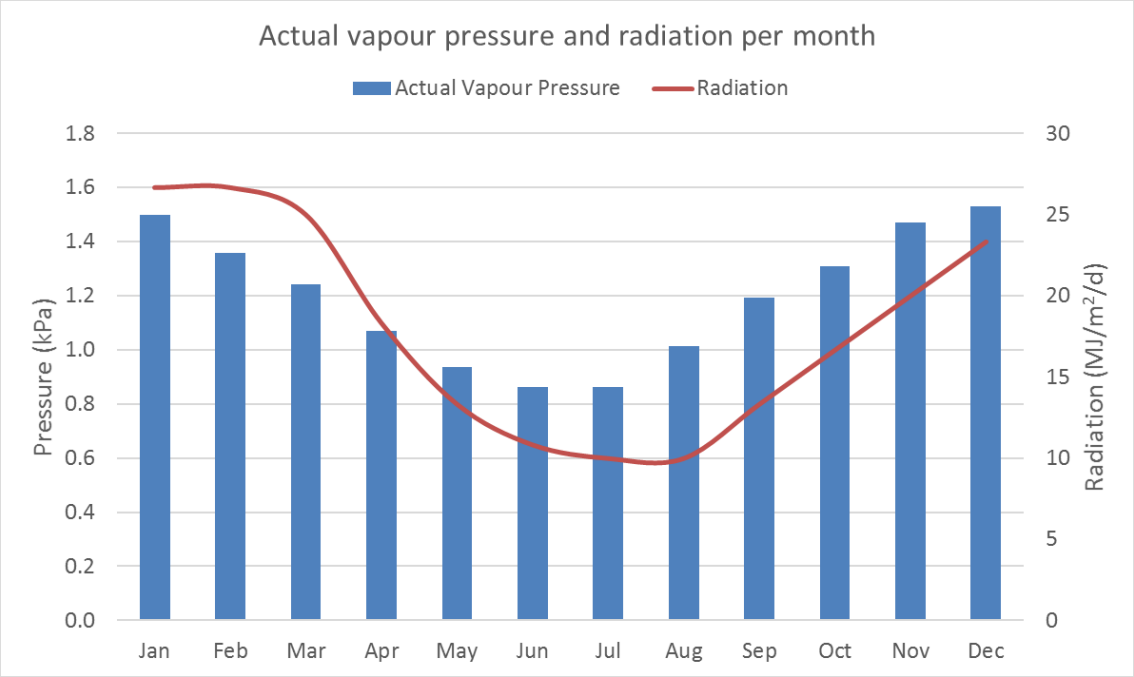

Figure 48: Actual vapour pressure and radiation per month

6.2 Field Measurements

6.2.1 Experimental Site Selection

Due to the sparse distribution of tree communities over the area, as can be seen in the sequence of images presented in Figure 49, experimental sites were selected based on the occurrence of *Eucalyptus* clusters across the study area. Seven experimental sites were identified, and two representative trees within each site were chosen for measurements and assessments. Coordinates of the experimental sites are presented in Table 13 and their localities are shown in Figure 50.

Table 13: Summary of experimental site information

Site	Longitude	Latitude	Altitude (mamsl)
Site 1	27.709358	-26.349950	1656
Site 2	27.711531	-26.346353	1654
Site 3	27.715047	-26.351761	1668
Site 4	27.726375	-26.367247	1686
Site 5	27.728458	-26.377975	1666
Site 6	27.709361	-26.373344	1693
Site 7	27.692806	-26.352053	1660

Figure 49: Patchy distribution of vegetation across the Cooke 4 study area

With the exception of Site 4 all other sites are situated in close proximity of areas with moderate to high agricultural potential.

6.2.2 Representative Vegetation Assessment

During field observations, it was clear that *Eucalyptus* trees that are in closer proximity to tailings dams, were larger in size and grows in denser clusters than trees further away from the tailings dams, thus leading to the conclusion that *Eucalypts* were established as wind breaks in earlier years of tailings dam development, and that clusters further away from tailings have establish in following years after spreading. Due to a significant difference in tree size and stem diameter at different experimental sites, younger trees of smaller height and stem diameter were selected as representative vegetation at the experimental sites, in order to account for stands that have not been established during the 1970's, to be comparable to sites consisting of mostly younger trees.

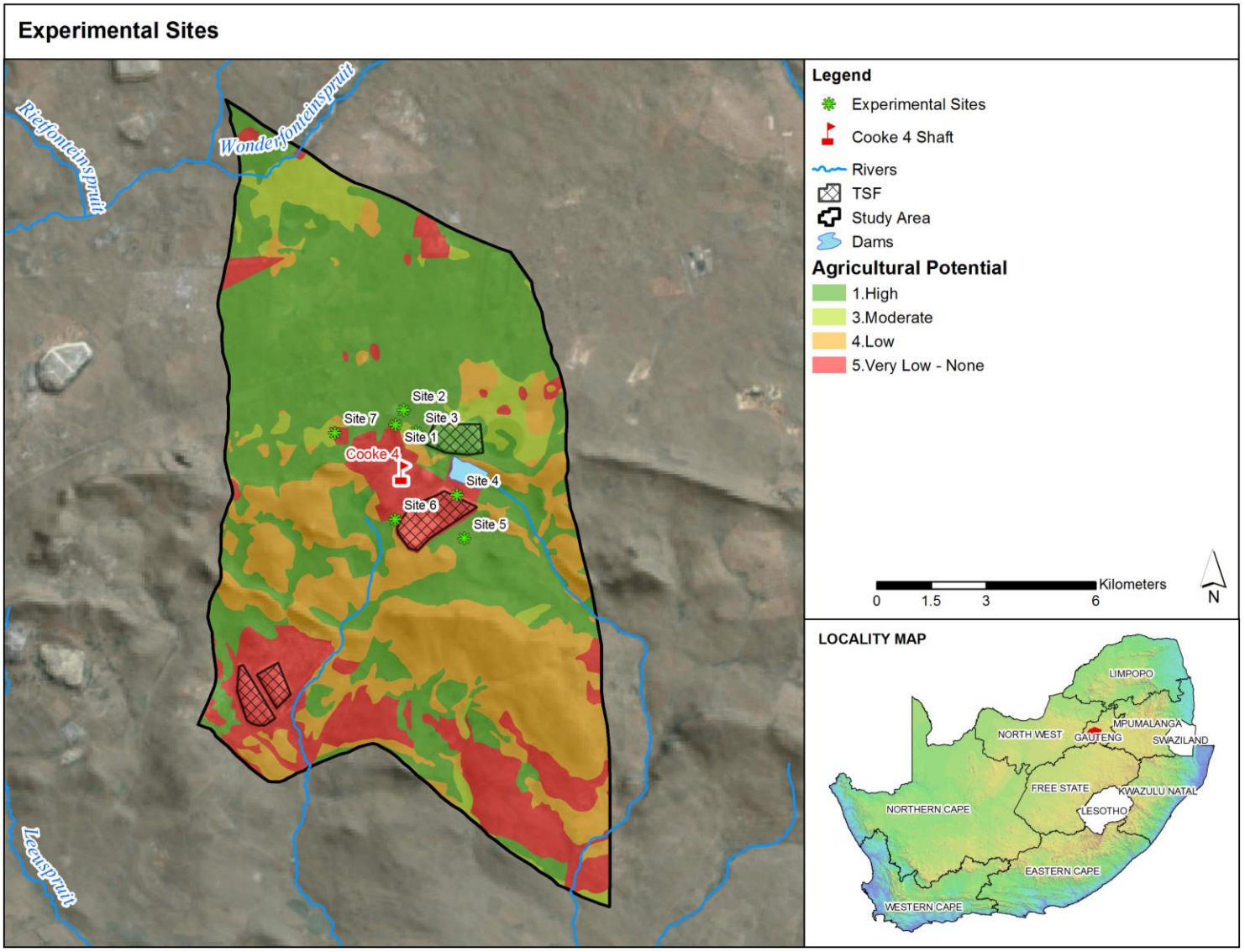

Figure 50: Locality map of selected experimental sites

6.2.2.1 Tree Height, Stem Circumference and Crown Diameter

The measured tree heights and stem diameters are presented in Table 14. The standard deviations are relatively large for considering the samples a uniform population. A better selection of trees was difficult due to sparse tree populations scattered through the area.

Table 14: Measured tree size parameters

Sample #	Site #	Tree Height (m)	Canopy Height (m)	Stem Circumference (cm)	Crown Diameter (m)
Sample 1	Site 1	6.5	3.0	63	4.1
Sample 2	Site 1	6.0	3.0	48	5.1
Sample 3	Site 4	5.0	4.5	82	5.1
Sample 4	Site 4	5.0	3.0	25	5.7
Sample 5	Site 6	7.0	4.5	46	6.0
Sample 6	Site 2	6.5	5.0	111	6.0
Sample 7	Site 6	8.0	4.0	96	6.0
Sample 8	Site 5	7.0	4.5	46	6.0
Sample 9	Site 2	7.0	4.5	119	6.4
Sample 10	Site 5	9.0	4.0	122	6.4
Sample 11	Site 3	8.5	4.5	29	6.4
Sample 12	Site 7	7.0	4.5	119	6.4
Sample 13	Site 3	9.0	4.0	64	6.4
Sample 14	Site 7	9.0	6.0	64	6.4
Average		7.2	4.3	74	5.9
Minimum		5.0	3.0	25	4.1
Maximum		9.0	6.0	122	6.4
Std. Deviation		1.3	0.9	33	0.7

6.2.2.2 Canopy Volume and Crown Projected Area

The calculated canopy volumes and crown projected area is presented in Table 15. The choice of multiplier is determined by the crown shape. A visual assessment of the canopies determined that the trees for this study were parabolic in shape, corresponding to studies on similar vegetation

types (Verma *et al.,* 2014). According to Coder (2000), the multiplier factor for parabolic vegetation is 0.393.

Table 15: Calculated tree parameters

Sample #	Site #	Canopy Volume (m^3)	Crown Projection Area (m^2)
Sample 1	Site 1	47	13.2
Sample 2	Site 1	73	20.4
Sample 3	Site 4	110	20.4
Sample 4	Site 4	92	25.5
Sample 5	Site 6	152	28.3
Sample 6	Site 2	169	28.3
Sample 7	Site 6	135	28.3
Sample 8	Site 5	152	28.3
Sample 9	Site 2	173	32.2
Sample 10	Site 5	154	32.2
Sample 11	Site 3	173	32.2
Sample 12	Site 7	173	32.2
Sample 13	Site 3	154	32.2
Sample 14	Site 7	231	32.2
	Average	142	27.5
	Minimum	47	13.2
	Maximum	231	32.2
	Std. Deviation	46	5.6

6.2.2.3 Leaf Area and Leaf Count

The average measured leaf length was 14 cm with an average leaf width of 1 cm which resulted in an average leaf area of 0.0014 m^2 to be used in the modelling. The leaf count based in the quadrant count delivered the following general result as presented in Table 16.

Table 16: General leaf count results

Stem Circumference	Leaf Count / m^3
< 90 cm	680
> 90 cm	1300

Since the average stem circumference is 74 cm (Table 14) the leaf count figure of 680 leaves per m^3 were used in the modelling.

6.2.2.4 Effective Leaf Area per Square Meter

The calculated leaf area per square meter is presented in Table 17. The average of 4.8 m^2 leaf area per square meter on the surface was used in the ET modelling.

Table 17: Calculated leaf area per square meter

Sample #	Leaf Area (m^2/m^2)
Sample 1	3.42
Sample 2	3.42
Sample 3	5.13
Sample 4	3.42
Sample 5	5.13
Sample 6	5.69
Sample 7	4.56
Sample 8	5.13
Sample 9	5.13
Sample 10	4.56
Sample 11	5.13
Sample 12	5.13
Sample 13	4.56
Sample 14	6.83
Average	4.80
Minimum	3.42
Maximum	6.83
Std. Deviation	0.91

6.2.3 Stomatal Conductance Measurements

A control site was selected to measure the stomatal conductance, leaf temperature and relative humidity profile over the course of 12 hours from 06:00 to 18:00. The control profile was done on 10 December 2015 since peak ET values are expected during the month of December. Refer to Figure 51 for a map depicting weather stations and control site localities.

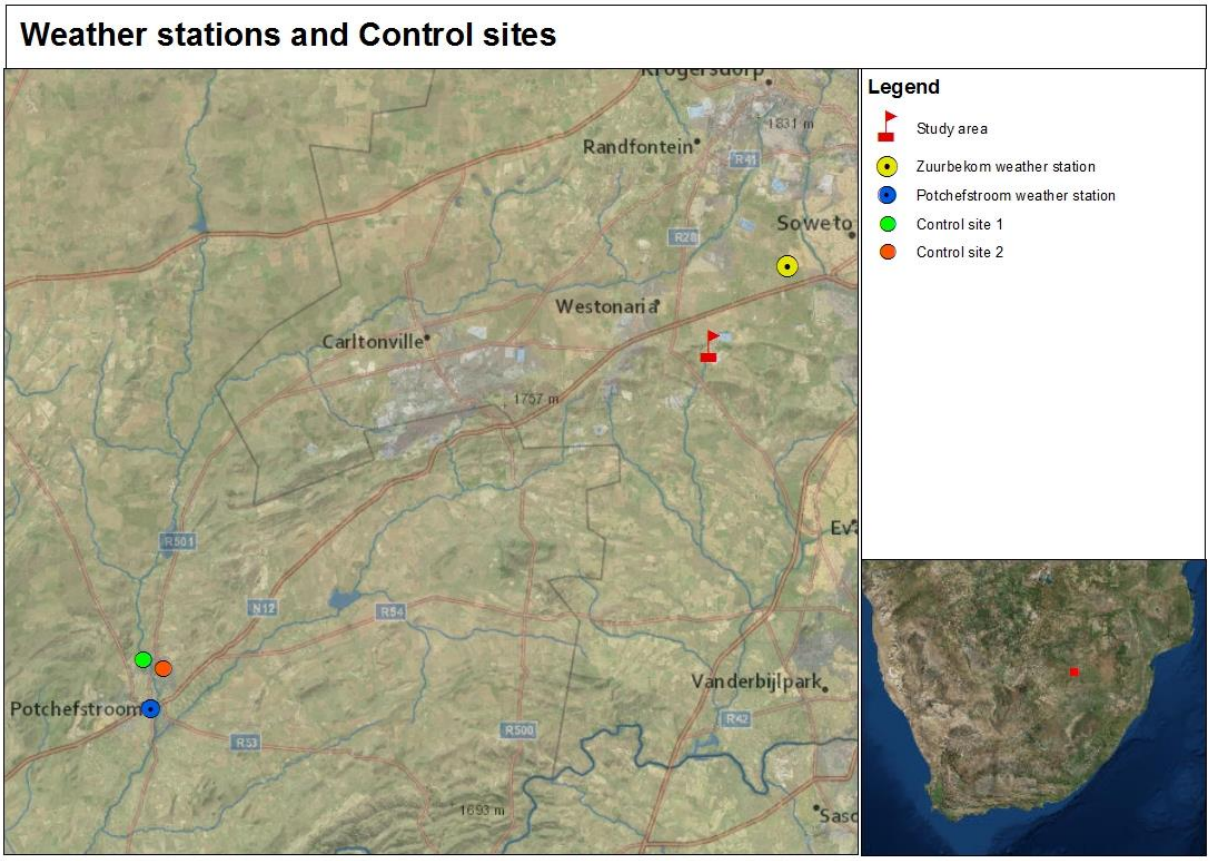

Figure 51: Control sites and weather station localities

The measured stomatal conductance together with the relative humidity and leaf temperature is shown in Figure 52 and Figure 53 respectively. It is clear from visual inspection form the aforementioned figures that that there exists some correlation between the stomatal conductance and the leaf temperature and this correlation is presented in Figure 54.

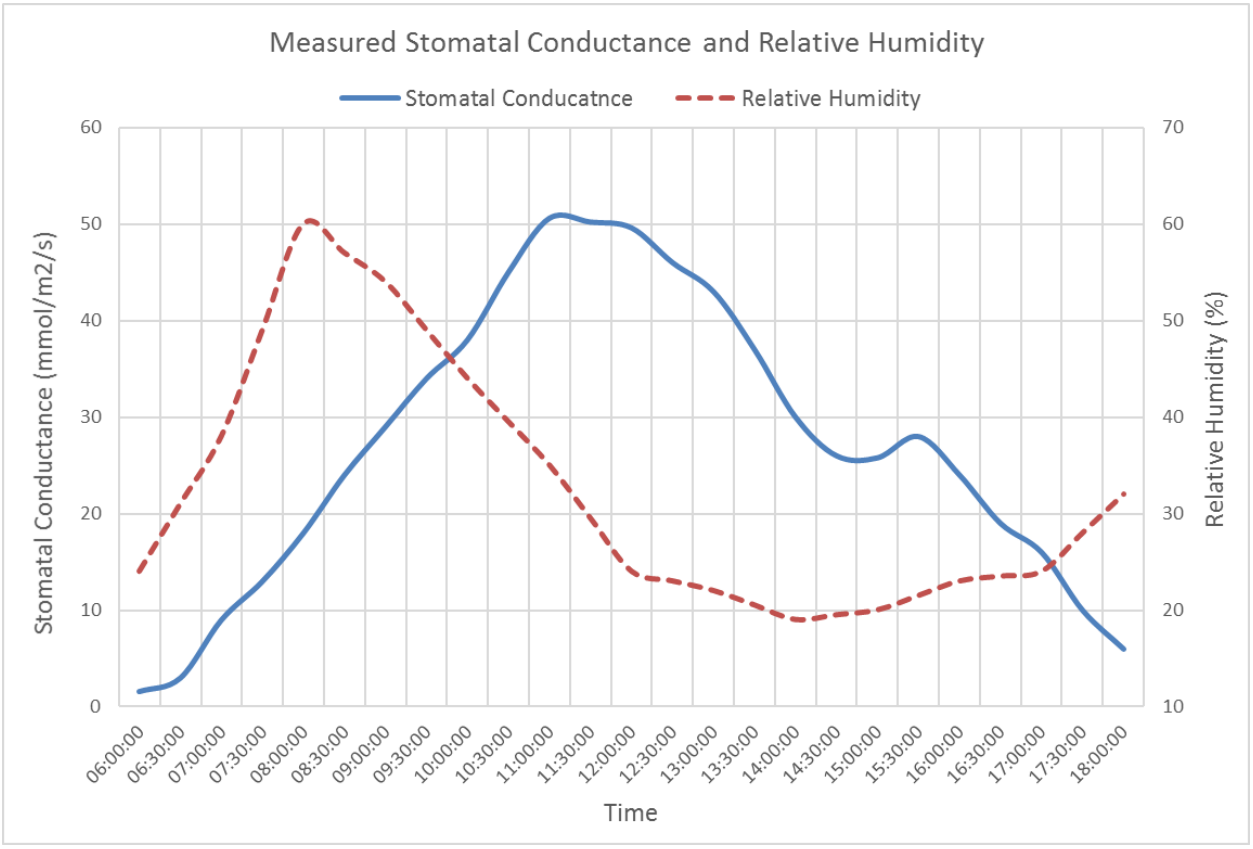

Figure 52: Measured stomatal conductance and measured relative humidity

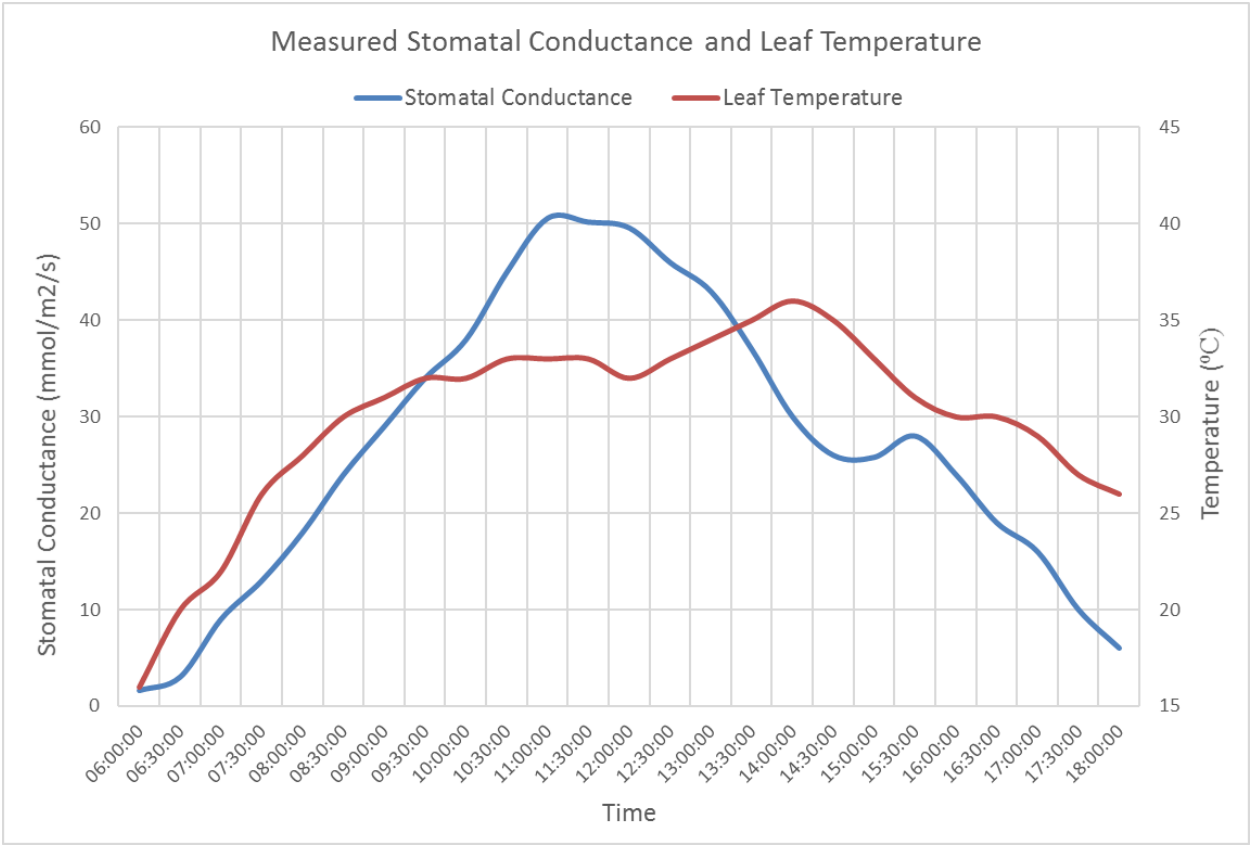

Figure 53: Measured stomatal conductance and measured leaf temperature

When considering the behaviour between stomatal conductance and leaf temperature some form of hysteresis is observed; a strong correlation exists between stomatal conductance and leaf temperature on the rising limb of the graph, but there is a delay in the drop of leaf temperature on the falling limb when compared to the stomatal conductance. Therefore, only the data points which contributed to a strong correlation were used in formulating the correlation function as shown in Figure 54.

By making use of the following relationship, stomatal conductance can be predicted based on leaf temperature:

$$C_s = 0.0863e^{0.1904T_L} \qquad (18)$$

where,

C_S = *Stomatal conductance (mmol/m^2/s)*

T_L = *Leaf temperature (^{o}C)*

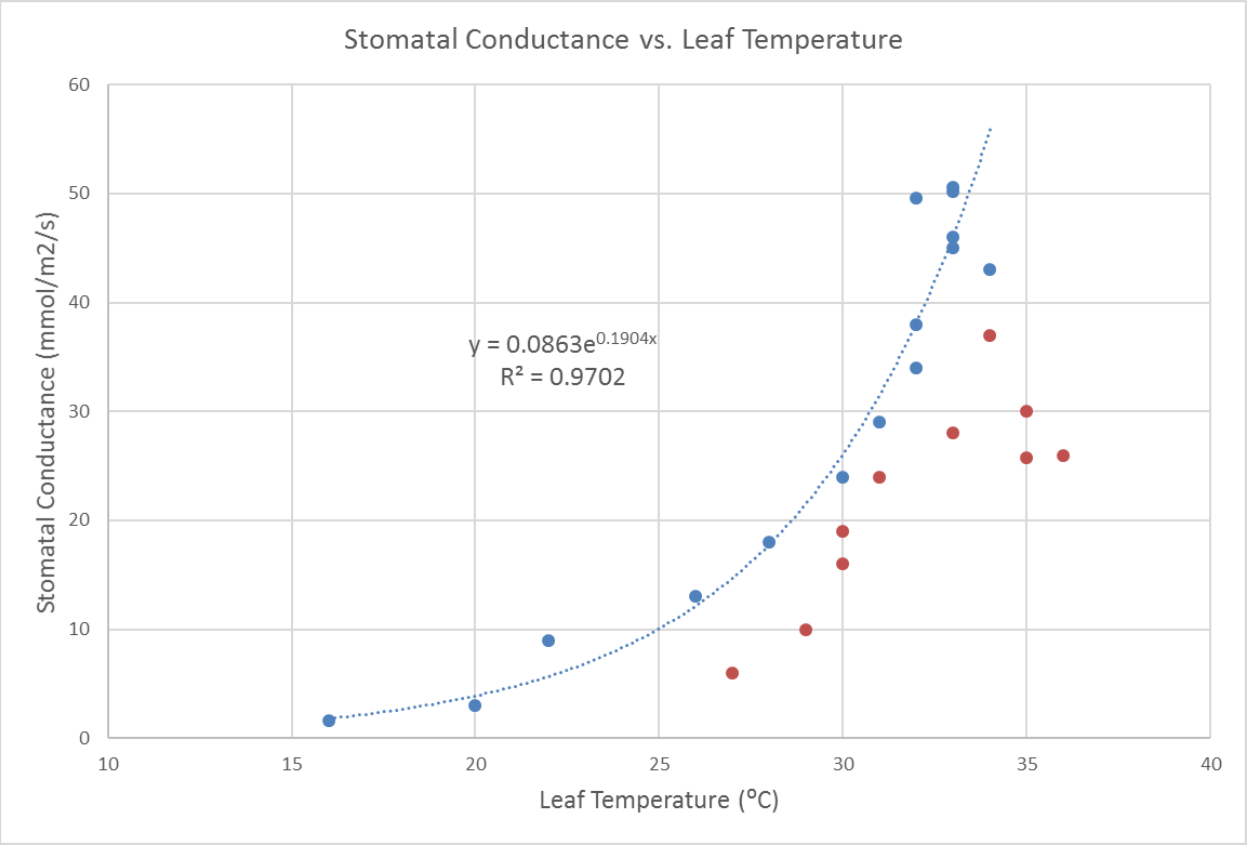

Figure 54: Stomatal conductance vs. leaf temperature

6.3 Evapotranspiration Modelling

The ET modelling is done through the formulation of a field model to predict stomatal conductance based on field measurements and then converting the predicted stomatal conductances to ET.

6.3.1 Formulation of the Field Model

The following steps are followed in the formulation of the field model:

1. Simulate leaf temperature making use of air temperature as described in Equation 4 to Equation 13 after Campbell and Norman (1998).
2. Use the relationship determined in Equation 18 to simulate stomatal conductance based on simulated leaf temperature from step 1.
3. Calibrate the field model based on field observations. Average stomatal conductances and leaf temperatures were used from the 14 experimental sites, as these sites are assumed to be homogenous in all respects for the purpose of this study.

6.3.1.1 Modelling Leaf Temperature

Since only air temperature is readily available from weather stations as opposed to leaf temperatures, leaf temperatures are simulated based on air temperatures as described in Campbell and Norman (1998). For the purpose of this study *Eucalyptus* leaves with and emissivity of 0.98 and leaf width of 0.01 meter were used in leaf temperature modelling. The absorbed radiation R_{abs} were used as a fitting parameter. The measured and simulated leaf temperature results are shown in Figure 55 and the parameters used in the calculation is presented in Appendix C.

A relatively good fit was obtained with the exception of the prediction on the rising and falling limbs of the graph. The correlation between the measured and simulated leaf temperatures is presented in Figure 56.

For the control site, the closest weather station temperature was used as this is also the methodology that is followed at the experimental sites. The correlation between the air and leaf temperature is shown Figure 57 which is in good agreement of what is expected (Figure 46).

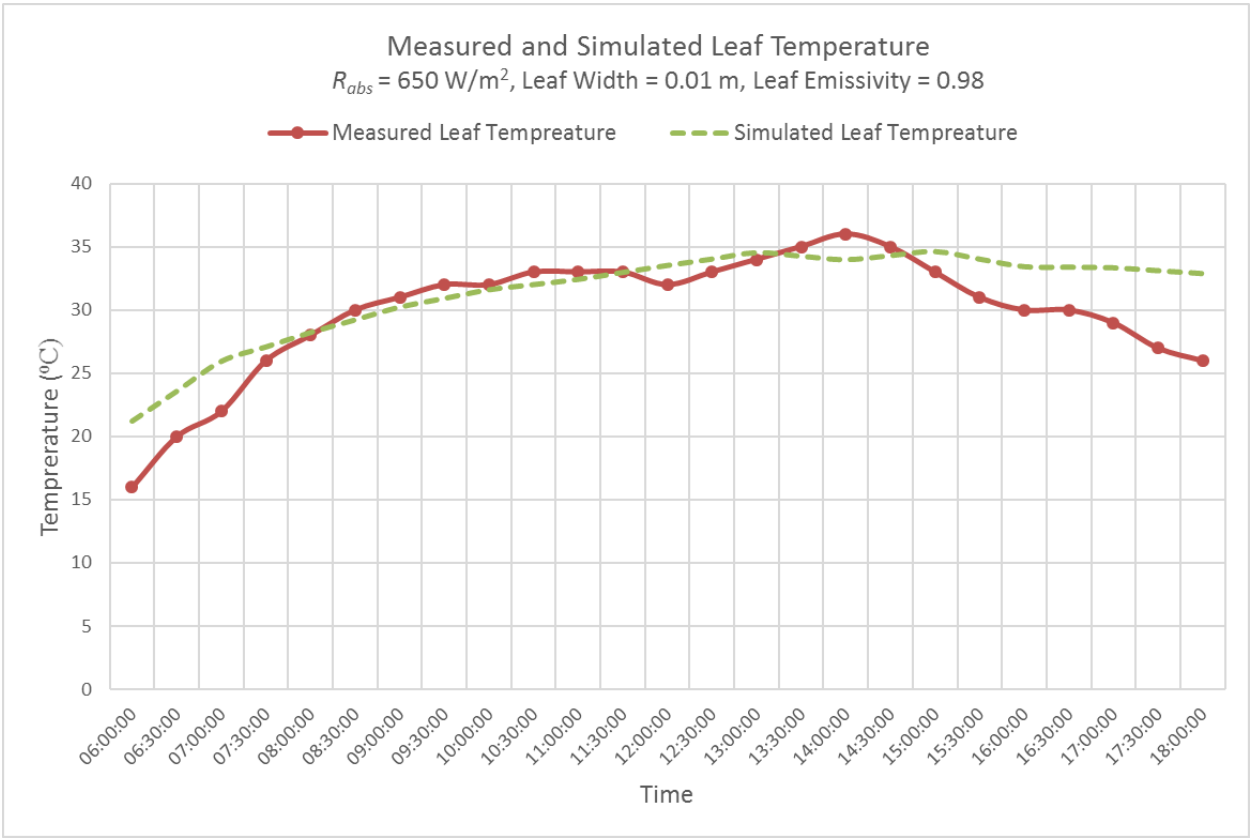

Figure 55: Measured and simulated leaf temperature

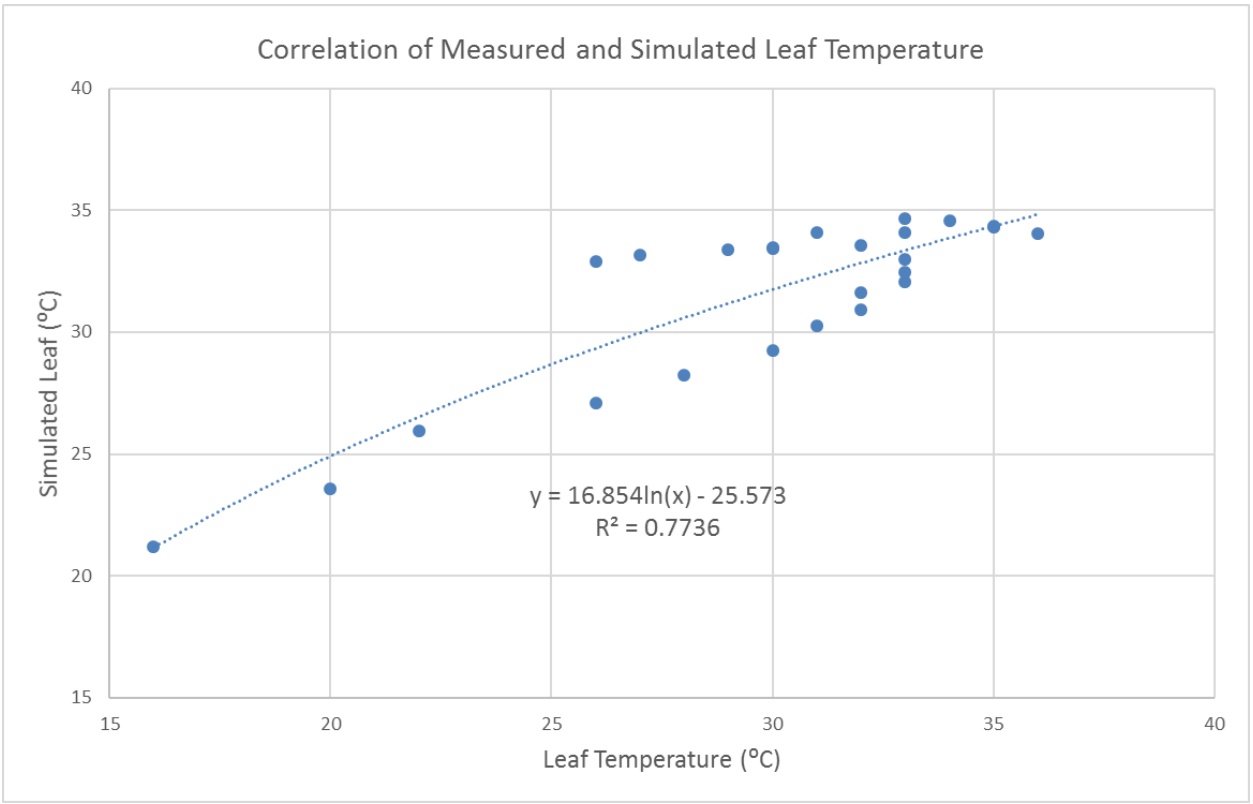

Figure 56: Correlation between measured and simulated leaf temperature

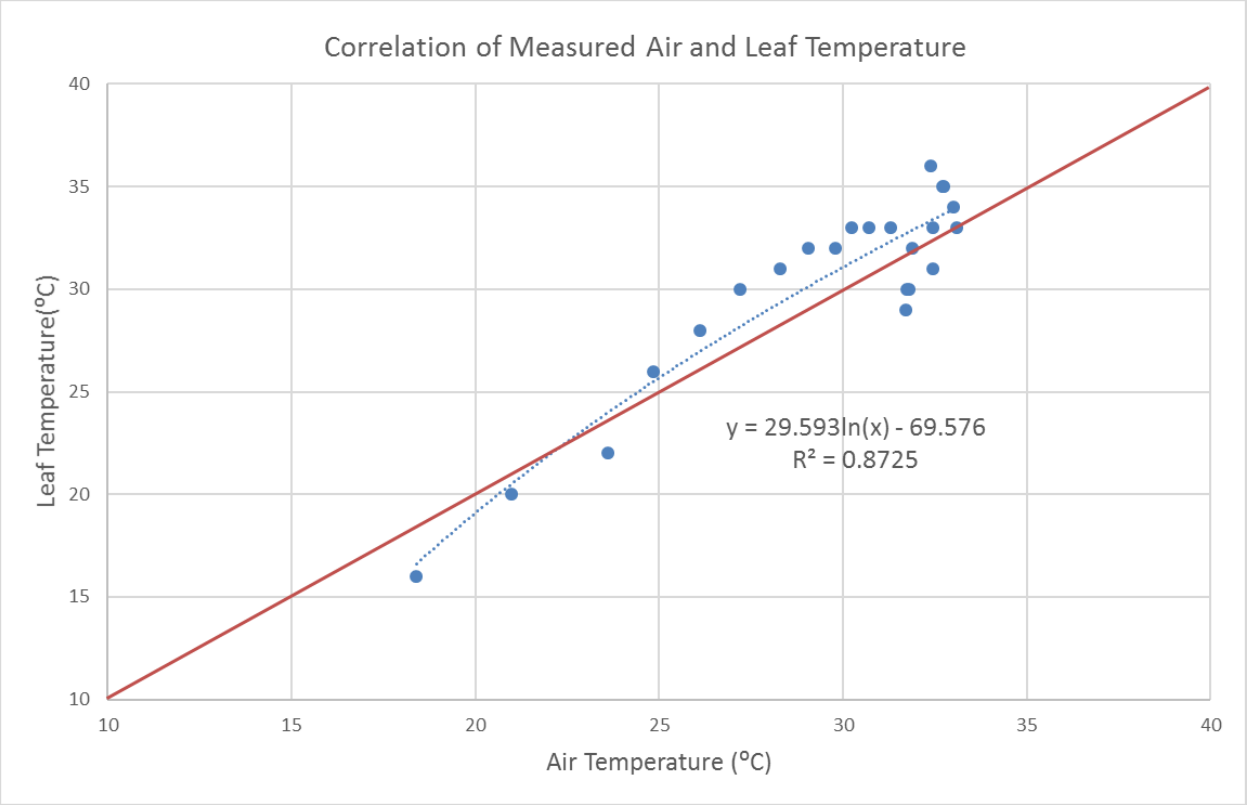

Figure 57: Correlation between air and leaf temperature

6.3.1.2 Field Model Calibration

Three sampling campaigns were conducted on the following dates during 2015: 22 September, 12 November and 8 December. On each occasion of stomatal conductance measurements, a 3m ladder was used to gain access to the tree canopies. Stomatal conductance measurements were performed on a set of 8 leaves per tree, distributed throughout the outer part of the lower and mid canopy. Porometer measurements were run until four readings per leaf were obtained. Stomatal conductances were measured at 15-minute intervals within a 3-hour period.

Table 18 provides a summary of average field measurements recorded at the 14 experimental sites. The averages were calculated using the average of 3 readings per site and then calculating the average for all sites.

Model calibration was achieved through applying a scaling factor to the regional radiation profile (Figure 48) to calculate an absorbed radiation figure per month to obtain the best fit to measured data across all months when sampling took place. The calibration results are presented in Figure 58. The simulated values presented in Figure 58 is based in the hourly air temperature data of the closest weather station for that specific day.

Table 18: Summary of average field measurements

Sample Time	22 September 2015		12 November 2015		8 December 2015	
	Leaf Temperature (ºC)	Stomatal Conductance (mmol/m²/s)	Leaf Temperature (ºC)	Stomatal Conductance (mmol/m²/s)	Leaf Temperature (ºC)	Stomatal Conductance (mmol/m²/s)
08:00					26.5	31.0
09:00	30.2	19.8	32.4	76.6	27.0	33.5
10:00	29.3	29.4	32.7	96.8	30.0	49.7
11:00	33.2	31.2	33.7	101.0		

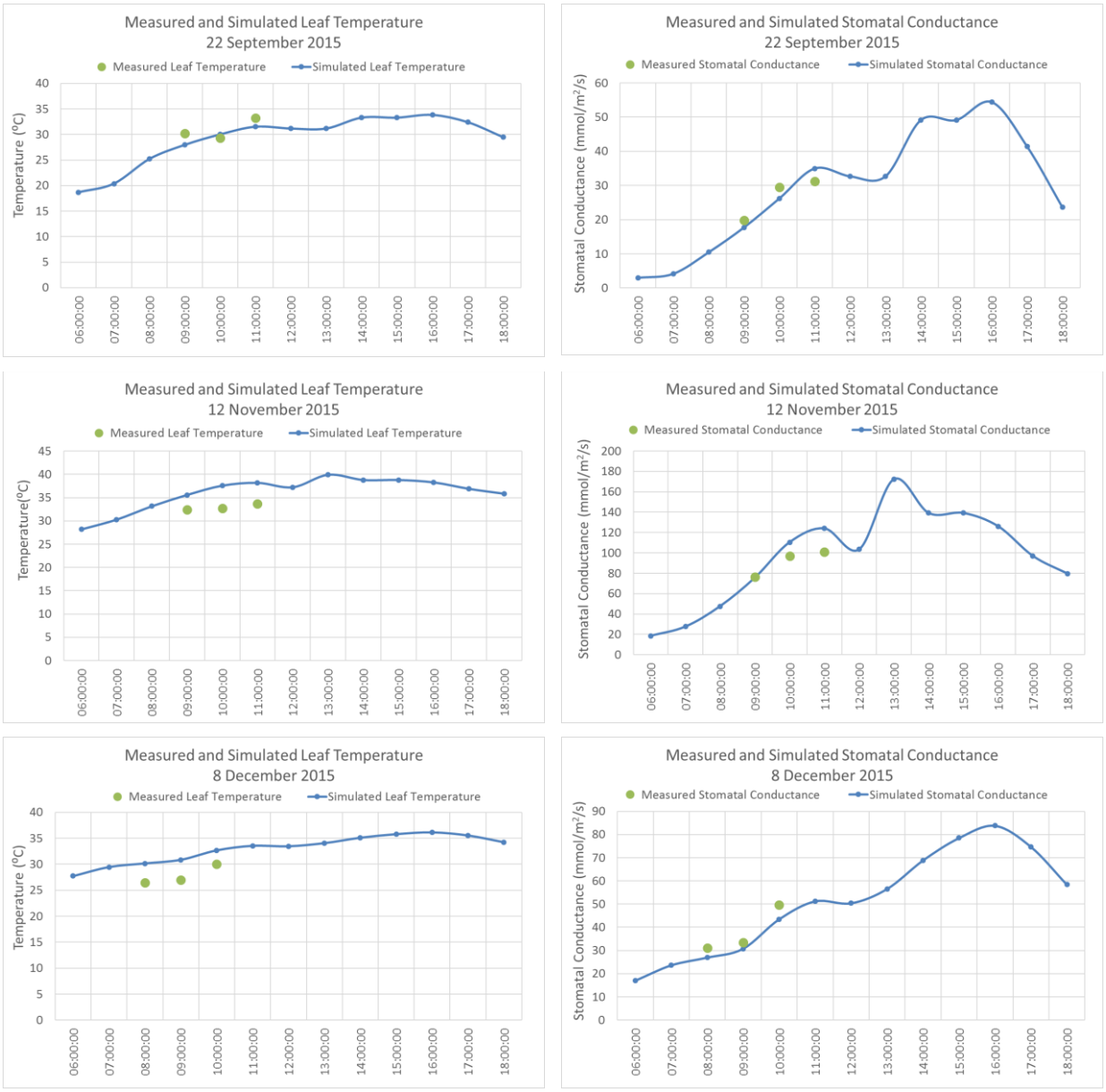

Figure 58: Field model calibration results

6.3.2 Converting Stomatal Conductance to ET

Making use of the monthly hourly average temperature data for the area (Figure 47) the stomatal conductances were calculated for each month of 2015 and converted to ET through the use of Equation 14. The modelling results for each month is presented in Appendix D.

Water loss during transpiration is an inevitable consequence of stomatal opening for carbon gain and gas exchange during photosynthesis. Gas exchange and water loss through stomata is regulated by the change in stomata size (open or closed). In general, stomata are open in light and closed in darkness. Despite reports of night time transpiration in a range of species native to a diversity of habitats including wetlands (Loftfield, 1921), deserts (Ludwig *et al.,* 2006), savannah biomes (Scholz *et al.,* 2007) and evergreen forests (Kavanagh *et al.,* 2007), the magnitude of water loss through transpiration have been documented to occur during daytime stomatal conductance, as the exchange of gasses to cool leaves are reduced during the night (Caird *et al.,* 2007).

The opening and closing of stomata are dependent on a number of environmental factors, including temperatures, light intensity, CO_2 concentrations, humidity, soil moisture and wind (Schulze and Hall, 1982). Complex interactions often exist among these different environmental factors, making it difficult to distinguish the role and relative importance of individual factors.

If assumed that stomatal conductance only takes place between the hours of 06:00 and 18:00 every day, then the total ET per day (mm/d) is calculated as the sum of the hourly ET values (mm/hour) presented in Appendix D. Since the temperature profiles used per month is based in the monthly averages, it is assumed that the calculated ET for each month (mm/d) is also a representation of the average monthly ET value (mm/d).

A summary of the calculated ET values per month is presented in Table 19. The figures obtained in Table 19 is calculated by multiplying the calculated ET values from Appendix D with the average effective leaf area per square meter which is 4.8 (Table 17) as the stomatal conductance is measured per leaf area.

Table 19: Summary of calculated monthly ET values

Month	ET (mm/d)	Month	ET (mm/d)	Month	ET (mm/d)
Jan	6.241	**May**	1.818	**Sep**	3.046
Feb	5.595	**Jun**	0.793	**Oct**	5.696
Mar	3.686	**Jul**	0.870	**Nov**	6.732
Apr	2.148	**Aug**	2.021	**Dec**	9.191

A comparison of the field model results to that of the FAO Penman-Monteith reference crop model and the Shuttleworth-Wallace ET model is shown in Figure 59. The average value for the Shuttleworth-Wallace ET model and the developed field model is basically identical, but the field model exhibits more pronounced minima and maxima compared to the Shuttleworth-Wallace ET model. During the winter months, the developed field model gives similar results to that of the FAO Penman-Monteith reference crop model and this is due to the fact that the model is temperature driven and a sudden drop in winter months is evident (Figure 47). The Shuttleworth-Wallace ET model assumed an evergreen broadleaf forest landcover with an average tree height of 7.2 m (Table 14). The calculations of the FAO Penman-Monteith and Shuttleworth-Wallace ET model is presented in Appendix E.

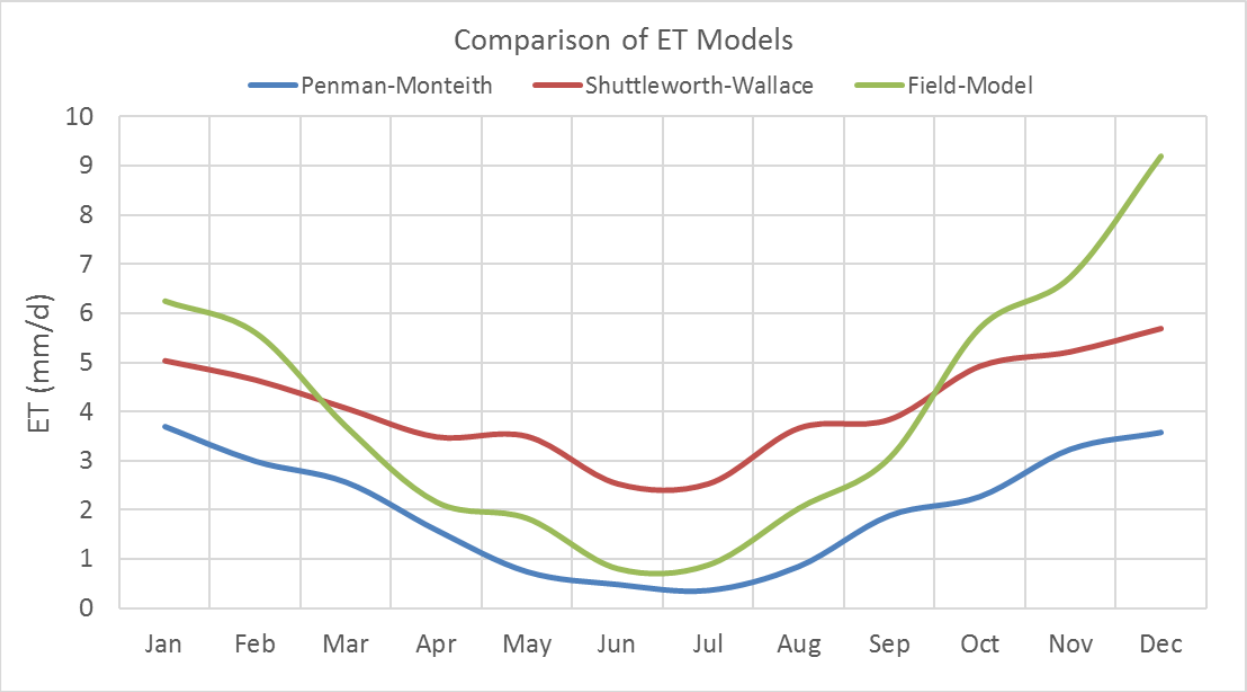

Figure 59: Comparison of ET model results

6.4 Water Balance Modelling

To determine the impact that the introduction of a plantation will have on the Cooke 4 water ingress into the mine workings, a water balance needs to be established. Since the study area is defined by dykes which are considered impermeable and the inflows from the adjacent compartments are known, the SVF model can be applied. The SVF model requires groundwater level data with time as well as rainfall data over the same time period.

An initial water balance will be calculated to represent the study area before any plantations are introduced after which the effect of the plantation will be modelled by introducing ET to the initial water balance.

6.4.1 Initial Water Balance

The position of the borehole selected to be used in the SVF model is shown in Figure 60. It is important to note that the borehole selected does not fall within the cone of depression that is caused around the Cooke 4 shaft, to ensure that a more natural water level response is used in the SVF model. The known inflows and outflows to the system are summarised in Table 22. It should be noted that the Cooke 3 shaft also reside within the study area.

Table 20: Summary of known inflows and outflows to the study area

Inflows	Ml/d	Outflows	Ml/d
Zuurbekom	9	**Cooke 4 Pumping**	68
Gemsbok East	6	**Cooke 3 Pumping**	9
Leeuspruit	7.5	**Gemsbokfontein Eye**	0
Rietspruit	5		

The average drop in water level from pre-mining to current water levels is estimated at 27 m (Figure 41). Making use of the aforementioned water level drop and current inflows to the system, Equation 16 was used to calculate the conductances for each of the inflows and the results are presented in Table 21. The conductances for each of the sources allow for the inflow to change as the head value changes.

Table 21: Calculated conductances

Source	Conductance (m^2/d)
Zuurbekom	315
Gemsbok East	210
Leeuspruit	260
Rietspruit	175

The model parameters that were used to obtain the best fit as shown in Figure 61 is presented in Table 22. The effective recharge was calculated by assigning a 12.8% (Table 10) to the areas where the surface geology is dolomite and a 5.3% (Table 10) to the areas where the surface geology is part of the Transvaal group. The study area size was calculated through GIS and the specific yield and dolomite storage was used as fitting parameters in the water balance model. The dolomite storage refers to the amount of water that is released from storage due to the dewatering of the compartment that is taking place. The detail around the SVF water balance calculation is available in Appendix F.

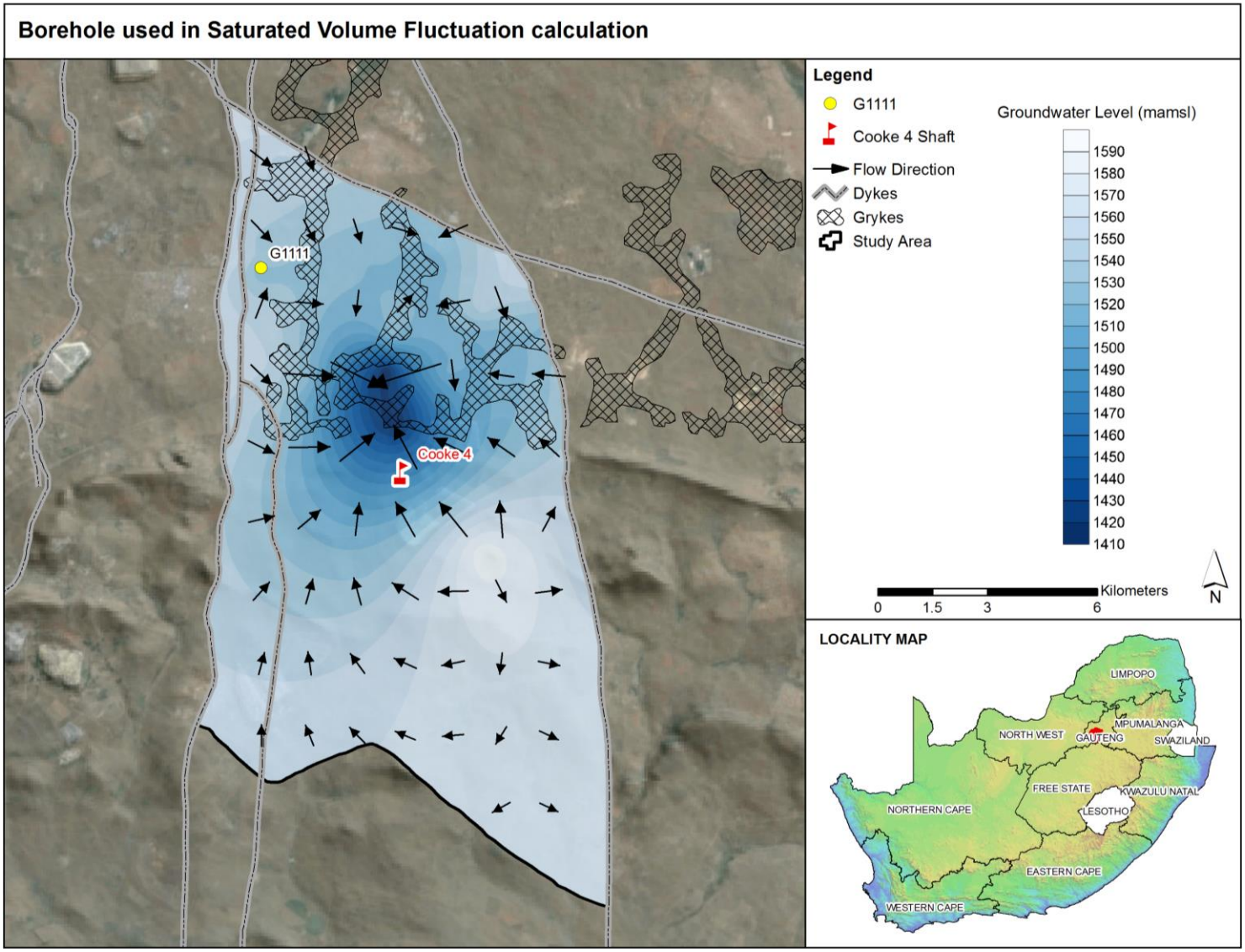

Figure 60: Locality of borehole used for SVF model

Table 22: SVF fitting parameters

Parameter	Value
Study Area (km^2)	161
Specific Yield	0.0043
Effective Recharge (%)	7.1
Dolomite Storage (Ml/d)	28

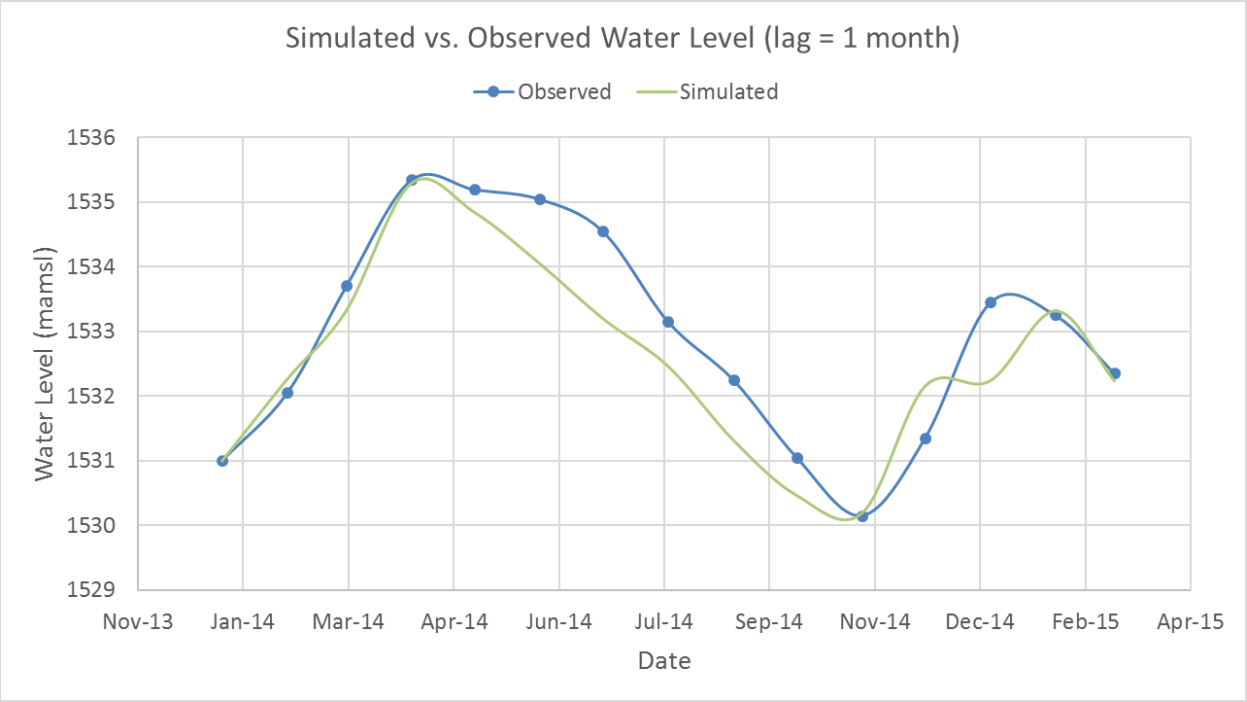

Figure 61: SVF model fit for borehole G1111

The assumptions associated with the water balance model can be summarised as follows:

- All inflows to the system are connected to the mine void via the network of faults within the study area
- All dykes are considered impermeable and inflows from adjacent compartments is head dependent and therefore controlled via a conductance term
- All leakage from rivers are also head dependent and are controlled via a conductance term.

6.4.2 Water Balance with ET

Before the calculated ET can be introduced to the water balance, the area where a possible plantation can be introduced must first be identified. The major criteria for establishing a plantation

will be the depth of the groundwater level. For the purpose of this study it is assumed that the maximum root depth of the proposed *Eucalyptus* is 8 mbgl (Nepstad *et al*., 1994). The reduction in recharge to the area is considered to be through extraction via root uptake only.

The only region where the average groundwater level is 8 mbgl or shallower is shown in Figure 63. By combining this region with areas with moderate to high agricultural potential, a probable area for the proposed plantation is identified as shown in Figure 64.

The initial water balance is modified by introducing the calculated ET over the proposed plantation area of 4.8 km^2. The effect of the proposed plantation is assumed to reduce direct recharge into the compartment and recharge for the plantation area was set to zero for months where the ET exceeded the recharge. The pumping rate of Cooke 3 were assumed to stay constant and the pumping rate of Cooke 4 was reduced until the water level response of the observed borehole and the predicted water level response with the ET delivered the same trend as shown in Figure 64.

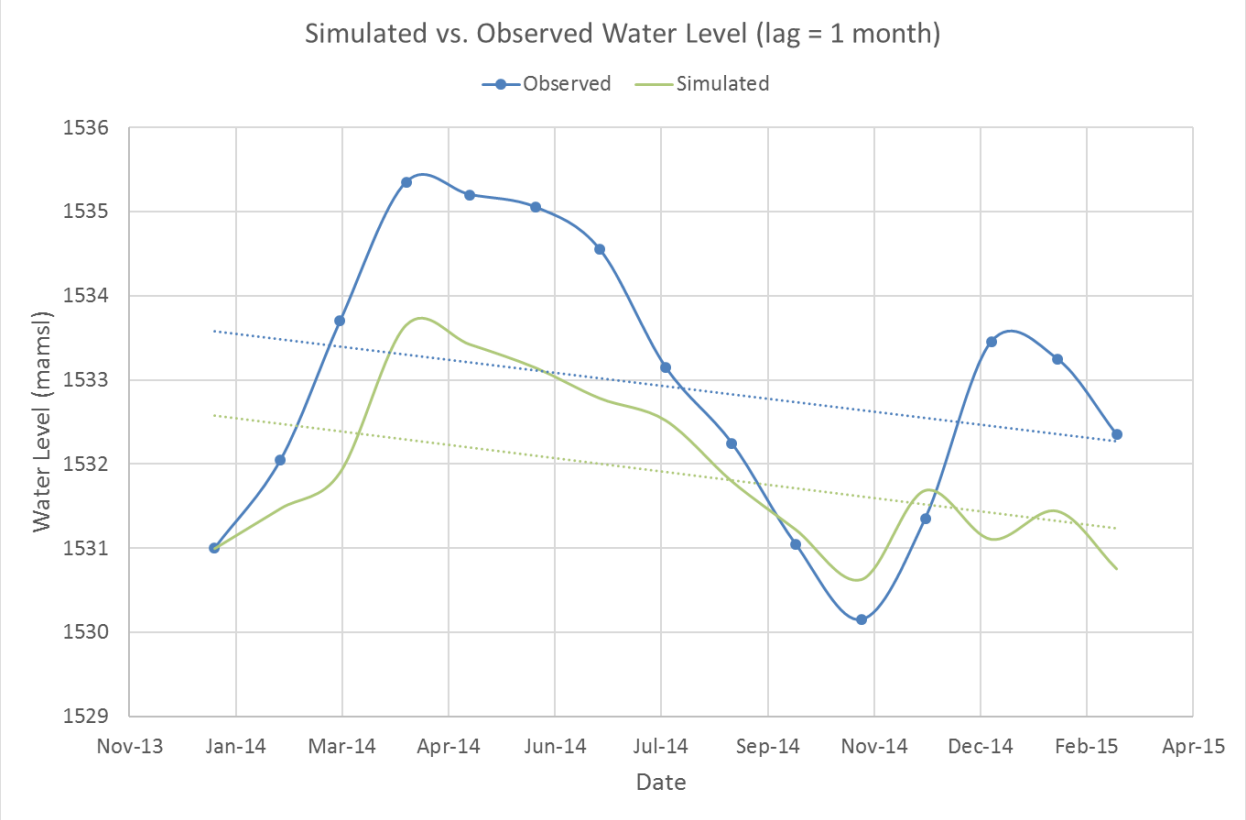

Figure 62: Predicted water level response with ET of proposed plantation

The resultant pumping rate of Cooke 4 were reduced with 11 Ml/d to obtain the results shown in Figure 62 .

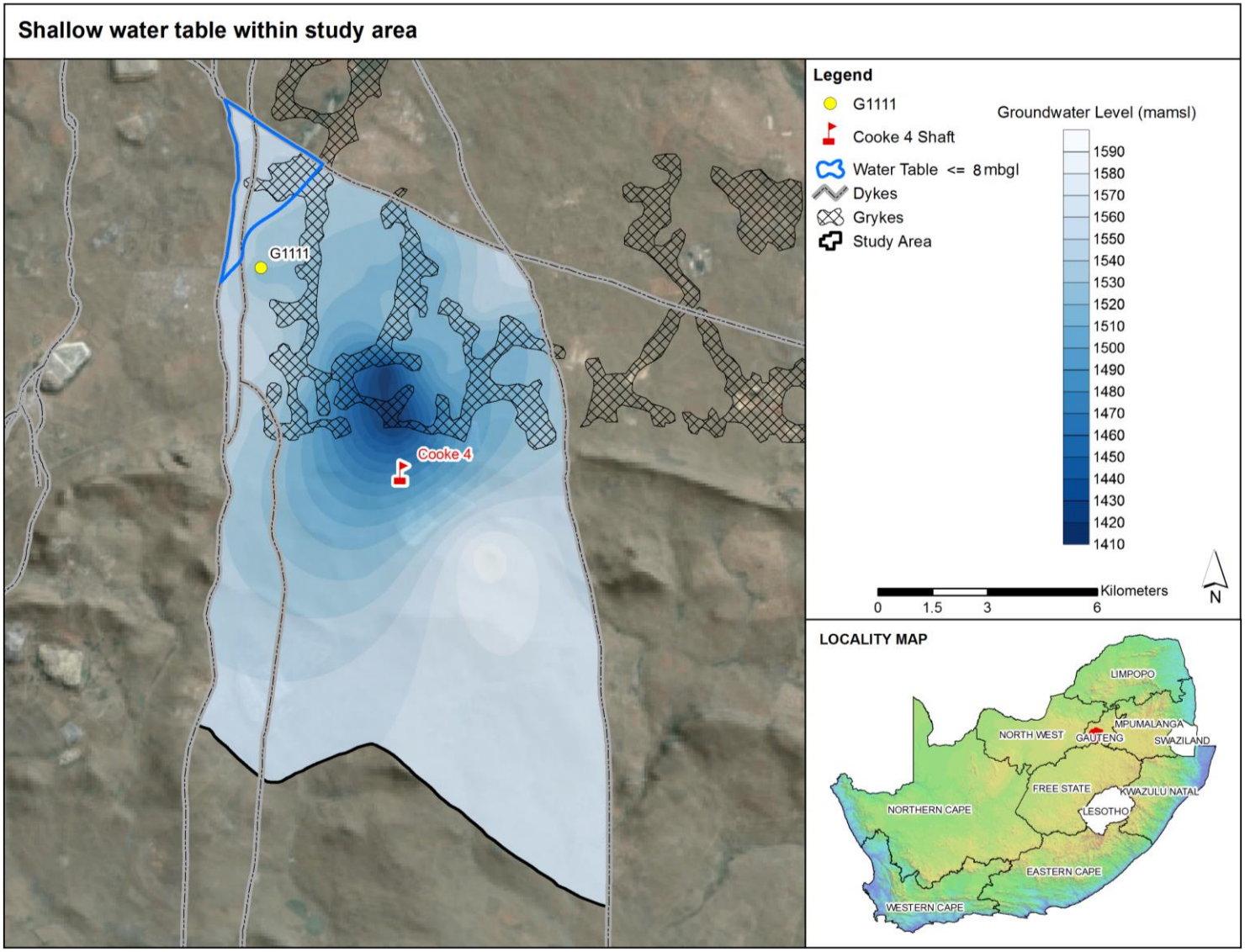

Figure 63: Area where water table are 8 mbgl or shallower

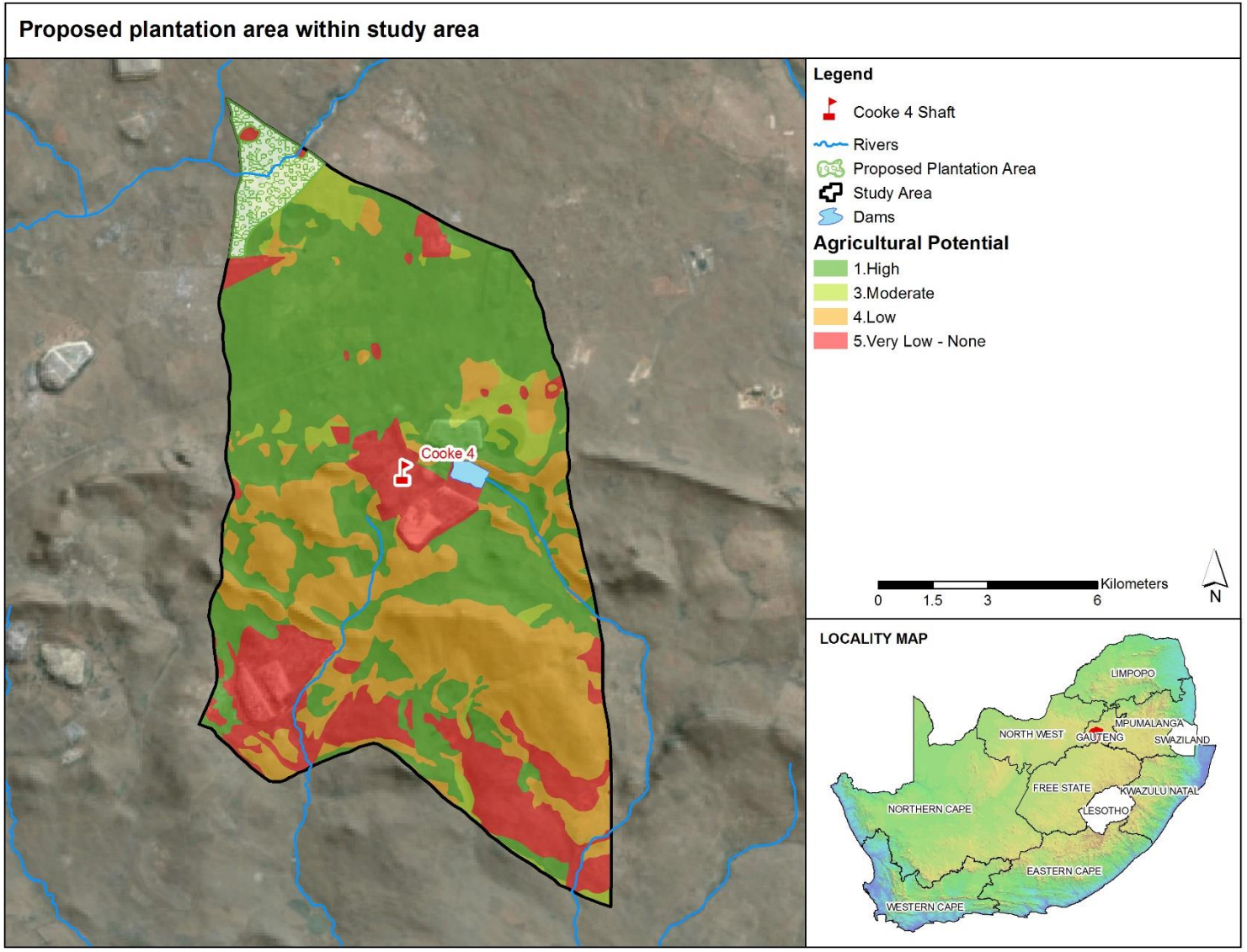

Figure 64: Proposed plantation area

The average direct ET of the proposed plantation area is 20 Ml/d, but not the whole 20 Ml/d is seen as a reduction in pumping rate. The predicted water level dropped at a maximum with 2 m and this increase in hydraulic gradient resulted in some increase from inflow sources described by a conductance term (Table 21). Furthermore, when ET exceeds recharge the recharge for the plantation area is set to zero and the effective ET equal the available recharge.

The water balance model with ET from the plantation are valid under the following assumptions:

- All assumptions from the initial water balance model
- No change in the storage from the dolomite
- The water level drop will not affect the ET due to increased root depth requirement
- ET is taking place at the predicted rate for each month and is not affected by factors such as the age of the plantation and availability of water.

7 CONCLUSIONS

There exists a correlation between stomatal conductance and leaf temperature even though some form of hysteresis is present. By fitting a curve to the correlated data an expression can be obtained to predict stomatal conductance when the leaf temperature is known.

Existing models can be used to simulate leaf temperature based on air temperature which in turn can be used to predict the stomatal conductance.

Through the use of field measurements, the formulated field model was successfully calibrated to predict stomatal conductance based on air temperature data from a close by weather station. This calibrated model was then used to predict average monthly stomatal conductance on an hourly basis from 06:00 to 18:00.

The stomatal conductance was converted to evapotranspiration through the use of the ideal gas law. The effective leaf area per square meter was used to scale the ET based on stomatal conductance to actual ET comparable to existing ET models.

The calculated ET based on the field model were compared with the FAO Penman-Monteith model for a reference crop ET as well as the Schuttleworth-Wallace model which is a variant of the Penman-Monteith model, but with the flexibility to select a specific type of landcover. On average the field model and the Schuttleworth-Wallace model compared very well, but the field model exhibited more extreme minima and maxima. Overall the comparison seemed realistic.

A water balance for the study area were determined making use of the SVF method under certain assumptions. Inflows to the SVF model were considered as head dependent and were therefore assigned appropriate conductance values. Pre-mining and existing groundwater levels in the area were used to determine the head loss required for head depended inflows.

The water balance model was then modified to account for the ET from the proposed plantation, which were assumed to reduce direct recharge. The most likely area to establish the proposed plantation were determined making use of a combination of where the groundwater levels are 8 mbgl or less and the agricultural potential is moderate to high.

The effective recharge was reduced based on the modelled ET values across the proposed plantation area and the water balance were adjusted so that the predicted water levels will follow the same trend as the measured water levels. This resulted in an average reduction of 11 Ml/d of the pumping at Cooke 4 assuming the pumping of 9 Ml/d of Cooke 3 is sustained. This will result in a 16% reduction in the pumping rate at Cooke 4 if all assumptions regarding the water balance model is valid. The average direct ET of the proposed plantation area is 20 Ml/d, but not the whole

20 Ml/d is seen as a reduction in pumping rate due to the fact that the water table drop will increase head dependent inflows and when ET exceeds recharge the recharge for the plantation area is set to zero and the effective ET equal the available recharge.

The predicted reduction of 16% in the pumping rate at Cooke 4 should be seen as a maximum. ET will vary with access to the water table and with age of the plantation. Physical constraints could also affect the effective area to be used for the plantation which in turn will also result in a reduced ET.

Given the fact that no long-term continuous data collection campaign was conducted, the water-use potential of a plantation in its various stages of establishment, and growing in the given environment, cannot be accurately comprehended. Such a study would require long-term data collection of tree growth patterns and root proliferation under site specific environmental conditions, chemical and physical soil characteristics, soil-moisture fluxes etc. For this reason, it cannot be confirmed that changing the natural vegetation to a plantation with high evaporative demands, will equal the available recharge in an area – thus the H_1 hypothesis cannot be confirmed. However, based on the evidence obtained from ET modelling, the outcome supports the predictions of a 16% reduction in the effective recharge across a potential *Eucalyptus* plantation area, therefore confirming H_0.

8 RECCOMENDATIONS

Model calibration has been done, but model validation has not taken place. It is recommended that stomatal conductance and leaf temperature readings are continued within the study area to also validate the response in the winter months.

As more information become available, a more detailed water balance could be developed through the use of a numerical model that can account for the different geological layers and structures and faults, which should give a better estimation of the effective reduction in pumping volumes at the Cooke 4 shaft.

Verification of the ET prediction methodology should be carried out within a different study area.

9 REFERENCES

Accuweather. 2015. www.accuweather.com

Ahmadi, M.T., Attarod, P., Marvi-Mohadjer, M.R., Rahmani, R. and Faithi, J. 2009. Partitioning of rainfall into throughfall, stemflow and interception loss in an oriental beech (*Fagus orientalis* Lipsky) forest during the rowing season. *Turkish Journal of Agriculture and Forestry*, 33:557-568.

Allen, R.G., Pereira, L.S., Raes, D. & Smith, M. 1998. Crop Evapotranspiration. Guidelines for Computing Crop Water Requirements. FAO Irrigation and Drainage Paper, 56. FAO, Rome, p.300.

Allison, G.B. & Hughes, M.W. 1983. The use of natural tracers as indicators of soil-water movement in a temperature semi-arid region. *Journal of Hydrology*, 60:157-173.

Anderson, J., Dybkjaer, G., Jensen, K.H., Refsgaard, J.C. & Rasmussen, K. 2002. Use of remote sensed precipitation and leaf area index in a distributed hydrological model. *Journal of Hydrology*, 264:34-50.

Bacon, P.E., Stone, C., Binns, C.L., Leslie, D.J., Edwards, EW. 1993. Relationship between water availability and *Eucalyptus camaldulensis* growth in a riparian forest. *Journal of Hydrology*, 150:541-561.

Bahmani, S.A., Attarod, P., Bayramzadeh, V., Ahmandi, M.T. & Radmehr, A. 2012. Throughfall, stemflow and rainfall interception in a natural forest of *Quercus castaneifolia* in Caspia Forest of Iran. *Forestry Journal*, 55(2): 197-206.

Beard, J.S. 1956. Results of the Mountain home rainfall interception and infiltration project in Black Wattle. *Journal of South African Forestry Association*, 27: 72-85.

Beets, P.N. & Oliver, G.R. 2006. Water use by managed stands of *Pinus radiata,* indigenous *Podocarpus/*Hardwood forests, and improved pasture in the central north island of New Zealand. *New Zealand Journal of Forestry Science,* 37(2):306-323.

Bennetts, D.A., Webbs, A., McCaskill, M. 2006. Dryland salinity processes within the discharge zone of a local groundwater system, southeastern Australia. *Hydrogeology Journal,*15:1197

Benyon, G.R., Theiveyanathan, S. & Doody, T. 2002. Impacts of tree plantations on groundwater in south-eastern Australia. *Australian Journal of Botany*, 54: 181-192.

Bilal, H., Ali, S.S. and Kim, K. 2014. Potential of *Eucalyptus* in the remediation of environmental problems: a review. *International Journal of Innovation and Scientific Research,* 4(2):136-144.

Bosch, J.M. 1979. Treatment effects of annual and dry period streamflow at Cathedral Peak. *South African Forestry Journal*, 108:29-38.

Bosch, J.M. & Hewlett, J.D. 1982. A review of catchment experiments to determine the effect of vegetation changes on water yield and evapotranspiration. *Journal of Hydrology*, 55(1-4):3-23.

Braune, E. 2000. Towards comprehensive groundwater resource management in South Africa. In: Sililo, O. et al. (Editors). Proceedings of the XXX IAH congress on Groundwater: Past achievements and future challenges. Cape Town, South Africa. 26 November to 1 December 2000. AA Balkeme, Rotterdam, pp 7-16.

Breda, N., Cochard, H., Dreyer, E. & Granier, A. 1993. Field comparison of transpiration, stomatal conductance and vulnerability to cavitation of *Quercus petraea and Quercus robur* under water stress. Annual Scientific *Forestry*, 50:571-582.

Bredenkamp, D.B., Botha, L.J., Van Tonder, G.J. & Van Rensburg, H.J. 1995. Manual on quantitative estimation of groundwater recharge and aquifer storativity. WRC Report TT 73/95. Water Research Commission, Pretoria.

Breman, H. & Kessler, J.J. 1995. Woody plants in agro-ecosystems of semi-arid regions. Advanced series in Agricultural Science No. 23, Springer-Verslag, Berlin.

Brisson, N., Itier, B., L'Hotel, J.C. & Lorendeau, J.Y. 1998. Parameterisation of the Shuttleworth-Wallace model to estimate daily maximum transpiration for use of crop models. *Ecological Modelling*, 107:159-169.

Brooks, S.D., Yan, M., Vidaurre, G., Khalizov, A.F. & Wang, L. 2013. Rapid modification of cloud-nucleating ability of aerosols by biogenic emissions. *Geophysical research letters,* 40:6293-6297.

Brooksbank, K., White, D.A., Veneklaas, E.J. & Carter, J.L. 2011. Hydraulic redistribution in *Eucalyptus kochii ssp. borealis* with variable access to groundwater. *Trees* DOI: 10.1007/s00468-011-0551-0.

Brutsaert, W., 1982. Evaporation into the Atmosphere. Dreidel, Dordrecht, Holland, pp.299.

Bryant, M.L., Bhat, S. & Jacobs, J.M. 2005. Measurements and modelling of throughfall variability for five forest communities in the southeaster US. *Journal of Hydrology,* 312(1-4):95-108.

Burch, G.J., Bath, R.K., Moore, I.D. & O'Loughlin, E.M. 1989. Comparative hydrological behaviour of forested and cleared catchments in south-eastern Australia. *Journal of Hydrology*, 90:19-42.

Burch, G.J., Moore, I.D. & Burns, J. 1989. Soil hydrophobic effects on infiltration and catchment runoff. Journal of *Hydrology*, 3:211-222.

Burgess, S.S.O., Pate, J.S., Adams, M.A. & Dawson, T.E. 2000. Seasonal water acquisition and redistribution in the Australian woody phreatophyte, *Banksia prionotes*. *Annual Botany*, 85: 215–224.

Caird, M.A., Richards, J.H. & Lisa, A.D. 2007. Nighttime stomatal conductance and transpiration in C3 and C4 plants. *Plant physiology*, 143:4-10.

Calder, I.R. 1992. Water use of eucalypts–a review. In: Calder, I.R., Hall, R.L., Adlard, P.G. (Eds.), Growth and Water Use of Forest Plantations. Wiley, Chichester, pp. 167–179.

Caldwell, M.M., Dawson & T.E., Richards, J.H. 1998. Hydraulic lift – consequences of water efflux from the roots of plants. *Oecologia*, 113:151–161.

Camillo, P.J. & Gurney, R.J. 1986. A resistance parameter for bare soil evaporation models. *Soil Science*, 141:95-106.

Campbell, G.S. & Norman, J.M. 1998. An Introduction to Environmental Biophysics (2nd Eds). Springer-Verlag, New York, United States of America.

Canadell, J., Jackson, R.B., Ehleringer, J.R., Mooney, H.S., Sala, O.E., Schulze, E.D. 1996. Maximum rooting depth of vegetation types at the global scale. *Oecologia*, 108: 583-595.

Chamberlain, D., Essop, H., Hougaard, C., Malherbe, S. & Walker, R. 2005. Part I: The contribution, cost and development opportunities of the Forestry, Timber, Pulp and Paper industries in South Africa. Final Report – 29 June 2005. Genesis Analytica (Pty) Ltd, South Africa.

Chimner, R. A., & Cooper, D. J. 2004. Using stable oxygen isotopes to quantify the water source used for transpiration by native shrubs in the San Luis Valley, Colorado, USA. *Plant Soil*, 260: 225– 236.

Choudhury, B.J. & Monteith, J.L. 1998. A four-layer model for the heat budget of homogenous land surfaces. *Quarterly Journal of the Royal Meteorological Society*, 114:373-398.

Coder, K.D. 2000. Crown Shape Factor and Volumes. Tree Biomechanics 672 Series. University of Georgia:Athens, G.A, USA, p. 1-5. Retrieved from: http://www.mdpi.com/2072-4292/3/11/2346/htm

Cohen, Y., Adar, E., Dody, A. & Schiller, G. 1997. Underground water use by *Eucalyptus trees in an arid climate. Trees, 11:356-362.*

Cooper, D.J., D'Amico, D.R. & Scott, M.L. 2003. Physiological and morphological response patterns of populus deltoides to alluvial groundwater pumping. *Environmental Management,* 31: 215–226.

Crombie, S.D. 1992. Root depth, leaf area and day time water relations of Jarrah (*Eucalyptus marginata*) forest over storey and understorey during summer drought. *Australian Journal of Botany*, 40: 113-122.

Davies, W.J., Wilkonson, S. & Loveus, B. 2002. Stomatal control by chemical signalling and exploitation of this mechanism to increase water use efficiency in agriculture. *New Phytologist,* 153, 449-460.

De Villiers, G. & De Jager, D.E. 1981. Net rainfall and interception losses in *Burkea Africana – Ochna pulchra* tree savannah. *Water SA*, 7(4): 249-254.

Dean, J.F., Webb, J.A., Jacobsen, G.E., Chisari, R. & Dresel, P.E. 2016. Biomass uptake and fire as controls on groundwater solute evolution on a southeast Australian granite: aboriginal land management hypothesis. *Biogeosciences,* 11(15):4099-4114.

Delin, G.G., Healy R.W., Landon, M.K. & Bhlke, J.K. 2000. Effects of topography and soil properties on recharge at two sites in an agricultural field. *Journal of American Water Resources Association*, 36(6):1041-1416.

Delzon, S. & Loustau, D. 2005. Age-related decline in stand water use: sap flow and transpiration in a pine forest chronosequence. *Agricultural and Forest Meteorology,* 129(3-4):105-119.

Dragun, J. 1988. The soil chemistry of hazardous material. Hazardous Martial Control Institute, Silver Spring, Maryland.

Duncan, M.J. 1995. The hydrological impact of converting pasture to Pine plantations. *Journal of Hydrology New Zealand*, 34(1): 15-41.

DWAF (Department of Water Affairs and Forestry). 1998. Water Law Principles – Discussion Document. Department of Water Affairs and Forestry, Pretoria.

Dye, P. & Jarmain, C. 2004. Water use by black wattle (*Acacia mearnsii*) : Implications for the link between removal of invading trees and catchment streamflow response. *South African Journal of Science,* 100(1-2):40-44.

Dye, P. J. 1996a. Response of *Eucalyptus grandis* trees to soil water deficits. *Tree Physiology*, 16: 233– 238.

Dye, P., Moses, G., Vilakazi, P., Ndlela, R. & Royappen, M. 2001. Comparative water used of wattle thickets and indigenous plant communities at riparian sites in the Western Cape and KwaZulu Natal. Water SA, 27(4):529-538.

Dye, P.J. 1996b. An investigation of sub-soil water penetration in the Mokobulaan research catchment, South-eastern Transvaal. *South African Forestry Journal*, 161:31-34.

Dye, P.J. 1996c. Climate forest and streamflow relationships in South African afforested catchments. *Commonwealth Forestry*, 75:31-38.

Dye, P.J., B.W. Olbrich and I.R. Calder. 1992. A comparison of the heat pulse method and deuterium tracing method for measuring transpiration from *Eucalyptus grandis* trees. *Journal of Botany*, 43:337-343.

Edwards, W.R.N. 1986. Precision weighting lysimetry for trees, using a simplified tared-balance design. Tree *Physiology*, 1:127-144.

Engel, V., Jobbagy E.G., Stieglitz, M., Williams, M. & Jackson, R.B. 2005. Hydrological consequences of *Eucalyptus* afforestation in the Argentine pampas. *Water Resources Research*, 4:1-14.

Enslin, J.F. & Kriel, J.P. 1968. The assessment and possible use of the dolomitic groundwater resources of the Far West Rand, Transvaal, Republic of South Africa. Proc. Int. Conf. Water for Peace, Washington, May 1967, Volume 2.

FAO (Food and Agricultural Organisation. 1989. Production Yearbook. Rome, FAO. Vol. 42

Farley, K.A., Jobbagy, E.G. & Jackson, R.B. 2005. Effects of afforestation on water yield: a global synthesis with implications for policy. *Global Change Biology*, 11: 1565-1576.

Farrington, P. & Bartle, G.A. (1991). Recharge beneath a *Banksia* woodland and a *Pinus pinaster* plantation on coastal deep sands in South Western Australia. *Forestry Ecology and Management*, 40:101-118.

Federer, C.A., Vorosmarty, C.J. & Fekete, B. 1996. Intercomparing of methods for potential evapotranspiration in regional or global water balance models. *Water Resources Research*, 32:2315-2321.

Fennesey, N.M. & Kirshen, P.H. 1994. Evaporation and evapotranspiration under climate change in New England. *Journal of Water Resources Planning and Management*, 12(1):48-69.

Ferro, A., J. Cassada, B. Berra, & D. Tsao. 2006. “Phytoremediation of TPH-Contaminated Groundwater,” presented at the Annual International Conference on Soils, Sediments, and Water, University of Massachusetts, Amherst.

Fleisher, J.N.E. 1981. Geohydrology of the dolomite aquifers of the Mamani Subgroup in the wouth-western Transvaal, RSA. Department of Water Affairs and Forestry, Technical Report GH3169.

Forestry Commission, 2005. Water Use by Trees. Retrieved from: http://www.northlandnemo.org/images/Water%20Use%20by%20Trees.pdf

Forrester, D.I., Theiveyyanathan, S., Collopy, J.J. & Marcar, N.E. 2010. Enhanced water use efficiency in a mixed *Eucalyptus globulus* and *Acacia mearnsii* plantation. *Forest Ecology and Management, 259:1761-1770.*

Fuchs, M. & Tanner, C.B. 1968. Evaporation from a drying soil. *Journal of Applied Meteorology*, 6:582-587.

Gardiol, J.M., Serio, L.A. & Maggiora, A.I.D. 2003. Modelling evapotranspiration of corn (Z*ea mays*) under different plant densities. *Journal of hydrology*, 217:188-196.

George, R.J., Nulsen, R.A., Ferdowsian, R. & Raper, G.P. 1999. Intercation between trees and groundwater in recharge and discharge areas – A survey of Western Australian sites. *Agricultural Water Management,* 39:91-113.

Global Agricultural Information Network. 2014. Update on the South African Lumber industry. Retrieved from http://www.unece.lsu.edu/marketing/documents/2015Mar/gme15-03.pdf

Granier, A., Bobay, V., Gash, J.H.C., Gelpe, J., Saugier, B. & Shuttleworth, W.J. 1990. Vapour flux density and transpiration rate comparison in a stand of Maritime pine *(Pinus pinaster* Ait.) in Les Landes forest. *Agricultural and Forest Meteorology*, 51:309-319.

Greenwood, E.A., Biddiscombe, E.F., Rogers, A.L., Beresford, J.D. & Watson, G.D. 1995. Growth of species in tree plantations and its influence on salinity and groundwater in a 400mm rainfall region of south-western Australia. *Water Management*, 28: 231-243.

Greenwood, E.A.N., Kleine, L., Bereford, J.D. & Watson, G.D. 1985. Differences in annual evaporation between grazed pasture and *Eucalyptus* species in plantations on a saline farm catchment. *Journal ofHydrology*, 78:261-278.

Gush, M.B., Dye, P.J., Geldenhuys, C.J. and Bulcock, H.H., 2011. Volumes and efficiencies of water-use within selected indigenous and introduced tree species in South Africa: Current results and

potential applications. *In:* Proceedings of the 5th Natural Forests and Woodlands Symposium, Richards Bay, 11-14 April.

Heuperman, A.F., Kapoor, A.S. & Denecke, H.W. 2002. Bio-drainage principles, experiences and applications. *In* International Programme for Technology and Research in Irrigation and Drainage. United Nations. p.2-79.

Hinckley, T.M., Brooks, J.R., Earmak, J., Ceulmans, R., Kueera, J., Meinzer, F.C. & Roberts, D.A. 1994. Water flux in a hybrid poplar stand. *Tree Physiology*, 14:1005-1018.

Hodgson, F.D.I., Usher, B.H., Scott, R., Zeelie, S., Cruywagen, L.M. & De Necker, E. 2001. Predictive techniques and preventative measures relating to the post operational impact of underground mines in the quality and quantity of groundwater resources. WRC Report no. 699/1/01, ISBN no. 1868451828, p. 272.

Hopkins, W.G. & Hüner, N.P.A. 2008. Introduction to plant physiology. 4th Edition ed. London: Wiley.

Horton, J.L. & Clark, J.L. 2001. Water table decline alters growth and survival of *Salix gooddomgii and Tamarix chinensis* seedlings. *Forest Ecology and Managemen*t, 140:239-247.

Huber, A., Iroumè, A. & Bathurst, J. 2007. Effect of *Pinus radiata* on water balance in Chile. *Hydrological Processes*, 22(1): 142-148.

ITRC (Interstate Technology and Regulatory Council). 2009. Phytotechnology Technical and Regulatory Guidance and Decision Trees, Revised. Phyto-3. Washington, D.C. Retrieved from: http://isites.harvard.edu/fs/docs/icb.topic1256177.files/READINGS/2009-ITRC%20PHYTO-3.pdf

Jackson, R.B., Canadell, J., Ehleringer, J.R., Mooney, H.A., Sala, O.E. & Schulze, E.D. 2005. A global analysis of root distributions for terrestrial biomes. *Oecologia*, 108:389-411.

Jarmain, C. 2003. Potential for using trees to limit the ingress of water into mine workings: A comparison of total evaporation and soil water relations for Eucalyptus and grassland. Pietermaritzburg: University of Natal. (Thesis – MSc Agric).

Johan Fourie and Associates Consulting. 2011. Ezulwini Mining Company (Pty) Ltd Strategic Water Management Plan. Paardekraal, South Africa.

Johnston, C.D. 1987. Preferred water flow and localised recharge in a variable regolith. *Journal ofHydrology,* 94:129–142

Joshi, M. & Palanisami, K. 2011. Imapct of Eucalytpus plantations on ground water availability in south Karnataka.

Kavanagh, K.L., Pangle, R. & Schotzko, A. 2007. Nocturnal transpiration causing disequilibrium between soil and stem predawn water potential in mixed conifer forests of Idaho. *Tree Physiology,* 27(4):621-629.

Kelliher, F.M., Leuning, R., Raupach, M.R. & Schulze, E.D. 1995. Maximum conductance for evaporation from global vegetation types. *Agricultural Forest Meteorology*, 7:1-16.

Kramer, P.J. 1969. Plant and soil water relationships: modern synthesis. McGraw-Hill, New York 482.

Kueera, J., Earmak, J. & Penka, M. 1977. Improved thermal method of continual recording the transpiration flow rate dynamics. *Plant Biology,* 19:413-420.

Lafleur, P.M & Ross, W.R., 1990. Application of an energy combination model for evaporation from sparse canopies. *Agricultural Forest Meteorology*, 49:135-153.

Langkamp, P.J., Farrel, G.K. & Dalling, M.J. 1982. Measurements of precipitation interception, seasonal acetylene reduction, plant growth and nitrogen requirement. *Australian Journal of Botany*, 30:87-106.

Larcher, W. (1983). Physiological Plant Ecology. Springer-Verlag, Berlin.

Le Maitre, D.C., Scott, D.F. & Colvin, C. 1999. A review on information on interaction between vegetation and groundwater. *Water SA*, 25:137-148.

Lhomme, J.P., Chehbouni, A. & Boulet, G. 1998. Stomatal control of transpiration: Examination of Monteith's formulation of canopy resistance. *Water Resources Research*, 34(9):2301-238.

Loftfiel J.V.G. 1921. The behaviour of stomata, volume 314. Carnegie Institution, Washington, D.C.

Loheide, S.P., Butler, I.J.J. & Gorelick, S.M. 2005. Estimation of groundwater consumption by phreatophytes using diurnal water table fluctuations: A saturated-unsaturated flow assessment. Water Resources 41, W07030, doi:10.1029/2005WR003942.

Loustau, D., Berbigier, P., Roumagnac, P., Arruda-Pacheco, C., Davids, M.I., Ferreira, J.S., Pereira, J.S. & Tavares, R. 1996. Transpiration of a 64-year old maritime pine stand in Portugal:seasonal course of water flux through maritime pine. Oecologia, *107*:33-42.

Ludwig, F., Jewitt, R.A. & Donovan, L.A. 2006. Nutrient and water addition effects on day-and night-time conductance and transpiration in a C3 desert annual. *Oecologia,* 148:219-225.

Lui, D.L. & Scott, B.J. 2001. Estimation of solar radiation in Australia from rainfall and temperature observations. *Agricultural and Forest Meteorology*, 106:41-59.

Lund, M.R. & Soegaard, H. 2003. Modelling of evaporation in a sparse millet crop using a two-source model including sensible heat advection with the canopy. *Journal of Hydrology*, 280:124-144.

Mahoney, J.M. & Rood, S.M. 1998. A device for studying the influence of declining water table on poplar growth and survival. *Tree physiology,* 8:305-314.

McCarthy, T.S. 2006. The Witwatersrand Supergroup. In: Johnson, M.R., Anhaeusser, C.R., Thomas, R.J. (Eds.s), The Geology of South Africa. Geological Society of South Africa, Johannesburg/Council for Geosciences, Pretoria, pp. 155-186.

McJannet, D.L., Vertessy, R.A. & Clifton, C.A. 2000. Observations of evapotranspiration in a break of slope plantations susceptible to periodic drought stress. *Tree Physiology*, 20(3):169-177.

McKenzie, R.C., George, R.J., Woods, S.A., Cannon, M.E., Bennett, D.L. 1997. Use of electromagnetic induction meters as a tool in managing salinization. *Journal of Hydrology*, 11:361-371

Mellor, E.T. 1917. The geology of the Witwatersrand: and explanation of geological map of the Witwatersrand goldfield. *Nature*, 100:156-156.

Minerals Act no. 50 of 1991. South African Government Gazette.

Mo, X., Liu, S. & Zhao, Z. 2004. Simulating temporal and spatial variation of evapotranspiration over the Lushi basin. *Journal of Hydrology*, 285:125-142.

Monteith, J.L. 1973. Principles of Environmental Physics. Edward Arnold, London, pp.214.

Monteith, J.L. 1995. Accommodation between transpiring vegetation and the convective boundary layer. *Journal of Hydrology*, 166(3-4):251-263.

Mucina, L. & Rutherford, M.C. 2006. The vegetation of South Africa, Lesotho and Swaziland. South African National Biodiversity Institute, Pretoria.

Mulvey, J.M., Vanderbei, R.J. & Zenois, S.A. 1995. Robust optimization of large-scale systems. *Operations Research*, 43:264-281.

Musto, J.W. 1994. Changes in soil properties and related hydraulic characteristics caused by *Eucalyptus* plantations (Unpublished M.Sc. (Agric) Thesis). University of Natal, Durban.

National Water Act no. 36 of 1998 (NWA). South African Government Gazette.

Naumberg, E., Hunter, R.M.R., Mclendon, T. & Martin, D.W. 2005. Phreatophytic Vegetation and Groundwater Fluctuations: A review of current research and application of ecosystem responses modelling with an emphasis on Great Basin Vegetation. *Environmental Management*, 35(6): 726-740

Navar, J. & Ryan, R. 1990. Interception loss and rainfall redistribution by three semi-arid growing shrubs in northeastern Mexico. *Journal of Hydrology*, 115:51-63.

Neal, C., Robson, A.J., Bhardwaj, C.L., Conway, T., Jeffery, H.A., Neal, M., Ryland, G.P., Smith, C.J. & Walls, J. 1993. Relationship between precipitation, stemflow and through fall for a lowland BlackvWood plantation in England: findings on interception at a forest edge and the effects of storm damage. *Journal of Hydrology*, 146: 221-233.

Nepstad, D.C., Carvalho, D.E., Davidson, E.A., Jipp, P.H., Lefbvre, P.A., Negreiros, G.H., Da Silva, E.D., Stone, T.A., Trumbore, S.E. & Veira, S. 1994. The role of deep roots in the hydrological and carbon cycles of Amazonian Forests. *Nature*, 372: 666-669.

Noilhan, J. & Planton, S. 1998. A simple parameterization of land surface process for meteorological models. *Monthly Weather Review*, 17:536-549.

O'Connor, T.G. 1985. A synthesis of field experiments concerning the grass layers in the savannah regions of Southern Africa. Report No. 114, South African National Scientific Programmes, Foundation for Research Development, Pretoria.

Olbrich, B., Olbrich, K., Dye, P. & Soko, S. 1996. A year-long comparison of water use efficiency of stressed and non-stressed *E. grandis and P. patula*: findings and management recommendations. Un-published Report FOR-DEA 958, CSIR, Pretoria.

Parsons, C.F. & Killisck, A.M. 1985. The surface geology of part of the WAGM: Property and Environs. Retrieved from: https://dspace.nwu.ac.za/handle/10394/613

Parsons, C.F. 1989. The geology of the dolomitic inliers on Jachtfontein 344 and Elandsfontein 308 of WAGM. Research Unit Not 4189. JCI Technical Services Division. Unpublished. Retrieved from:

Pepper, R.G. & Craig, G.F. 1986. Resistance of selected *Eucalyptus* species to soil salinity in Western Australia. *Journal of Applied Ecology*, 23:977-987.

Pienaar, L.V. 1964. Reënvalonderskepping deur ‘n jong opstand van *Pinus radiate* D. Don. *Forestry in South Africa*, 5:23-37.

Raper, G.P. 1998. Agroforestry water use in Mediterranean regions of Australia:Water and salinity issues. Rural Industries Research and Development Corporation, Canberra.

Raschke, K. 1979. Movement of stomata. *In:* Haupt, W., Feinlien, M.E. (eds) Physiology of movements, Encyclopaedia of plant physiology, new series, volume 7. New York: Spinger-Verlag, p.383-390.

Rawls, J. & Brakensiek, D.L. 1985. Predication of soil water properties for hydrological modelling. Watershed Management in the Eighties, ASCE, 293-299.

Richards, J.H. & Caldwell, M.M. 1987. Hydraulic lift: substantial nocturnal water transport between soil layers by *Artemisia tridentate* roots. *Oecologia*, 73:486-489.

Rison Groundwater Consulting. 2011. Groundwater Monitoring Borehole Installation: Ezulwini Mining Company (Pty) Ltd Tailings Storage Facility. Krugersdorp, South Africa.

Roberts, S., Vertessy, R. & Grayson, R. 2001. Transpiration from *Eucalyptus sieberi* (L. Johnson) forests of different age. *Forest Ecology and Management*, 143:153-161.

Rood, S.B. & Mahoney, J.M. 2002. The collapse of riparian poplar forest downstream form dams on western prairies: Probable cause and prospects for mitigation. *Environmental Management,* 14:451-464.

Rowe, P.B. & Hendrix, T.M. 1951. Interception of rain and snow by second-growth ponderosa pine. *Transactions American Geophysical Union*, 32:903-908.

Rowntree, P.R. 1991. Atmospheric parameterization schemes for evaporation over land: basic concepts and climate modelling aspects. In: Schmugge, T.J. & Andre, J.C. (Eds.), Land surface evaporation: measurement and parameterization, pp.5-29.

Ryel, R.J., Caldwell, M.M., Yoder, C.K., Or, D. & Leffler, A.J. 2002. Hydraulic redistribution in a stand of *Artemisia tridentata*: evaluation of benefits to transpiration assessed with a simulation model. *Oecologia*, 130:173-184.

SACS, 2006. A revised stratigraphic framework for the Witwatersrand Supergroup. Lithostratigraphic Series, 42. Geological Surveys of South Africa, Pretoria, p. 7.

Salama, R.B., Bartle, G.A. & Farrington, P. 1994. Water use of plantation *Eucalyptus camaldulensis* estimated by groundwater hydrograph separation techniques and heat pulse method. *Journal of Hydrology*, 156, (1-4):163-180.

SANBI (South African National Biodiversity Institute). 2016. South African Trees A to Z. Retrieved from http://www.plantzafrica.com/plants/treesae.htm

Sansigolo, C.A. & Ferraz, E.S.B. 1982. Measurement of transpiration and biomass in a tropical *Pinus caribaea* plantation with tritiated water. *Agricultural Meteorology*, 26:25-*33.*

Sappi. 1994. Tree Farming Guidelines Part 4. Retrieved from: https://cdn-s3.sappi.com/s3fs-public/Part-4-References-Reference-material.pdf

SAWS (South African Weather Services). 2015. Retrieved from http://www.weathersa.co.za

Schilling, K. E., M. K. Jha, Y.-K. Zhang, P. W. Gassman, & C. F. Wolter. 2008. Impact of land use and land cover change on the water balance of a large agricultural watershed: Historical effects and future directions, Water Resources Research, 45(7).

Schnoor, J.L., Licht, L.A., McCutchein, S.C., Wolfe, N.L. & Carrerira, L.H. 1995. Phytoremediation of organic and nutrient contaminants. Environmental Science and Technology, 29:318-323

Schofiled, N.J., Loh, I.C., Scott, P.R., Bartle, J.R., Riston, R., Bell, R.W., Borg, H., Anson, B. & Moore, R. 1989. Vegetation strategies to reduce stream salinities of water resources ctahcments in South-West Western Australia, Water Authority of Western Australia, Leederville, W.A.

Scholes, R.J. & Walker, B.H. 1993. An African Savanna - Synthesis of the Nylsvley Study. Cambridge University Press, Cambridge.

Scholz, F.G., Bucci, S.J., Goldstein, G., Meinzer, F.C., Franco, A.C. & Miralles-Wilhelm, F. 2007. Removal of nutrient limitations by long-term fertilization decrease nocturnal water loss in savanna trees*. Tree Physiology*, 27:551-559.

Schulze, E.D. & Hall, A.E. 1982. Stomatal responses, water loss and CO2 assimilation rates of plants in contrasting environments. In: Lange, O.L., Nobel, P.S., Osmond, C.B. & Ziegler, H. (Eds.) Encyclopaedia of Plant Physiology Volume 12B. Physiological Plant Ecology II. Water relations and Carbon Assimilation. Springer-Verslag, Berlin, pp.181-230.

Schulze, R.E. 2006. Solar Radiation: Background. *In:* Schulze, R.E. (Ed). 2006. South African Atlas of Climatology and Agrohydrology. Water Research Commission, Pretoria, RSA, WRC Report 1489/1/06, Section 5.1.

Schulze, R.E. and Chapman 2006. Estimation of Daily Solar Radiation over South Africa. *In:* Schulze, R.E. (Ed). 2006. South African Atlas of Climatology and Agrohydrology. Water Research Commission, Pretoria, RSA, WRC Report 1489/1/06, Section 5.2.

Schulze, R.E., Maharaj, M. and Moult, N. 2006. Reference Crop Evaporation by the Penman-Monteith Method. In: Schulze, R.E. (Ed). 2006. South African Atlas of Climatology and Agrohydrology. Water Research Commission, Pretoria, RSA, WRC Report 1489/1/06, Section 13.3.

Scott, D.F. & Lesch, W. 1997. Streamflow responses to afforestation with *Eucalyptus grandis* and *Pinus patula* and to felling in the Mokobulaan experimental catchments, South Africa. *Journal of Hydrology*, 199(3):360-377.

Scott, M., Shafroth, P. & Auble, G. 1999a. Response of riparian Cottonwoods to alluvial water table declines. *Environmental Management*, 23:347.

Scott, R.L., Shuttleworth, W.J., Goodrich, D.C. & Maddock III, T. 1999b. The water use of two dominant vegetation communities in a semiarid riparian ecosystem. *Agricultural and Forest Meteorology*, 150: 241–256.

Sellers, P.J., Los, S.O., Tucker, C.J, Uistice, Co., Dazlich, D.A., Collatz, G.J. & Randall, D.A. 1996. A revised and surface parameterization (SiB_2) for atmospheric GCM's. Part II: The generation of global fields of terrestrial biophysical parameters for satellite data. *Journal of Climate*, 9:706-737.

Shafroth, P.B., Stromberg, J.C. & Patten, D.T. 2000. Woody riparian vegetation response to different alluvial water table regimes. Westerns North American Naturalist, 60:66-76.

Sharma, M.L., Barron, R.J.W. & Fernie, M.S. 1987a. Aerial distribution of infiltration parameters and some soil properties in lateritic catchments. *Journal of Hydrology*, 94:109-127.

Sharma, M.L., Barron, R.W.J. & Williamson, D.R. 1987b. Soil water dynamics of lateritic catchment as affected by forest clearing for pasture. *Journal of Hydrology*, 94:29-46.

Shuttleworth, W.J. 1993. Evaporation. In: Maidment, D.R.(Ed.), Handbook of Hydrology/ McGraw-Hill, New York, pp.4.1-4.53.

Shuttleworth, W.J. & Gurney, R.J. 1990. The theoretical relationship between foliage temperature and canopy resistance in sparse crops. *Quarterly Journal of the Royal Meteorological Society*. 116, 497-519.

Sikka, A.K., Samra, J.S., Sharda, V.N., Samraj, P. & Lakshmanan, V. 2003. Ow flow and yield response to converting natural grassland into bluegum (*Eucalyptus globulus*) in Nilgiris watersheds of South India. *Journal of Hydrology,* 270:12-26.

Smedema, L.K. 1997. Biological drainage: myth or opportunity? GRID, magazine of the IPTRID network, 11:3.

Smith, D.M., P.G. Jarvis & J.C.W. Odongo. 1998. Management of windbreaks in the Sahel: the strategic implications of tree water use. *Agroforestry Systems*, 40:83–93.

Soares, J.V. & Almeida, A.C. 2001. Modeling the water balance and soil water fluxes in a fast growing Eucaluptus plantation in Brazil. *Journal of Hydrology*, 253; 130-137.

South African National Biodiversity Institute (SANBI). 2009. 2009 National Mosaic Land-cover. Retrieved from: http://bgis.sanbi.org/landcover/project.asp

Srivastava, R.J., Kumar, A. & Prasa, K. 2003. Studies on Soil Moisture Variations under Eucalyptus Plantation. XII World Forestry Congress, 2003, Quebec City, Canada.

SRK Consulting. 2013. Independent Technical Report: Gold One Cooke Four Underground operation, Gauteng, South Africa.

Stannard, D.I. 1993. Comparison of Penman-Monteith, Shuttleworth-Wallace and modified Priestly-Taylor evapotranspiration models for wildland vegetation in semiarid rangeland. *Water Resources Research*, 29(5):1379-1392.

Stone, E.L. & Kalitz, P.J. 1991. On the maximum extent of tree roots. *Forestry Ecology and Management,* 46:59–102.

Sudmeyer, R.A., Speijers, J. & Nicolas, B.D. 2004. Root distribution of *Pinus pinaster, P. radiata, Eucalyptus globulus and E. kochii* and associated soil chemistry in agricultural land adjacent to tree lines. *Tree Physiology,* 24:1333-1346.

Teskey R.O. & Sheriff D.W. 1996. Water use by Pinus radiata trees in a plantation. *Tree Physiology*, 16: 273–280.

Tèson, N., Conzonno, V.H., Arturi, M.F. & Frangi, J.L. 2014. Dissolved organic carbon in water fluxes for *E. grandis* plantations in northeastern Etaerios Province, Argentina. *Bosque*, 35(3): 279-288.

Tucker, R.F. 1980. The sedimentary and mineralogy of the Composite Reef on Cooke Section, Randfontein Estates Gold Mines, Witwatersrand, South Africa, (Unpublished M.Sc. Thesis), University of Witwatersrand, Johannesburg, South Africa, p.335.

Tucker, R.F. & Viljoen, R.P. 1986. The geology of the West Rand Goldfields, with special reference to the Southern Limb. *In:* Anhauesse, C.R. & Maske, S. (*Eds*). Mineral Depost of South Africa, Volume 2, Geological Society of South Africa, Johannesburg, 649-688.

Tyree, M.T. & Ewers, F.W. 1991. Transley Review No. 34. The hydraulic architecture of trees and other woody plants. *New Phytologist,* 199(3):345-360.

Valente, F., David, J.S. & Gash, J.H.C. 1999. Modelling interception loss from two sparse eucalypt and pine forests in central Portugal using reformulated Rutter and Gash analytic models. *Journal of Hydrology,* 190(1):141-162.

Valentini, R., Scarascia, G.E., De Angelis, P. & Bimbi, R. 1991. An experimental test of the eddy correlation and technique over a Mediterranean canopy. *Plant Cell Environment*, 14:987-994.

Van Dijk, A.I.J.M., Hairsine, P.B., Pena Arancibia, J. & Dowling, T.I. 2007. Reforestation, water availability and stream salinity: a multi-scale analysis in the Murray-Darling Basin, Australia. Forestry and Ecological *Management*: 251:94-109.

Van Hylckama, T.E.A. 1974. Water use by salt cedars as measured by the water budget method. US Geological Survey Papers.

Van Lill, W.S., Kruger, F.J. & van Dyk, D.B. 1980. The effect of afforestation with *Eucalyprus grandis* Hill ex Maiden and *Pinus patula* Schlecht. Et. Cham. on streamflow from experimental catchments at Mokubalaan, Transvaal. *Journal of Hydrology*, 48:107-118.

Van Tonder, G. Xu, Y. 2000. A guide for the estimation of groundwater recharge in South Africa. Water South Africa. 27(3): 341 - 343 p.

Van Wyk, D. B. 1987. Some effects of afforestation on streamflow in the Western Cape Province, South Africa. *Water SA*, 13:31–36.

Verma, N.K., Lamb, D.W., Reid, N. & Wilson, B. 2014. An allomeric model for estimating DBH of isolated clustered Eucalyptus trees from measurements of crown projection area. *Forest Ecology and Management,* 326:125-132.

Versfeld, D.B. 1988. Rainfall interception in stands of *Pinus radiata* and *Protea neriifolia*. (*In* Research Contribution to Plantation Forestry. Stellenbosch. p. 130-149).

Versfeld, D.B., Everson, C.S. & Pulter, A.G. 1998. The use of vegetation in the amelioration of the impacts of mining on water quality: An assessment of species and water use. WRC Report no. 413/1/98, ISBN no 1868454975, p.172.

Vertessy, R.A., Hatton, T.J., Benyon, R.G. & Dawes, W.R. 1997. Long-term growth and water balance predictions for mountain ash (*E. regnans*) forest catchment subject to clear-felling and regeneration. *Tree Physiology*, 16:221-232.

Webb, J.A., Williams, B.G., Bailue, K., Walker, J. & Anderson, J.W. 2008. Short-term groundwater dynamics at a paddock scale. Proceedings of Water Down Under Adelaide, South Australia. Retrieved from: https://www.researchgate.net/publication/238621818_Short-term_groundwater_dynamics_at_a_paddock_scale?_sg=EEdafDzPz65QsA1MJ2bIQLlc-VY14ltRTzFs-GnnN7VHsMpkh1Wo9e-SKXXE_XAcatDucpc42NA7wuD1A35tTQ

Weiersbye, I.M., Witkowski, E.T.F. & Reichardt, M. 2002. Floristic composition of gold and uranium tailings dams, and adjacent polluted areas, on South Africa's deep level mines. *Bothalia*, 36:101-127.

White, D., Beadle, C. & Worledge, D. 1998. The influence of drought on the relationship between leaf and conducting sapwood area in *Eucalyptus globulus* and *Eucalyptus niten*. *Trees*, 12: 406-414

White, D.A., Dunin, F.X., Turner, N.C., Ward, B.H. & Galbraith, J.H. 2002. Water use by contour-planted belts of tree comprised of four *Eucalyptus* species. *Agricultural Water Management*, 53:133-152.

Winter, T.C. 2001. The concept of hydrologic landscapes. *Journal of American Water Resources Association,* 37(2):335-349.

Wolmerans, J.F. & Guise-Brown, F.H. 1978. The water hazard in deep gold mining of the Far West Witwatersrand – South Africa. SAIMOS-7, Granada, p.329-346

Wullschleger, S.D., Meinzer, F.C. & Vertessy, R.A. 1997. A review of whole-plant water use studies in trees. *Tree Physiology, 18:499-512.*

Zhang, L., Dawes, W.R. & Walker, G.R. 2001. Response of mean annual evapotranspiration to vegetation change at catchment scale. *Water Resources Research,* 37(3):701-708.

Zhou, M.C., Ishidaira, H., Hapuarachchi, H.P., Magome, J., Kiem, A.S. & Takeuchi, K. 2006. Estimating potential evapotranspiration using Shuttleworth-Wallace model and NOAA-AVHRR

NDVI data to feed a distributed hydrological model over the Mekong River Basis. *Journal of Hydrology*, 327:151-173.

Zimmermann, A., Wilcke, W. &Elsenbeer, H. 2007. Spatial and temporal patterns of througfall quantity and quality in a tropical montane forest in Ecuador. *Journal of Hydrology,* 343, 80-96.

Zinke, P.J. 1967. Rainfall interception studies in the United States. *Forest Hydrology*, 137-161.

APPENDIX A - PENMAN-MONTEITH MODEL FORMULATION

Formulation of the simplified E_{rpm} parameters

The formulation of the equation parameters is a combination of the simplifications of the FAO (1992) derived equations and empirical expressions developed specifically from South African Research, as described by Schulze *et al*. (2006).

Atmospheric parameters

Atmospheric pressure (P_a)

Atmospheric pressure (P_a) is defined as the pressured exerted by the weight of the Earth's atmosphere. The atmospheric pressure is a function of altitude viz. Using the equation specifically designed for South African described by Schulze *et al.* (2006), and given an altitude of 1500 meters above mean sea level (mamsl) for the study area, the atmospheric pressure is calculated by:

$$Pa = 101.3[\frac{293 - 0.065z}{293}]^{5.26} \quad (A1)$$

where:

P_a = *Atmospheric pressure (kPa)*

z = *Elevation (mamsl)*

Psychrometric constant (γ)

As the average pressure is constant for each altitude, a psychrometric constant is constant for each location. The psychrometric constant is calculated by:

$$\gamma = 0.665/(10^3 Pa) \quad (A2)$$

where,

γ = *Psychrometric constant (kPa/℃)*

Pa = *Atmospheric pressure (kPa)*

Mean daily air temperature (T_{xd})

The mean daily temperature (T_{xd}) is used in the simplified FAO Penman-Moneteith equation to calculate the slope of saturation vapor pressure (Δ) as the effect of temperature variation on other climatic parameter values are small. The daily maximum air temperature (T_{mxd}) and daily

minimum air temperature (T_{mnd}) are the maximum and minimum air temperature observed during the 24-hour period. Minimum and maximum temperatures were obtained from the South African Weather Services (SAWS). Mean temperature was obtain using the follow equation:

$$Txd = \frac{Tmxd - Tmnd}{2} \qquad (A3)$$

where,

T_{xd} = *Mean daily air temperature (℃)*

T_{mxd} = *Maximum Daily air temperature (℃)*

T_{mnd} = *Minimum daily air temperature (℃)*

Vapour pressure

Water vapour is a gas and its associated pressure contributes to the total atmospheric pressure. The amount of water in the air is related directly to the partial pressure exerted by the water vapor in the air, and is therefore a direct measure of the air water content. When an equilibrium is reached between the water molecules escaping from and returning to evaporating surfaces, the air has reached its maximum capacity of storing moisture. The corresponding pressure to saturated air is called the saturation vapour pressure (e_a). A direct relationship exists between the moisture capacity of the air, and the ambient air temperature – as temperature rises, the moisture storage capacity of the air increases. The relationship between the mean saturation vapour pressure (e_a) and the ambient air temperature, is referred to as the slope of vapour pressure curve (Δ).

Saturated Vapour Pressure (e_a)

As described by Schulze et al. (2006), the saturated vapour pressure is calculated as follow:

$$ea = 0.6108\, exp\{(17.27\, Txd)(Txd + 237.3)\} \qquad (A4)$$

where,

e_a = *Saturated vapour pressure (kPa)*

T_{xd} = *Mean daily temperature (℃)*

Actual vapour pressure (e_d)

As described by Schulze et al. (2006), the actual vapour pressure (e_a) is the variable expressing the atmospheric moisture content through the partial pressure exerted by the water vapour present in the atmosphere. For the simplification of the FAO Penman-Monteith equation, the actual vapour pressure (ed) is calculated as follow:

$$ed = [\frac{293 - 0.0065z}{293}]^{5.26} \quad (A5)$$

where,

e_d = *Actual vapour pressure (kPa)*

z = *Altitude (mamsl)*

Slope of saturation vapour pressure (∆)

The slope of the vapour pressure curve (∆) for the simplified FAO Penman-Monteith equation, specifically for South African research as described by Schulze et al. (2006), is calculated as follow:

$$\Delta = \frac{[4098\left\{0.6108\ exp\left(\frac{(17.27Txd)}{Txd + 237.3}\right)\right\}]}{(Txd + 237.3)^2} \quad (A6)$$

where,

∆ = *Slope of saturation vapour pressure (kPa/℃)*

T_{xd} = *Mean daily temperature (℃)*

Radiation

Net radiation (R_n)

The net radiation is expressed as:

$$Rn = Rsn - Riw \quad (A7)$$

where,

R_n = *Net radiation (MJ/m^2/d)*

R_{sn} = *Solar radiation (MJ/m^2/d)*

R_{iw} = *Net longwave radiation (MJ/m^2/d)*

Calculation of these parameters are based on research by Schulze and Chapman (2006) developed specifically for South African research, as discussed below:

Net shortwave radiation (R_{sn})

The net shortwave radiation (R_{sn}) resulting from the balance between incoming and reflected solar radiation is given by the following equation:

$$Rsn = (1 - a)Rs \qquad (A8)$$

where,

R_{sn} = *Incoming solar radiation ($MJ/m^2/d$)*

α = *Albedo or canopy reflection coefficient*

Based on the IGB classification land cover parameters the albedo for evergreen broadleaf forests are set as 0.2 as suggested by Brutsaert (1982); Shuttleworth (1993) and Fennessey and Kirsten (1994).

Extra-terrestrial radiation (R_a)

The radiation striking a surface perpendicular to the sun's rays at the top of the earth's atmosphere, called the solar constant, is about 0.082 MJ/m^2/day. The solar radiation received at the top of the earth's atmosphere on a horizontal surface is called the extraterrestrial radiation (R_a). If the sun is directly overhead, the angle of incidence is zero and the extra-terrestrial radiation is 0.0820 MJ/m^2/min (Allen *et al.,* 1998). As seasons change, the position of the sun, the length of the day and, hence, R_a change as well. R_a is thus a function of latitude, date and time of day. R_a values used in this study is based on literature, described by the FAO (1992).

Daily temperature range (T_{ra})

For the simplified FAO Penman-Monteith equation, the daily temperature range (T_{ra}) is calculated using the Liu and Scott's (2001) formulation of the daily temperature range, viz. The Lui and Scott (2001) formulation are as follow:

$$Tra = \frac{Tmxd - (Tmnd + (Tmnd + 1))}{2} \qquad (A9)$$

where,

T_{ra} = *Daily transpiration range (℃)*

T_{mxd} = *Maximum daily temperature (℃)*

T_{mnd} = *Minimum daily temperature (℃)*

T_{mnd+1} = *Minimum temperature of the following morning (℃)*

Empirical constants (b and c)

The empirical constants, *b* and *c*, governs the depletion of the solar beam due to cloudiness and rainfall, and for which daily T_{ra} is used as an estimator on the premise that cloudy/rainy conditions are associated with high atmospheric humidity, hence a low diurnal T_{ra} while under clear skies high temperature ranges prevail (Schulze et al., 2006). Optimized values for *b* and *c* by region in South Africa as well as month, as described by Schulze et al. (2006) and in the Bristow and Campbell extinction expression for cloudiness and rainfall, is presented in the table below:

Table A1: Optimize values for b and c, as describe by Bristow and Campbell for semi-arid regions with a low MAP falling predominantly in summer months.

Month	b	c
January	0,0116	1,9204
February	0,0102	1,9666
March	0,0106	1,9611
April	0,109	1,9152
May	0,0149	1,796
June	0,0523	1,3391
July	0,0408	1,3914
August	0,0215	1,618
September	0,0271	1,5165
October	0,0089	1,9218
November	0,0163	1,7438
December	0,0076	2,0669

Solar radiation (R_s)

The calculation of the solar radiation (R_s), is required for computing net longwave radiation. R_s is calculated using the following equation as discussed by Schulze (2006):

$$Rs = 0.75Ra\left(\frac{1-1}{Tra^{2.5}}\right)[1-exp(-bTra^{c})] \qquad (A10)$$

where,

R_s = *Solar radiation (MJ/m^2/d)*

R_a = *Extra-terrestrial radiation (MJ/m^2/d)*

T_{ra} = *Daily transpiration range (℃)*

b and c = *Regression constants (Refer to Table A1)*

Net longwave radiation (R_{iw})

The rate of longwave energy (R_{iw}) emission is proportional to the absolute temperature of the surface raised to the fourth power. The net longwave radiation (R_{iw}) was calculated using the following equation:

$$Riw = 0.5\left(\frac{4.903}{10^9}\right)[((Tmxd + 273.16)^4 + (Tmxd + 273.16)^4](0.34 - 0.14ed^{0.5})[\frac{1.35Rs}{\left\{Ra\left(0.75 + \frac{2z}{10^5}\right)\right\}}] \quad (A11)$$

where,

R_{iw} = *Net longwave radiation (MJ/m^2/d)*

R_a = *Extra-terrestrial radiation (MJ/m^2/d)*

R_s = *Incoming solar radiation (MJ/m^2/d)*

T_{mxd} = *Maximum daily temperature (℃)*

e_d = *Actual vapour pressure (kPa)*

z = *Elevation (mamsl)*

APPENDIX B - SHUTTLEWORTH-WALLACE MODEL FORMULATION

This section describes the formulation of the Shuttleworth-Wallace model, as described by Zhou *et al.* (2005):

Climate related parameters

Parameters e_s, Δ, p, c_p, λ and γ were calculated using the following equations, as described by Shuttleworth (1993) and Allen *et al.* (1998):

Latent heat of vaporisation (λ)

The latent heat of vaporisation (λ) is defined as the energy required to convert 1 unit of water in liquid phase to a gas. λ is estimated with the following equation:

$$\lambda = 2.501 - 0.002361 T_s \qquad (B1)$$

where,

λ = *Latent heat of vaporisation (MJ/kg)*

T_s = *Temperature of water surface (°C)*

However, for simplicity of this model, T_s is substituted with the daily mean air temperature, equal to the arithmetic average of the mean maximum and minimum daily temperatures (T_{max} and T_{min}).

Saturated vapour pressure ($e^0(T)$)

For the simplified Shuttleworth-Walace equation the temperature of the water surface (T_s) is substituted with the daily mean air temperature (T), which is equal to arithmetic average of the daily maximum temperature (T_{max}) and the daily minimum temperature (T_{min}) in °C.

$$e^0(T) = 0.6108\, exp\left(\frac{17.27T}{T+237.3}\right)$$

$$and \qquad (B2)$$

$$e_s = \frac{e0(Tmax)+e0(Tmin)}{2}$$

where,

T = *Mean air temperature (°C)*

$e^0(T)$ = *Saturation vapour pressure (kPa) at T*

T_{max} = *Maximum air temperature (°C)*

T_{min} = *Minimum air temperature (°C)*

e_s = *Mean saturation vapour pressure (kPa)*

Slope of vapour pressure curve (∆)

The slope of the vapour pressure curve (∆) is defined as the relationship between the saturation vapor pressed (kPa) and the atmospheric air temperature (°C).

$$\Delta = \frac{[4098\left\{0.6108\ exp\left(\frac{(17.27T)}{T+237.3}\right)\right\}]}{(T+237.3)^2} \quad \textit{(B3)}$$

where,

Δ, = *Slope of vapour pressure curve (kPa/℃)*

T = *Mean daily air temperature (℃)*

Ideal gas law (ρ)

The following equation is based on the ideal gas law:

$$\rho = \frac{P}{TkvR} \quad \textit{(B4)}$$

where,

P = *Mean air density at constant pressure (kJ/m^3)*

T_{kv} = *Virtual air temperature (K) [273+T]*

R = *Specific gas constant [0.287 kJ/kg]*

Atmospheric pressure (P)

The atmospheric pressure (P) is the pressure exerted by the earth's weight, and is a function of the elevation. P is expressed in kPa and is estimated using the following equation:

$$P = 101.3\ (\frac{293-0.0065z}{293})^{5.26} \quad \textit{(B5)}$$

where,

P = *Atmospheric pressure (kPa)*

z = *Altitude (mamsl)*

Psychrometric constant (γ)

The psychrometric constant (γ) relates the partial pressure of the moisture in the air to the air temperature, and is calculated as follow:

$$\gamma = CpP/\varepsilon\lambda = 0.665 \text{ x } 10\text{-}3P \qquad (B6)$$

where,

γ = *Psychrometric constant (kPa/℃)*

ε = *Ration of molecular weight of water vapour to that of dry air*

c_p = *Specific heat of moist air at constant pressure (MJ/kg/℃)*

For calculation of the psychrometric constant, a value of 1.013 x 10^{-3} MJ/kg for C_p (a value used under average atmospheric conditions), λ = 2.45 MJ/kg (when temperature is about 20°C) and ε = 0.622 was used.

Aerodynamic resistance (r^s_a and r^a_a)

The aerodynamic resistance, r^s_a and r^a_a, are derived by integrating the eddy coefficients within and above the canopy, referred to as the K-theory. Shuttleworth and Gurney (1990) applied the K-theory directly to sparse vegetation canopy through an assumed "preferred" height. Shuttleworth and Gurney (1990) estimated the roughness length and zero plane displacement of the canopy by using a second-order closure theory. The following equations were used for calculating the aerodynamic parameters required for long-term monthly PET:

$$r^s_a = \frac{hc\, exp(n)}{nKh} \text{ x } [exp(-nz_{0g}/h) - exp\{-n(Z_0+d_p)/h_c\}]$$
$$r^s_a = \frac{1}{ku*} ln(\frac{za-d0}{hc-d0}) + \frac{hc}{nKh} [exp\{n[1 - (Z_0 + d_p/h_c]\} -1] \qquad (B7)$$

where,

r^s_a *and* r^a_s = *Aerodynamic resistances (s/m)*

h_c = *Vegetation height (m) [h_c=90m]*

n = *Eddy diffusivity decay constant of vegetation*

k_h = *Eddy diffusion coefficient at the top of the canopy (m^2/s)*

z_{og} = *Roughness length of the ground (m)*

z_0 = *Preferred roughness length (m) [z_0=0.13h_c]*

z_a = *Reference height 2m above vegetation (m) [h_c+2]*

d_p = *Preferred zero plane displacement (m)*

k = *Von Karman Constant [0.41]*

u* = *Friction velocity (m/s)*

d_o = *Zero plane displacement of the canopy (m)*

The above mentioned parameters are calculated as follow: (Montieth, 1973; Choudhury and Monteith, 1998; Shuttleworth and Gurney, 1990; Federer *et al.*, 1996):

$$K_h = k u_* (h_c - d_0) \quad (B8)$$

$$u_* = k u_a / \ln\{(z_a - d_0)/z_0\} \quad (B9)$$

$$d_0 = \begin{cases} h_c - z_{oz}/0.3, & LAI \geq 4 \\ \text{or} & \\ 1.1 h_c \ln[1+(c_d LAI)^{0.25}], & LAI < 4 \end{cases} \quad (B10)$$

$$Z_{oc} = \begin{cases} 0.13 h_c, & h_c \leq 1 \\ 0.139 h_c - 0.09 h_c^2, & 1 < h_c < 10 \\ [-1+\exp(0.909-3.03 z_{oc}/h_c)]^4/4, & h_c \geq 0 \end{cases} \quad (B11)$$

$$d_p = 0.63\, h_c \quad (B12)$$

$$Z_0 = \min\{0.3 (h_c - d_o), \quad z_{0g} + 0.3 h_c (c_d LAI)^{0.5}\} \quad (B13)$$

$$Z_a = h_c + 2 \quad (B14)$$

$$n = \begin{cases} 2.5 & h_c \leq \\ 2.306+0.194 h_c & 1 < h_c < 10 \\ 4.25 & h_c \geq 10 \end{cases} \quad (B15)$$

where,

Assumed c_d = 0.412 for tall vegetation ($h_c \geq 10$) (Shuttleworth and Gurney, 1990), $z_{oc} = 0.05\ h_c$ ($hc \geq 10m$) and n = 4.25 ($h_c \geq 10 = 4.25$) and z_a described as 2m above the vegetation height ($z_a = h_c + 2$). The Von Karman's constant *k* = 0.41.

According to a formulation described by Brutsaert, 1982; Federer *et al.,* 1996), wind speed data obtained from the weather station, is converted to the reference height using a logarithmic profile in that the internal boundary layer height over the weather-ground and canopy surface, are matched and a step change in surface roughness from z_0 to z_{ow} is assumed:

Wind speed at reference height (u_a)

$$u_a = u_w \frac{ln(\frac{zb}{zow})}{ln(\frac{zb}{zo})} X \frac{ln[\frac{za-do}{za}]}{ln(\frac{zw}{zow})} \qquad (B16)$$

where,

u_a	=	*Windspeed at reference height (m/s)*
u_w	=	*Wind speed observed at weather station (m/s)*
z_w	=	*Height of observation (m)*
z_{ow}	=	*Zero plane displacement over the weather station ground (m)*
z_b	=	*Roughness length of the ground (m)*
z_o	=	*Roughness length of canopy (m)*
z_a	=	*Reference height 2m above vegetation (m) [=h_c +2]*
d_o	=	*Zero plane displacement (m) [=.63h_c]*

For the purpose of this study z_w = 10m based on CRU data (New *et al.,* 1999). The zero plane displacement over the weather station ground, is assumed z_{0w} = 0.005m (Federer *et al.,* 1996). The height of internal boundary layer (z_b) is calculated as follow:

$$Z_b = 0.334\ F^{0.875}{}_w\ z^{0.125}{}_{0w} \qquad (B17)$$

where,

z_b	=	*Height of internal boundary layer (m)*
F_w	=	*Fetch at the weather station (m)*

For this study it is assumed that F_w = 5000m (Brutsaert, 1982).

Vegetation parameters

Apart from soil surface resistance, all other resistance factors and components of radiation, are related to the vegetation parameters including Leaf Area Index (LAI), tree height and leaf width. Morphological characteristics changes dynamically with the surrounding environmental conditions and seasons.

Leaf Area Index (LAI)

For this study the SiB2 method, described by Sellers et al. (1996), was used to determine the LAI:

$$= \frac{1 + NDVI}{1 - NDVI} \quad (B18)$$

$$FPAR = FPAR_{min} + (FPAR_{max} - FPAR_{min})\left(\frac{SR - SRmin}{SRmax - SRmin}\right) \quad (B19)$$

$$LAI = (1\text{-}F_{cl})LAI_{max}\frac{ln(1-FPAR)}{ln(1-FPARmax)} + F_{cl}LAI_{max}\frac{FPAR}{FPARmax} \quad (B20)$$

where,

SR	=	*Simple ration of hemisphere reflectance of near-infrared (NIR) light to that for visible*
NDVI	=	*Normalised Difference Vegetation Index*
FPAR	=	*Fraction of Photosynthetically Active Radiation*
$FPAR_{min}$	=	*Minimum Fraction of Photosynthetically Active Radiation*
$FPAR_{max}$	=	*Maximum Fraction of Photosynthetically Active Radiation*
F_{cl}	=	*Fraction of clumped vegetation*
SR_{min}	=	*SR with 5% NDVI population*
SR_{max}	=	*SR with 98% of NDVI population*
LAI_{max}	=	*Maximum Leaf Area Index*

For this study, F_{cl} =0 as described by Sellers et al. (1996) and Mo et al. (2004). SR_{min} =0.039 and SR_{max} = 0.721 (Sellers *et al.,* 1996; Mo *et al.,* 2004), $FPAR_{min}$ = 0.001 and $FPAR_{max}$ = 0.95. LAI_{max} is set as 7 for estimation based on data for evergreen broadleaf forests as described by Anderson et al. (2002).

Prescribed parameters

For the simplified Shuttleworth-Wallace equation, land cover threshold parameter values are adopted from the SiB2 for all vegetation types. Table B1 presents the land cover threshold parameters based on the IGBP classification from literature.

Table B1: SiB2 vegetation classification and land cover threshold parameters based on the IGBP classification

Code	Type	α_m	LAI_{max}	h_c (m)	w_{max} (m)	F_{cl}	$r_{ST\ min}$ (s m^{-1})	$NDVI_{98\%}$	d_{rz} (m)	z_{0g} (m)
1	Evergreen needleleaf forests	0.16	5.5	17.0–17.0	0.001	1.0	150	0.689	2.5	0.020
2	Evergreen broadleaf forests	0.20	7.0	30.0–30.0	0.05	0.0	150	0.611	2.5	0.020
3	Deciduous needleleaf forests	0.15	3.3	17.0–17.0	0.001	1.0	150	0.689	2.5	0.020
4	Deciduous broadleaf forests	0.18	7.0	25.0–25.0	0.08	0.0	150	0.721	2.5	0.020
5	Mixed forests	0.17	5.7	20.0–20.0	0.04	0.5	150	0.721	2.0	0.020
6	Closed shrublands	0.20	4.6	1.5–1.5	0.01	0.0	150	0.674	1.0	0.020
7	Open shrublands	0.15	3.0	1.0–1.0	0.01	1.0	100	0.674	1.0	0.020
8	Woods savannas	0.20	1.5	0.8–0.8	0.01	0.5	180	0.611	1.0	0.020
9	Savannas	0.25	0.9	0.1–0.8	0.01	0.8	120	0.674	1.0	0.020
10	Grasslands	0.23	1.8	0.05–0.8	0.01	0.0	115	0.674	0.5	0.010
11	Permanent wetlands	0.10	6.0	0.05–1.0	0.01	0.0	65	0.674	1.0	0.010
12	Croplands	0.20	7.0	0.0–0.8	0.01	0.0	90	0.674	0.7	0.005
13	Urban and built-up	0.18	–	–	–	0.0	0	0.674	0.001	0.020
14	Cropland/natural vegetation mosaic	0.20	6.5	0.1–0.8	0.01	0.5	120	0.674	1.0	0.010
15	Permanent snow and ice	0.70	–	–	–	0.0	0	0.674	1.3	0.001
16	Barren or sparsely vegetated	0.15	0.3	0.05–0.8	0.01	1.0	120	0.674	1.0	0.001
17	Water bodies	0.08	–	–	–	0.0	0	0.674	1.3	0.001

Code is IGBP number for vegetation type, α_m is maximum albedo (full cover), LAI_{max} is maximum leaf area index, h_c is vegetation height (a function of LAI), w_{max} is maximum vegetation leaf width, F_{cl} is fraction of clumped vegetation, $r_{ST\,min}$ is minimum stomatal resistance of individual leaf, d_{rz} is root depth, z_{0g} is roughness length of substrate ground.
Perennial vegetations: codes from 1 to 8, and annual vegetations: others; tall vegetations: codes from 1 to 5, and short vegetations: others; root depth for codes 15 and 17 represents the average water depth.

Thus, prescribed parameters for this study, based on classification of evergreen broadleaf forests:

- Vegetation height (h_c): Vegetation height for the Shuttleworth and Wallace equation is calculated by differentiating between annual and perennial vegetation. For perennial vegetation, the height is assumed to be constant. As described by Sellers et al. (1996) and Mo et al. (2004). **h_c = 30m**
- Leaf width (w): As decribed by the leaf width is also determined by differentiating between annual and perennial vegetation. For perennial vegetation, **w = wmax = 0.05** (Seller et al. (1996) and Mo et al. (2004)).
- The maximum albedo ($\propto_m$): The maximum albedo-value for deciduous broadleaf forests are **$\propto_m$ = 0.2** for full cover (Brutsaert, 1982; Shuttleworth,1993; Fennesey and Kirshen, 1994).
- Minimum stomatal resistance for an individual leaf (r_{STmin}): For this study, **r_{STmin} = 150** (Rowntree (1991).
- Root depth (d_{rz}): For this study **d_{rz} = 2.5m** (Sellers *et al.,* 1998; Vorosmarty *et al.,* 1998; Ohnuki *et al.,* 2004).
- Roughness length of substrate ground (z_{0g}): For this study, **z_{0g} = 0.02** (Federer *et al.,* 1996).

Bulk stomatal and boundary layer resistance

Bulk stomatal canopy resistance (r^c_s)

The bulk stomatal canopy resistance is influenced by the LAI and various environmental variables. Bulk stomatal resistance of a canopy is express as (Jarvis, 1976):

$$= \frac{1 + NDVI}{1 - NDVI} \quad (B21)$$

$$FPAR = FPAR_{min} + (FPAR_{max} - FPAR_{min})(\frac{SR - SRmin}{SRmax - SRmin}) \quad (B22)$$

$$r^c_s = \frac{rstmin}{LIAe\ \Pi i\ Fi(Xi)} \quad (B23)$$

where,

LAI_e	=	*Effective Leaf Area Index*
r_{stmin}	=	*Minimal stomatal resistance for individual leaves under optimal conditions (s/m)*
r^c_s	=	*Bulk stomatal resistance of the canopy*
SR	=	*Simple ration of hemisphere reflectance of near-infrared (NIR) light to that for visible*
NDVI	=	*Normalised Difference Vegetation Index*
FPAR	=	*Fraction of Photosynthetically Active Radiation*
$FPAR_{min}$	=	*Minimum Fraction of Photosynthetically Active Radiation*
$FPAR_{max}$	=	*Maximum Fraction of Photosynthetically Active Radiation*
SR_{min}	=	*SR with 5% NDVI population*
SR_{max}	=	*SR with 98% of NDVI population*

Where LAI_e is expressed as LAI/2 when LAI ≥ 4 (Gardiol *et al.,* 2003). As per Equation B20, LAI was calculated to be 7.5 for evergreen broadleaf forests. r^c_s was given a maximum value of 50 000s/m, corresponding to the molecular diffusivity of water vapour through leaf cuticula, as suggested by Tourla and Heikinhemo (1998). $F_i(X_i)$ is the environmental stress factors of X_i,0 ≤ $F_i(X_i)$ ≤ 1. Environmental stress factors are calculated as follow:

$$F_1\ (S) = (dS)/(c+S) \quad (B24)$$

$$F_2\ (D) = \begin{cases} 1\text{-}0.238D, & \text{for tall vegetation} \\ Or & \\ 1\text{-}0.409D, & \text{for short vegetation} \end{cases} \quad (B25)$$

$$F_3(T) = \begin{cases} 1, & T \geq 298 \\ 1 - 1.6 \times 10^{-3}(298-T)^2, & 273 < T < 298 \\ 0, & T \leq 273 \end{cases} \quad (B26)$$

where,

S = *Incoming photosynthetically active radiation (PAR)*

d = *1+c/1000*

D = *Coefficient of water vapor pressure deficit* $[D=e_s-e_a]$

T = *Mean Air temperature (℃)*

Incoming photosynthetically active radiation (PAR) is generally in the range of 0.4 -0.72 um flux (W/m^2) and d = 1+c/1000; where c=100 for forest. For simplicity, the net radiation was used rather than the solar radiation and averaged over the day time in daily simulation, as described by Monteith (1995). The coefficient of water vapour pressure deficit for this study is representative for tall vegetation data as suggested by Noilhan and Planton, (1998); and Lhomme *et al.* (1998). When the air temperature exceeds 25°C, stomata opens; however less than 0°C, stomata closes. For this study, temperature exceeded 298°K, therefore the temperature function of 1 is used (Shuttleworth and Wallace, 1985).

Bulk boundary layer resistance of canopy (r^c_a)

The bulk boundary layer resistance of the canopy is calculated as follow (Shuttleworth and Wallace, 1985; Brisson *et al.,* 1998):

$$rca = rb\sigma b/LAI \quad (B27)$$

where,

σb = *Shielding factor*

r_b = *Canopy characteristic leaf width (s/m)*

r^c_a = *Bulk boundary layer resistance of canopy (s/m)*

LAI = *Leaf Area Index*

Where σ_b = 0.5 as described by Shuttleworth and Wallace (1985) and Brisson *et al.,* (1998). R_b is obtained by (Shuttleworth and Wallace, 1998; Brisson *et al.,* 1998):

$$r_b = \frac{100}{n}\left(\frac{w}{uh}\right)^{0.5}\left[1 - exp\left(\frac{-n}{2}\right)^{-1}\right. \quad (B28)$$

where,

u_h = *Wind speed at the top of the canopy*

r_b = *Canopy characteristic leaf width (m)*

n = *Eddy coefficient* $[h_{c=} 4.25 \quad h_c \geq 10]$

u_h is estimated by substituting the vegetation height (h_c) with the reference height (z_a).

Surface resistance of substrate soil (r^s_s)

Generally surface resistance of the substrate soil (r^s_s) is calculated as follow:

$$r_s^s = \frac{\tau l}{pDv} \qquad (B29)$$

$$r_s^s = 10exp\,[\alpha\theta(\theta min - \theta], \qquad \theta \leq \theta \qquad (B30)$$

where,

r_s^s = *Surface resistance of substrate soil (s/m)*

τl = *Depth of the upper dry soil layer (m)*

p = *Soil porosity*

θ = *Soil moisture content in the top 1cm*

θmin = *Empirical minimum value which soil is able to deliver vapour at a potential rate*

$\alpha\theta$ = *Coefficient*

For this study, r^s_s is set as 500s/m for potential evapotranspiration estimation, as suggested by Shuttleworth and Wallace (1985), and Federer et al. (1996). This value for r_s^s is reasoned by results from research over a large variety of soil types as described by Fuchs and Tanner, 1968; Camillo and Gurney, 1986; Mahfouf and Noilhan, 1991; Griend and Owe 1994; Lund and Soegaard, 2003; Rawls and Brakensiek, 1985.

Net radiation over vegetation canopy (R_{nl})

The Shuttleworth-Wallace model is highly dependent on the accuracy of the net radiation. For the application of net radiation in the Shuttleworth-Wallace model, solar radiation is estimated using the following equations:

$$R_n = R_{ns} - R_{nl} \qquad (B31)$$

$$R_{ns} = (1-\alpha)\, R_{solar} \qquad (B32)$$

$$R_{nl} = \sigma \left(\frac{Tmax+Tmin}{2}\right) x\, (0.34-0.14\sqrt{ea}) \left(1.35\frac{Rsolar}{Ro\ solar}\right) - 0.35 \qquad (B33)$$

where,

R_n = *Net Solar Radiation (MJ/m^2/d)*

R_{nl} = *Net loss of energy in longwave radiation to the atmosphere (MJ/m^2/d)*

R_{solar} = *Solar Radiation (MJ/m^2/d)*

R^0_{solar} = *Clear-sky solar radiation (MJ/m^2/d)*

R_{ns} = *Net solar radiation (MJ/m^2/d)*

T_{min} = *Minimum air temperature (K)*

T_{max} = *Maximum air temperature (K)*

α = *Land surface albedo*

σ = *Stefan-Boltzmann content [4.903 x 10^{-9}MJ/m^2/d]*

e_a = *Actual Vapour pressure (kPa)*

R_{solar} and R^0_{solar} values in MJ/m^2/d for the study area, were obtained from Solargis Direct Horizontal Irradiation (DHI) and Direct Normal Irradiation (DMI) maps. The land and surface albedo are estimated using the following equation:

$$\alpha = \alpha_m - (\alpha_m - \alpha_s)\, exp\,(0.56LAI) \qquad (B34)$$

where,

α = *Albedo of vegetation*

α_m = *Maximum albedo for vegetation*

α_s = *Albedo for bare soils*

LAI = *Leaf Area Index*

Albedo changes with the vegetation type. For the purpose of this study, α_m was set as 0.2, representing evergreen broadleaf forests, as suggested by Brutsaert (1982); Shuttleworth (1993), Fennesey and Kirshen (1999), and presented in B1. For the estimation of potential ET, the α_s – value for this model is set as 0.1 for bare wet soils, as described by Shuttleworth and Wallace (1985).

Radiation flux over the substrate surface (R^s_n)

The radiation flux over the substrate surface, R^s_n, is calculated by applying the Beer's law relationship expressed as:

$$Rsn = Rn\, exp\,(-CrLAI) \qquad (B35)$$

where,

R^s_n = *Radiation flux over the substrate surface (MJ/m^2/d)*

C_r = *Extinction coefficient of vegetation for net radiation*

LAI = *Leaf Area Index*

R_n = *Net radiation ($MJ/m^2/d$)*

The C_r value varies between 0.3 and 0.8 for different vegetation types, as presented in research by Monteith (1973); Kelliher et al. (1995); Lafleur and Ross (1990); Brisson et al. (1998). However, for this study C_r variations in response to structural vegetation differences are ignores. For this reason, $C_r = 0.5$ as described by Shuttleworth and Wallace (1985), Stannard (1993) and Mo et al. (2004).

Soil heat flux (G)

The soil heat flux (G) is defined as the energy required to heat the soil surface. For this study, G was estimated using the equation described by Allen et al. (1998):

$$G = 0.07\,(T_{i+1} - T_{i-1}) \qquad (B36)$$

where,

G = *Soil heat flux (°C)*

T_{i+1} = *Mean air temperature for the following month (°C)*

T_{i-1} = *Mean air temperature for the previous month (°C)*

APPENDIX C – SIMULATED LEAF TEMPERATURE CALCULATIONS

Control Inputs

R_{abs} [W/m^2]	650
Surface	Popular Leaf
Leaf Width [m]	0.01
Wind Speed [m/s]	1.6

Date	Time	Temp [°C]	Leaf [°C]	$Leaf_{sim}$ [°C]	Rni [W/m^2]	B [W/m^2]	e_s(T) [kPa]	e_a [kPa]	D [kPa]	s [C^{-1}]	g_{Ha} [mol/m^2/s]	g_{va} [mol/m^2/s]	g_r [mol/m2/s]	g_{Hr} [mol/m^2/s]	v [mol/m^2/s]	γ* [C^{-1}]	Relative Humidity (%)	SC [mmol/m^2/s]
10/12/2015	06:00:00	18.4	16.0	21.2	242.4	415.9	2.0	2.1	0.00	0.0012	2.391	2.603	0.193	2.584	0.2097	0.0082	24.0	1.6
10/12/2015	06:30:00	21.0	20.0	23.6	227.8	430.9	2.4	2.5	0.00	0.0014	2.391	2.603	0.199	2.589	0.2097	0.0082	31.0	3.0
10/12/2015	07:00:00	23.6	22.0	25.9	213.1	445.8	2.8	2.9	0.00	0.0016	2.391	2.603	0.204	2.594	0.2097	0.0082	38.0	9.0
10/12/2015	07:30:00	24.9	26.0	27.1	206.1	453.0	3.0	3.1	0.00	0.0017	2.391	2.603	0.206	2.597	0.2097	0.0082	49.0	13.0
10/12/2015	08:00:00	26.1	28.0	28.2	199.1	460.1	3.2	3.4	0.00	0.0019	2.391	2.603	0.209	2.599	0.2097	0.0083	60.0	18.0
10/12/2015	08:30:00	27.2	30.0	29.2	192.9	466.4	3.5	3.6	0.00	0.0020	2.391	2.603	0.211	2.602	0.2097	0.0083	57.0	24.0
10/12/2015	09:00:00	28.3	31.0	30.3	186.7	472.8	3.7	3.8	0.00	0.0021	2.391	2.603	0.213	2.604	0.2097	0.0083	54.0	29.0
10/12/2015	09:30:00	29.1	32.0	30.9	182.5	477.1	3.9	4.0	0.00	0.0022	2.391	2.603	0.215	2.605	0.2097	0.0083	49.0	34.0
10/12/2015	10:00:00	29.8	32.0	31.6	178.3	481.4	4.1	4.2	0.00	0.0023	2.391	2.603	0.216	2.607	0.2097	0.0083	44.0	38.0
10/12/2015	10:30:00	30.3	33.0	32.0	175.7	483.9	4.2	4.3	0.00	0.0023	2.391	2.603	0.217	2.608	0.2097	0.0083	39.5	45.0
10/12/2015	11:00:00	30.7	33.0	32.5	173.2	486.5	4.3	4.4	0.00	0.0024	2.391	2.603	0.218	2.609	0.2097	0.0083	35.0	50.6
10/12/2015	11:30:00	31.3	33.0	33.0	169.8	490.0	4.5	4.6	0.00	0.0025	2.391	2.603	0.219	2.610	0.2097	0.0083	29.5	50.2
10/12/2015	12:00:00	31.9	32.0	33.6	166.5	493.4	4.7	4.7	0.00	0.0026	2.391	2.603	0.220	2.611	0.2097	0.0083	24.0	49.6
10/12/2015	12:30:00	32.5	33.0	34.1	163.4	496.6	4.8	4.9	0.00	0.0026	2.391	2.603	0.221	2.612	0.2097	0.0083	23.0	46.0
10/12/2015	13:00:00	33.0	34.0	34.6	160.3	499.7	5.0	5.0	0.00	0.0027	2.391	2.603	0.223	2.613	0.2097	0.0083	22.0	43.0
10/12/2015	13:30:00	32.7	35.0	34.3	162.0	498.0	4.9	4.9	0.00	0.0027	2.391	2.603	0.222	2.613	0.2097	0.0083	20.5	37.0
10/12/2015	14:00:00	32.4	36.0	34.0	163.6	496.3	4.8	4.9	0.00	0.0026	2.391	2.603	0.221	2.612	0.2097	0.0083	19.0	30.0
10/12/2015	14:30:00	32.8	35.0	34.3	161.7	498.3	4.9	5.0	0.00	0.0027	2.391	2.603	0.222	2.613	0.2097	0.0083	19.5	26.0
10/12/2015	15:00:00	33.1	33.0	34.7	159.7	500.3	5.0	5.1	0.00	0.0027	2.391	2.603	0.223	2.613	0.2097	0.0083	20.0	25.8
10/12/2015	15:30:00	32.5	31.0	34.1	163.4	496.6	4.8	4.9	0.00	0.0026	2.391	2.603	0.221	2.612	0.2097	0.0083	21.5	28.0
10/12/2015	16:00:00	31.8	30.0	33.5	167.0	492.8	4.6	4.7	0.00	0.0025	2.391	2.603	0.220	2.611	0.2097	0.0083	23.0	24.0
10/12/2015	16:30:00	31.8	30.0	33.4	167.3	492.6	4.6	4.7	0.00	0.0025	2.391	2.603	0.220	2.611	0.2097	0.0083	23.5	19.0
10/12/2015	17:00:00	31.7	29.0	33.4	167.6	492.3	4.6	4.7	0.00	0.0025	2.391	2.603	0.220	2.611	0.2097	0.0083	24.0	16.0
10/12/2015	17:30:00	31.5	27.0	33.1	169.0	490.8	4.5	4.6	0.00	0.0025	2.391	2.603	0.219	2.610	0.2097	0.0083	28.0	10.0
10/12/2015	18:00:00	31.2	26.0	32.9	170.4	489.4	4.5	4.5	0.00	0.0025	2.391	2.603	0.219	2.610	0.2097	0.0083	32.0	6.0

APPENDIX D – MONTHLY ET MODEL RESULTS

Jan-15	Temp [°C]	$Leaf_{sim}$ [°C]	Rni [W/m^2]	B [W/m^2]	$e_s(T)$ [kPa]	e_a [kPa]	D [kPa]	s [C^{-1}]	g_{Ha} [$mol/m^2/s$]	g_{va} [$mol/m^2/s$]	g_r [mol/m2/s]	g_{Hr} [$mol/m^2/s$]	v [$mol/m^2/s$]	γ* [C^{-1}]	SC [$mmol/m^2/s$]	n	T [K]	P [atm]	V [m^3]	mm/hr
06:00:00	16.9	25.0	700.3	407.3	1.8	1.9	0.00	0.0011	2.391	2.603	0.190	2.581	0.2097	0.0082	10.1	0.01015	289.9	0.0190	0.013	0.046
07:00:00	18.7	26.6	690.2	417.7	2.0	2.2	0.00	0.0013	2.391	2.603	0.194	2.585	0.2097	0.0082	13.7	0.01370	291.7	0.0213	0.015	0.055
08:00:00	20.6	28.3	679.4	428.7	2.3	2.4	0.00	0.0014	2.391	2.603	0.198	2.588	0.2097	0.0082	18.8	0.01885	293.6	0.0240	0.019	0.068
09:00:00	22.1	29.6	670.9	437.4	2.5	2.7	0.00	0.0015	2.391	2.603	0.201	2.591	0.2097	0.0082	24.2	0.02422	295.1	0.0263	0.022	0.080
10:00:00	23.5	30.8	663.5	444.9	2.8	2.9	0.00	0.0016	2.391	2.603	0.203	2.594	0.2097	0.0082	30.1	0.03011	296.5	0.0285	0.026	0.093
11:00:00	24.8	31.9	655.9	452.7	3.0	3.1	0.00	0.0017	2.391	2.603	0.206	2.597	0.2097	0.0082	37.7	0.03765	297.8	0.0309	0.030	0.107
12:00:00	25.8	32.8	650.2	458.5	3.2	3.3	0.00	0.0018	2.391	2.603	0.208	2.599	0.2097	0.0083	44.5	0.04448	298.8	0.0328	0.033	0.120
13:00:00	26.4	33.3	647.2	461.6	3.3	3.4	0.00	0.0019	2.391	2.603	0.209	2.600	0.2097	0.0083	48.6	0.04864	299.4	0.0339	0.035	0.127
14:00:00	26.7	33.5	645.5	463.3	3.4	3.5	0.00	0.0019	2.391	2.603	0.210	2.600	0.2097	0.0083	51.1	0.05108	299.7	0.0345	0.036	0.131
15:00:00	26.1	33.1	648.5	460.3	3.3	3.4	0.00	0.0019	2.391	2.603	0.209	2.599	0.2097	0.0083	46.8	0.04679	299.1	0.0334	0.034	0.124
16:00:00	26.2	33.1	648.0	460.8	3.3	3.4	0.00	0.0019	2.391	2.603	0.209	2.600	0.2097	0.0083	47.5	0.04746	299.2	0.0336	0.035	0.125
17:00:00	25.9	32.9	649.8	458.9	3.2	3.3	0.00	0.0018	2.391	2.603	0.208	2.599	0.2097	0.0083	45.1	0.04505	298.9	0.0330	0.034	0.121
18:00:00	24.5	31.6	657.7	450.8	2.9	3.1	0.00	0.0017	2.391	2.603	0.205	2.596	0.2097	0.0082	35.7	0.03566	297.5	0.0303	0.029	0.103

Feb-15	Temp [°C]	$Leaf_{sim}$ [°C]	Rni [W/m^2]	B [W/m^2]	$e_s(T)$ [kPa]	e_a [kPa]	D [kPa]	s [C^{-1}]	g_{Ha} [$mol/m^2/s$]	g_{va} [$mol/m^2/s$]	g_r [mol/m2/s]	g_{Hr} [$mol/m^2/s$]	v [$mol/m^2/s$]	γ* [C^{-1}]	SC [$mmol/m^2/s$]	n	T [K]	P [atm]	V [m^3]	mm/hr
06:00:00	15.8	22.9	600.8	401.2	1.7	1.8	0.00	0.0011	2.391	2.603	0.188	2.579	0.2097	0.0082	6.7	0.00670	288.8	0.0177	0.009	0.032
07:00:00	17.2	24.1	592.9	409.3	1.9	2.0	0.00	0.0012	2.391	2.603	0.191	2.582	0.2097	0.0082	8.5	0.00851	290.2	0.0194	0.010	0.038
08:00:00	20.3	26.8	575.8	426.7	2.3	2.4	0.00	0.0014	2.391	2.603	0.197	2.588	0.2097	0.0082	14.2	0.01417	293.3	0.0235	0.015	0.052
09:00:00	22.4	28.6	564.0	438.7	2.6	2.7	0.00	0.0015	2.391	2.603	0.201	2.592	0.2097	0.0082	20.1	0.02015	295.4	0.0267	0.018	0.066
10:00:00	23.9	30.0	555.4	447.5	2.8	3.0	0.00	0.0017	2.391	2.603	0.204	2.595	0.2097	0.0082	26.0	0.02601	296.9	0.0293	0.022	0.078
11:00:00	25.4	31.3	547.2	455.9	3.1	3.2	0.00	0.0018	2.391	2.603	0.207	2.598	0.2097	0.0083	33.3	0.03326	298.4	0.0319	0.025	0.092
12:00:00	26.7	32.4	539.8	463.4	3.4	3.5	0.00	0.0019	2.391	2.603	0.210	2.601	0.2097	0.0083	41.4	0.04136	299.7	0.0345	0.029	0.106
13:00:00	27.6	33.2	534.6	468.8	3.6	3.7	0.00	0.0020	2.391	2.603	0.212	2.602	0.2097	0.0083	48.3	0.04833	300.6	0.0364	0.033	0.118
14:00:00	28.0	33.6	532.3	471.1	3.7	3.8	0.00	0.0021	2.391	2.603	0.213	2.603	0.2097	0.0083	51.7	0.05167	301.0	0.0373	0.034	0.123
15:00:00	28.0	33.6	532.3	471.1	3.7	3.8	0.00	0.0021	2.391	2.603	0.213	2.603	0.2097	0.0083	51.7	0.05167	301.0	0.0373	0.034	0.123
16:00:00	28.0	33.6	532.5	470.9	3.6	3.8	0.00	0.0021	2.391	2.603	0.212	2.603	0.2097	0.0083	51.4	0.05139	301.0	0.0372	0.034	0.123
17:00:00	27.6	33.2	534.6	468.7	3.6	3.7	0.00	0.0020	2.391	2.603	0.212	2.602	0.2097	0.0083	48.3	0.04830	300.6	0.0364	0.033	0.118
18:00:00	25.9	31.7	544.2	458.9	3.2	3.3	0.00	0.0018	2.391	2.603	0.208	2.599	0.2097	0.0083	36.3	0.03631	298.9	0.0330	0.027	0.097

Mar-15	Temp [°C]	$Leaf_{sim}$ [°C]	Rni [W/m^2]	B [W/m^2]	$e_s(T)$ [kPa]	e_a [kPa]	D [kPa]	s [C^{-1}]	g_{Ha} [$mol/m^2/s$]	g_{va} [$mol/m^2/s$]	g_r [mol/m2/s]	g_{Hr} [$mol/m^2/s$]	v [$mol/m^2/s$]	γ* [C^{-1}]	SC [$mmol/m^2/s$]	n	T [K]	P [atm]	V [m^3]	mm/hr
06:00:00	14.8	21.0	523.1	395.2	1.6	1.7	0.00	0.0010	2.391	2.603	0.186	2.577	0.2097	0.0082	4.7	0.00466	287.8	0.0166	0.007	0.024
07:00:00	15.4	21.5	519.9	398.4	1.7	1.7	0.00	0.0010	2.391	2.603	0.187	2.578	0.2097	0.0082	5.1	0.00513	288.4	0.0172	0.007	0.025
08:00:00	18.0	23.8	505.1	413.5	2.0	2.1	0.00	0.0012	2.391	2.603	0.192	2.583	0.2097	0.0082	8.0	0.00802	291.0	0.0203	0.009	0.034
09:00:00	20.1	25.7	493.0	426.0	2.2	2.4	0.00	0.0014	2.391	2.603	0.197	2.587	0.2097	0.0082	11.6	0.01157	293.1	0.0233	0.012	0.043
10:00:00	22.0	27.4	482.7	436.5	2.5	2.6	0.00	0.0015	2.391	2.603	0.200	2.591	0.2097	0.0082	15.8	0.01579	295.0	0.0261	0.015	0.053
11:00:00	23.5	28.7	474.1	445.3	2.8	2.9	0.00	0.0016	2.391	2.603	0.204	2.594	0.2097	0.0082	20.5	0.02046	296.5	0.0286	0.017	0.063
12:00:00	24.7	29.8	467.4	452.1	3.0	3.1	0.00	0.0017	2.391	2.603	0.206	2.597	0.2097	0.0082	25.0	0.02501	297.7	0.0307	0.020	0.072
13:00:00	25.6	30.6	462.1	457.5	3.2	3.3	0.00	0.0018	2.391	2.603	0.208	2.598	0.2097	0.0083	29.3	0.02931	298.6	0.0325	0.022	0.080
14:00:00	25.9	30.9	460.4	459.2	3.2	3.3	0.00	0.0019	2.391	2.603	0.208	2.599	0.2097	0.0083	30.8	0.03085	298.9	0.0330	0.023	0.082
15:00:00	26.2	31.1	458.9	460.7	3.3	3.4	0.00	0.0019	2.391	2.603	0.209	2.600	0.2097	0.0083	32.3	0.03228	299.2	0.0336	0.024	0.085
16:00:00	25.5	30.5	463.0	456.5	3.1	3.3	0.00	0.0018	2.391	2.603	0.207	2.598	0.2097	0.0083	28.5	0.02852	298.5	0.0321	0.022	0.078
17:00:00	24.4	29.5	469.1	450.4	2.9	3.1	0.00	0.0017	2.391	2.603	0.205	2.596	0.2097	0.0082	23.8	0.02378	297.4	0.0302	0.019	0.069
18:00:00	23.1	28.4	476.3	443.0	2.7	2.8	0.00	0.0016	2.391	2.603	0.203	2.593	0.2097	0.0082	19.1	0.01915	296.1	0.0279	0.017	0.060

Apr-15	Temp [°C]	$Leaf_{sim}$ [°C]	Rni [W/m^2]	B [W/m^2]	$e_s(T)$ [kPa]	e_a [kPa]	D [kPa]	s [C^{-1}]	g_{Ha} [$mol/m^2/s$]	g_{va} [$mol/m^2/s$]	g_r [mol/m2/s]	g_{Hr} [$mol/m^2/s$]	v [$mol/m^2/s$]	γ* [C^{-1}]	SC [$mmol/m^2/s$]	n	T [K]	P [atm]	V [m^3]	mm/hr
06:00:00	12.4	17.3	409.0	381.5	1.4	1.4	0.00	0.0009	2.391	2.603	0.181	2.572	0.2097	0.0082	2.3	0.00232	285.4	0.0142	0.004	0.014
07:00:00	12.5	17.4	408.6	381.9	1.4	1.4	0.00	0.0009	2.391	2.603	0.181	2.572	0.2097	0.0082	2.4	0.00235	285.5	0.0143	0.004	0.014
08:00:00	15.7	20.3	390.3	400.6	1.7	1.8	0.00	0.0011	2.391	2.603	0.188	2.579	0.2097	0.0082	4.1	0.00412	288.7	0.0176	0.006	0.020
09:00:00	18.3	22.6	375.7	415.5	2.0	2.1	0.00	0.0012	2.391	2.603	0.193	2.584	0.2097	0.0082	6.4	0.00642	291.3	0.0208	0.007	0.027
10:00:00	20.3	24.4	364.8	426.6	2.3	2.4	0.00	0.0014	2.391	2.603	0.197	2.588	0.2097	0.0082	9.0	0.00896	293.3	0.0234	0.009	0.033
11:00:00	21.7	25.7	356.5	435.1	2.5	2.6	0.00	0.0015	2.391	2.603	0.200	2.591	0.2097	0.0082	11.6	0.01155	294.7	0.0257	0.011	0.039
12:00:00	23.0	26.8	349.6	442.1	2.7	2.8	0.00	0.0016	2.391	2.603	0.202	2.593	0.2097	0.0082	14.3	0.01426	296.0	0.0277	0.013	0.045
13:00:00	23.6	27.4	345.9	445.9	2.8	2.9	0.00	0.0016	2.391	2.603	0.204	2.594	0.2097	0.0082	16.0	0.01596	296.6	0.0288	0.014	0.049
14:00:00	23.7	27.5	345.3	446.5	2.8	2.9	0.00	0.0016	2.391	2.603	0.204	2.595	0.2097	0.0082	16.3	0.01628	296.7	0.0290	0.014	0.049
15:00:00	23.2	27.0	348.4	443.4	2.7	2.8	0.00	0.0016	2.391	2.603	0.203	2.594	0.2097	0.0082	14.8	0.01480	296.2	0.0280	0.013	0.046
16:00:00	22.7	26.6	350.9	440.8	2.6	2.8	0.00	0.0016	2.391	2.603	0.202	2.593	0.2097	0.0082	13.7	0.01372	295.7	0.0273	0.012	0.044
17:00:00	21.4	25.4	358.2	433.3	2.4	2.6	0.00	0.0015	2.391	2.603	0.199	2.590	0.2097	0.0082	10.9	0.01095	294.4	0.0252	0.011	0.038
18:00:00	19.4	23.6	369.6	421.8	2.1	2.3	0.00	0.0013	2.391	2.603	0.195	2.586	0.2097	0.0082	7.8	0.00775	292.4	0.0222	0.008	0.030

May-15	Temp [°C]	$Leaf_{sim}$ [°C]	Rni [W/m^2]	B [W/m^2]	$e_s(T)$ [kPa]	e_a [kPa]	D [kPa]	s [C^{-1}]	g_{Ha} [$mol/m^2/s$]	g_{va} [$mol/m^2/s$]	g_r [mol/m2/s]	g_{Hr} [$mol/m^2/s$]	v [$mol/m^2/s$]	γ* [C^{-1}]	SC [$mmol/m^2/s$]	n	T [K]	P [atm]	V [m^3]	mm/hr
06:00:00	9.1	13.1	330.8	362.5	1.1	1.2	0.00	0.0007	2.391	2.603	0.175	2.565	0.2097	0.0081	1.1	0.00105	282.1	0.0114	0.002	0.008
07:00:00	9.0	13.1	331.1	362.2	1.1	1.2	0.00	0.0007	2.391	2.603	0.175	2.565	0.2097	0.0081	1.0	0.00104	282.0	0.0114	0.002	0.008
08:00:00	14.2	17.7	302.4	391.6	1.5	1.6	0.00	0.0010	2.391	2.603	0.185	2.575	0.2097	0.0082	2.5	0.00252	287.2	0.0159	0.004	0.013
09:00:00	18.5	21.7	278.1	416.4	2.0	2.1	0.00	0.0012	2.391	2.603	0.193	2.584	0.2097	0.0082	5.3	0.00534	291.5	0.0210	0.006	0.022
10:00:00	20.7	23.7	265.4	429.3	2.3	2.4	0.00	0.0014	2.391	2.603	0.198	2.589	0.2097	0.0082	7.9	0.00789	293.7	0.0241	0.008	0.028
11:00:00	22.4	25.3	255.9	439.0	2.6	2.7	0.00	0.0015	2.391	2.603	0.201	2.592	0.2097	0.0082	10.6	0.01060	295.4	0.0268	0.010	0.035
12:00:00	23.5	26.2	249.8	445.2	2.8	2.9	0.00	0.0016	2.391	2.603	0.204	2.594	0.2097	0.0082	12.8	0.01278	296.5	0.0286	0.011	0.039
13:00:00	24.3	26.9	245.5	449.6	2.9	3.0	0.00	0.0017	2.391	2.603	0.205	2.596	0.2097	0.0082	14.6	0.01458	297.3	0.0299	0.012	0.043
14:00:00	24.9	27.5	242.2	453.0	3.0	3.1	0.00	0.0017	2.391	2.603	0.206	2.597	0.2097	0.0082	16.2	0.01615	297.9	0.0310	0.013	0.046
15:00:00	24.8	27.4	242.4	452.8	3.0	3.1	0.00	0.0017	2.391	2.603	0.206	2.597	0.2097	0.0082	16.1	0.01606	297.8	0.0309	0.013	0.046
16:00:00	23.3	26.0	251.1	443.9	2.7	2.9	0.00	0.0016	2.391	2.603	0.203	2.594	0.2097	0.0082	12.3	0.01228	296.3	0.0282	0.011	0.038
17:00:00	21.9	24.8	258.8	436.0	2.5	2.6	0.00	0.0015	2.391	2.603	0.200	2.591	0.2097	0.0082	9.7	0.00966	294.9	0.0259	0.009	0.032
18:00:00	18.1	21.3	280.2	414.2	2.0	2.1	0.00	0.0012	2.391	2.603	0.193	2.583	0.2097	0.0082	5.0	0.00500	291.1	0.0205	0.006	0.021

Jun-15	Temp [°C]	$Leaf_{sim}$ [°C]	Rni [W/m^2]	B [W/m^2]	$e_s(T)$ [kPa]	e_a [kPa]	D [kPa]	s [C^{-1}]	g_{Ha} [$mol/m^2/s$]	g_{va} [$mol/m^2/s$]	g_r [mol/m2/s]	g_{Hr} [$mol/m^2/s$]	v [$mol/m^2/s$]	γ* [C^{-1}]	SC [$mmol/m^2/s$]	n	T [K]	P [atm]	V [m^3]	mm/hr
06:00:00	4.5	8.3	303.8	336.3	0.8	0.8	0.00	0.0006	2.391	2.603	0.166	2.556	0.2097	0.0081	0.4	0.00042	277.5	0.0083	0.001	0.004
07:00:00	4.5	8.3	304.0	336.1	0.8	0.8	0.00	0.0006	2.391	2.603	0.165	2.556	0.2097	0.0081	0.4	0.00042	277.5	0.0083	0.001	0.004
08:00:00	7.9	11.4	284.9	355.6	1.0	1.1	0.00	0.0007	2.391	2.603	0.172	2.563	0.2097	0.0081	0.8	0.00075	280.9	0.0105	0.002	0.006
09:00:00	12.3	15.4	260.1	380.8	1.4	1.4	0.00	0.0009	2.391	2.603	0.181	2.572	0.2097	0.0082	1.6	0.00162	285.3	0.0141	0.003	0.010
10:00:00	14.5	17.4	247.7	393.5	1.6	1.6	0.00	0.0010	2.391	2.603	0.185	2.576	0.2097	0.0082	2.4	0.00238	287.5	0.0163	0.003	0.012
11:00:00	15.8	18.6	240.6	400.8	1.7	1.8	0.00	0.0011	2.391	2.603	0.188	2.579	0.2097	0.0082	3.0	0.00296	288.8	0.0177	0.004	0.014
12:00:00	17.0	19.7	233.5	408.0	1.8	1.9	0.00	0.0011	2.391	2.603	0.191	2.581	0.2097	0.0082	3.7	0.00369	290.0	0.0191	0.005	0.017
13:00:00	17.7	20.4	229.4	412.1	1.9	2.0	0.00	0.0012	2.391	2.603	0.192	2.583	0.2097	0.0082	4.2	0.00419	290.7	0.0200	0.005	0.018
14:00:00	18.3	20.9	226.2	415.4	2.0	2.1	0.00	0.0012	2.391	2.603	0.193	2.584	0.2097	0.0082	4.6	0.00463	291.3	0.0208	0.005	0.019
15:00:00	18.6	21.1	224.9	416.8	2.0	2.1	0.00	0.0012	2.391	2.603	0.194	2.584	0.2097	0.0082	4.8	0.00482	291.6	0.0211	0.005	0.020
16:00:00	17.1	19.8	233.3	408.2	1.8	1.9	0.00	0.0011	2.391	2.603	0.191	2.581	0.2097	0.0082	3.7	0.00372	290.1	0.0192	0.005	0.017
17:00:00	15.9	18.7	239.6	401.7	1.7	1.8	0.00	0.0011	2.391	2.603	0.188	2.579	0.2097	0.0082	3.1	0.00305	288.9	0.0178	0.004	0.015
18:00:00	12.7	15.7	258.0	383.0	1.4	1.5	0.00	0.0009	2.391	2.603	0.182	2.572	0.2097	0.0082	1.7	0.00173	285.7	0.0144	0.003	0.010

Jul-15	Temp [°C]	$Leaf_{sim}$ [°C]	Rni [W/m^2]	B [W/m^2]	$e_s(T)$ [kPa]	e_a [kPa]	D [kPa]	s [C^{-1}]	g_{Ha} [$mol/m^2/s$]	g_{va} [$mol/m^2/s$]	g_r [mol/m2/s]	g_{Hr} [$mol/m^2/s$]	v [$mol/m^2/s$]	γ* [C^{-1}]	SC [$mmol/m^2/s$]	n	T [K]	P [atm]	V [m^3]	mm/hr
06:00:00	5.5	9.2	298.1	342.1	0.9	0.9	0.00	0.0006	2.391	2.603	0.168	2.558	0.2097	0.0081	0.5	0.00050	278.5	0.0089	0.001	0.005
07:00:00	5.4	9.1	298.7	341.5	0.9	0.9	0.00	0.0006	2.391	2.603	0.167	2.558	0.2097	0.0081	0.5	0.00049	278.4	0.0089	0.001	0.005
08:00:00	8.3	11.8	282.5	358.0	1.1	1.1	0.00	0.0007	2.391	2.603	0.173	2.564	0.2097	0.0081	0.8	0.00081	281.3	0.0108	0.002	0.006
09:00:00	12.2	15.3	260.9	380.1	1.4	1.4	0.00	0.0009	2.391	2.603	0.181	2.571	0.2097	0.0082	1.6	0.00158	285.2	0.0140	0.003	0.010
10:00:00	14.7	17.6	246.6	394.6	1.6	1.7	0.00	0.0010	2.391	2.603	0.186	2.577	0.2097	0.0082	2.5	0.00246	287.7	0.0165	0.004	0.013
11:00:00	16.5	19.2	236.5	405.0	1.8	1.9	0.00	0.0011	2.391	2.603	0.189	2.580	0.2097	0.0082	3.4	0.00337	289.5	0.0185	0.004	0.016
12:00:00	17.7	20.4	229.4	412.2	1.9	2.0	0.00	0.0012	2.391	2.603	0.192	2.583	0.2097	0.0082	4.2	0.00419	290.7	0.0200	0.005	0.018
13:00:00	18.6	21.2	224.4	417.2	2.0	2.1	0.00	0.0012	2.391	2.603	0.194	2.584	0.2097	0.0082	4.9	0.00489	291.6	0.0212	0.006	0.020
14:00:00	19.3	21.8	220.6	421.2	2.1	2.2	0.00	0.0013	2.391	2.603	0.195	2.586	0.2097	0.0082	5.5	0.00551	292.3	0.0221	0.006	0.022
15:00:00	19.4	21.9	220.1	421.7	2.1	2.3	0.00	0.0013	2.391	2.603	0.195	2.586	0.2097	0.0082	5.6	0.00559	292.4	0.0222	0.006	0.022
16:00:00	18.0	20.6	227.9	413.7	2.0	2.1	0.00	0.0012	2.391	2.603	0.193	2.583	0.2097	0.0082	4.4	0.00439	291.0	0.0204	0.005	0.019
17:00:00	17.0	19.7	233.4	408.1	1.8	1.9	0.00	0.0011	2.391	2.603	0.191	2.581	0.2097	0.0082	3.7	0.00370	290.0	0.0192	0.005	0.017
18:00:00	14.1	17.0	250.2	391.0	1.5	1.6	0.00	0.0010	2.391	2.603	0.185	2.575	0.2097	0.0082	2.2	0.00220	287.1	0.0158	0.003	0.012

Aug-15	Temp [°C]	$Leaf_{sim}$ [°C]	Rni [W/m^2]	B [W/m^2]	$e_s(T)$ [kPa]	e_a [kPa]	D [kPa]	s [C^{-1}]	g_{Ha} [$mol/m^2/s$]	g_{va} [$mol/m^2/s$]	g_r [mol/m2/s]	g_{Hr} [$mol/m^2/s$]	v [$mol/m^2/s$]	γ* [C^{-1}]	SC [$mmol/m^2/s$]	n	T [K]	P [atm]	V [m^3]	mm/hr
06:00:00	8.2	13.0	393.0	357.4	1.1	1.1	0.00	0.0007	2.391	2.603	0.173	2.564	0.2097	0.0081	1.0	0.00103	281.2	0.0107	0.002	0.008
07:00:00	8.1	12.9	393.7	356.7	1.1	1.1	0.00	0.0007	2.391	2.603	0.173	2.563	0.2097	0.0081	1.0	0.00101	281.1	0.0106	0.002	0.008
08:00:00	13.1	17.4	365.7	385.3	1.4	1.5	0.00	0.0009	2.391	2.603	0.183	2.573	0.2097	0.0082	2.4	0.00238	286.1	0.0148	0.004	0.014
09:00:00	17.2	21.2	342.3	409.2	1.9	2.0	0.00	0.0012	2.391	2.603	0.191	2.582	0.2097	0.0082	4.9	0.00487	290.2	0.0194	0.006	0.022
10:00:00	19.8	23.5	327.9	423.9	2.2	2.3	0.00	0.0013	2.391	2.603	0.196	2.587	0.2097	0.0082	7.6	0.00759	292.8	0.0228	0.008	0.029
11:00:00	21.7	25.2	317.4	434.6	2.5	2.6	0.00	0.0015	2.391	2.603	0.200	2.590	0.2097	0.0082	10.5	0.01047	294.7	0.0255	0.010	0.036
12:00:00	23.1	26.6	309.0	443.2	2.7	2.8	0.00	0.0016	2.391	2.603	0.203	2.593	0.2097	0.0082	13.5	0.01354	296.1	0.0280	0.012	0.042
13:00:00	24.1	27.4	303.8	448.4	2.9	3.0	0.00	0.0017	2.391	2.603	0.205	2.595	0.2097	0.0082	15.9	0.01585	297.1	0.0295	0.013	0.047
14:00:00	24.7	28.0	300.2	452.1	3.0	3.1	0.00	0.0017	2.391	2.603	0.206	2.597	0.2097	0.0082	17.7	0.01774	297.7	0.0307	0.014	0.051
15:00:00	24.9	28.1	299.1	453.2	3.0	3.1	0.00	0.0017	2.391	2.603	0.206	2.597	0.2097	0.0082	18.3	0.01831	297.9	0.0311	0.014	0.052
16:00:00	24.0	27.3	304.2	448.1	2.8	3.0	0.00	0.0017	2.391	2.603	0.204	2.595	0.2097	0.0082	15.7	0.01568	297.0	0.0294	0.013	0.047
17:00:00	22.6	26.1	311.9	440.2	2.6	2.7	0.00	0.0015	2.391	2.603	0.202	2.592	0.2097	0.0082	12.4	0.01237	295.6	0.0271	0.011	0.040
18:00:00	19.2	23.0	331.2	420.5	2.1	2.2	0.00	0.0013	2.391	2.603	0.195	2.586	0.2097	0.0082	6.8	0.00685	292.2	0.0219	0.007	0.027

Sep-15	Temp [°C]	$Leaf_{sim}$ [°C]	Rni [W/m^2]	B [W/m^2]	$e_s(T)$ [kPa]	e_a [kPa]	D [kPa]	s [C^{-1}]	g_{Ha} [$mol/m^2/s$]	g_{va} [$mol/m^2/s$]	g_r [mol/m2/s]	g_{Hr} [$mol/m^2/s$]	v [$mol/m^2/s$]	γ* [C^{-1}]	SC [$mmol/m^2/s$]	n	T [K]	P [atm]	V [m^3]	mm/hr
06:00:00	11.0	17.1	509.3	373.4	1.3	1.3	0.00	0.0008	2.391	2.603	0.178	2.569	0.2097	0.0082	2.3	0.00225	284.0	0.0129	0.004	0.015
07:00:00	12.0	18.1	503.4	379.5	1.4	1.4	0.00	0.0009	2.391	2.603	0.181	2.571	0.2097	0.0082	2.7	0.00270	285.0	0.0139	0.005	0.016
08:00:00	16.0	21.6	481.3	402.0	1.7	1.8	0.00	0.0011	2.391	2.603	0.188	2.579	0.2097	0.0082	5.3	0.00527	289.0	0.0179	0.007	0.025
09:00:00	18.5	23.8	467.2	416.3	2.0	2.1	0.00	0.0012	2.391	2.603	0.193	2.584	0.2097	0.0082	8.1	0.00807	291.5	0.0210	0.009	0.033
10:00:00	20.6	25.7	455.2	428.6	2.3	2.4	0.00	0.0014	2.391	2.603	0.198	2.588	0.2097	0.0082	11.6	0.01161	293.6	0.0239	0.012	0.042
11:00:00	22.3	27.3	445.6	438.4	2.6	2.7	0.00	0.0015	2.391	2.603	0.201	2.592	0.2097	0.0082	15.5	0.01551	295.3	0.0266	0.014	0.051
12:00:00	23.8	28.6	437.2	446.9	2.8	2.9	0.00	0.0016	2.391	2.603	0.204	2.595	0.2097	0.0082	20.0	0.01998	296.8	0.0291	0.017	0.060
13:00:00	24.8	29.5	431.8	452.5	3.0	3.1	0.00	0.0017	2.391	2.603	0.206	2.597	0.2097	0.0082	23.5	0.02354	297.8	0.0308	0.019	0.067
14:00:00	25.5	30.1	427.8	456.6	3.1	3.3	0.00	0.0018	2.391	2.603	0.207	2.598	0.2097	0.0083	26.5	0.02655	298.5	0.0322	0.020	0.073
15:00:00	25.6	30.2	427.2	457.2	3.1	3.3	0.00	0.0018	2.391	2.603	0.208	2.598	0.2097	0.0083	27.1	0.02705	298.6	0.0324	0.020	0.074
16:00:00	25.0	29.7	430.6	453.8	3.0	3.2	0.00	0.0018	2.391	2.603	0.206	2.597	0.2097	0.0082	24.4	0.02443	298.0	0.0312	0.019	0.069
17:00:00	24.0	28.8	435.8	448.4	2.9	3.0	0.00	0.0017	2.391	2.603	0.205	2.595	0.2097	0.0082	20.8	0.02083	297.0	0.0295	0.017	0.062
18:00:00	21.7	26.8	448.8	435.2	2.5	2.6	0.00	0.0015	2.391	2.603	0.200	2.591	0.2097	0.0082	14.1	0.01409	294.7	0.0257	0.013	0.048

Oct-15	Temp [°C]	$Leaf_{sim}$ [°C]	Rni [W/m^2]	B [W/m^2]	$e_s(T)$ [kPa]	e_a [kPa]	D [kPa]	s [C^{-1}]	g_{Ha} [$mol/m^2/s$]	g_{va} [$mol/m^2/s$]	g_r [mol/m2/s]	g_{Hr} [$mol/m^2/s$]	v [$mol/m^2/s$]	γ* [C^{-1}]	SC [$mmol/m^2/s$]	n	T [K]	P [atm]	V [m^3]	mm/hr
06:00:00	14.5	21.2	573.3	393.4	1.6	1.6	0.00	0.0010	2.391	2.603	0.185	2.576	0.2097	0.0082	4.9	0.00492	287.5	0.0163	0.007	0.026
07:00:00	17.0	23.5	559.1	407.9	1.8	1.9	0.00	0.0011	2.391	2.603	0.190	2.581	0.2097	0.0082	7.6	0.00755	290.0	0.0191	0.009	0.034
08:00:00	20.5	26.6	539.4	428.0	2.3	2.4	0.00	0.0014	2.391	2.603	0.198	2.588	0.2097	0.0082	13.6	0.01364	293.5	0.0238	0.014	0.050
09:00:00	23.2	29.0	524.4	443.3	2.7	2.8	0.00	0.0016	2.391	2.603	0.203	2.594	0.2097	0.0082	21.4	0.02138	296.2	0.0280	0.019	0.067
10:00:00	25.2	30.7	513.0	454.8	3.1	3.2	0.00	0.0018	2.391	2.603	0.207	2.598	0.2097	0.0082	30.0	0.02998	298.2	0.0316	0.023	0.084
11:00:00	26.8	32.2	503.9	464.1	3.4	3.5	0.00	0.0019	2.391	2.603	0.210	2.601	0.2097	0.0083	39.4	0.03935	299.8	0.0348	0.028	0.100
12:00:00	28.1	33.3	496.4	471.8	3.7	3.8	0.00	0.0021	2.391	2.603	0.213	2.603	0.2097	0.0083	49.2	0.04922	301.1	0.0376	0.032	0.116
13:00:00	28.9	34.0	492.2	476.1	3.9	4.0	0.00	0.0022	2.391	2.603	0.214	2.605	0.2097	0.0083	55.9	0.05586	301.9	0.0393	0.035	0.127
14:00:00	29.2	34.3	490.3	478.1	3.9	4.1	0.00	0.0022	2.391	2.603	0.215	2.606	0.2097	0.0083	59.2	0.05916	302.2	0.0401	0.037	0.132
15:00:00	29.2	34.3	490.5	477.9	3.9	4.0	0.00	0.0022	2.391	2.603	0.215	2.606	0.2097	0.0083	58.8	0.05877	302.2	0.0400	0.036	0.131
16:00:00	28.9	34.0	492.4	475.9	3.9	4.0	0.00	0.0022	2.391	2.603	0.214	2.605	0.2097	0.0083	55.5	0.05553	301.9	0.0392	0.035	0.126
17:00:00	27.6	32.9	499.3	468.9	3.6	3.7	0.00	0.0020	2.391	2.603	0.212	2.602	0.2097	0.0083	45.2	0.04523	300.6	0.0365	0.031	0.110
18:00:00	25.2	30.8	512.8	455.1	3.1	3.2	0.00	0.0018	2.391	2.603	0.207	2.598	0.2097	0.0082	30.2	0.03016	298.2	0.0317	0.023	0.084

Nov-15	Temp [°C]	$Leaf_{sim}$ [°C]	Rni [W/m^2]	B [W/m^2]	$e_s(T)$ [kPa]	e_a [kPa]	D [kPa]	s [C^{-1}]	g_{Ha} [$mol/m^2/s$]	g_{va} [$mol/m^2/s$]	g_r [mol/m2/s]	g_{Hr} [$mol/m^2/s$]	v [$mol/m^2/s$]	γ* [C^{-1}]	SC [$mmol/m^2/s$]	n	T [K]	P [atm]	V [m^3]	mm/hr
06:00:00	13.9	22.1	695.3	390.1	1.5	1.6	0.00	0.0010	2.391	2.603	0.184	2.575	0.2097	0.0082	5.8	0.00584	286.9	0.0157	0.009	0.032
07:00:00	17.1	25.0	677.1	408.7	1.9	2.0	0.00	0.0012	2.391	2.603	0.191	2.581	0.2097	0.0082	10.0	0.01004	290.1	0.0193	0.012	0.045
08:00:00	19.8	27.3	662.1	423.9	2.2	2.3	0.00	0.0013	2.391	2.603	0.196	2.587	0.2097	0.0082	15.6	0.01562	292.8	0.0228	0.016	0.059
09:00:00	22.0	29.2	650.0	436.3	2.5	2.6	0.00	0.0015	2.391	2.603	0.200	2.591	0.2097	0.0082	22.4	0.02240	295.0	0.0260	0.021	0.075
10:00:00	24.1	31.0	638.0	448.5	2.9	3.0	0.00	0.0017	2.391	2.603	0.205	2.595	0.2097	0.0082	31.9	0.03186	297.1	0.0296	0.026	0.095
11:00:00	25.8	32.5	628.5	458.2	3.2	3.3	0.00	0.0018	2.391	2.603	0.208	2.599	0.2097	0.0083	42.2	0.04220	298.8	0.0327	0.032	0.114
12:00:00	27.1	33.7	621.1	465.8	3.5	3.6	0.00	0.0020	2.391	2.603	0.211	2.601	0.2097	0.0083	52.4	0.05244	300.1	0.0354	0.037	0.131
13:00:00	28.2	34.6	614.8	472.2	3.7	3.8	0.00	0.0021	2.391	2.603	0.213	2.604	0.2097	0.0083	63.1	0.06313	301.2	0.0378	0.041	0.149
14:00:00	28.7	35.1	611.9	475.1	3.8	3.9	0.00	0.0021	2.391	2.603	0.214	2.605	0.2097	0.0083	68.6	0.06860	301.7	0.0389	0.044	0.157
15:00:00	28.7	35.1	611.8	475.2	3.8	3.9	0.00	0.0022	2.391	2.603	0.214	2.605	0.2097	0.0083	68.8	0.06882	301.7	0.0389	0.044	0.158
16:00:00	28.4	34.8	613.9	473.1	3.7	3.9	0.00	0.0021	2.391	2.603	0.213	2.604	0.2097	0.0083	64.7	0.06468	301.4	0.0381	0.042	0.151
17:00:00	27.1	33.7	620.9	466.0	3.5	3.6	0.00	0.0020	2.391	2.603	0.211	2.601	0.2097	0.0083	52.8	0.05279	300.1	0.0354	0.037	0.132
18:00:00	25.0	31.9	632.7	453.9	3.0	3.2	0.00	0.0018	2.391	2.603	0.207	2.597	0.2097	0.0082	37.2	0.03723	298.0	0.0313	0.029	0.105

Dec-15	Temp [°C]	$Leaf_{sim}$ [°C]	Rni [W/m^2]	B [W/m^2]	$e_s(T)$ [kPa]	e_a [kPa]	D [kPa]	s [C^{-1}]	g_{Ha} [$mol/m^2/s$]	g_{va} [$mol/m^2/s$]	g_r [mol/m2/s]	g_{Hr} [$mol/m^2/s$]	v [$mol/m^2/s$]	γ* [C^{-1}]	SC [$mmol/m^2/s$]	n	T [K]	P [atm]	V [m^3]	mm/hr
06:00:00	18.1	26.4	715.5	414.3	2.0	2.1	0.00	0.0012	2.391	2.603	0.193	2.583	0.2097	0.0082	13.0	0.01304	291.1	0.0205	0.015	0.055
07:00:00	20.6	28.5	701.5	428.6	2.3	2.4	0.00	0.0014	2.391	2.603	0.198	2.588	0.2097	0.0082	19.7	0.01969	293.6	0.0239	0.020	0.071
08:00:00	22.6	30.2	690.5	439.8	2.6	2.7	0.00	0.0015	2.391	2.603	0.202	2.592	0.2097	0.0082	27.2	0.02722	295.6	0.0270	0.024	0.088
09:00:00	24.5	31.9	679.6	450.9	2.9	3.1	0.00	0.0017	2.391	2.603	0.205	2.596	0.2097	0.0082	37.4	0.03744	297.5	0.0303	0.030	0.109
10:00:00	26.1	33.3	670.6	460.1	3.2	3.4	0.00	0.0019	2.391	2.603	0.209	2.599	0.2097	0.0083	48.7	0.04873	299.1	0.0334	0.036	0.129
11:00:00	27.6	34.5	662.4	468.5	3.6	3.7	0.00	0.0020	2.391	2.603	0.212	2.602	0.2097	0.0083	61.9	0.06195	300.6	0.0363	0.042	0.151
12:00:00	28.6	35.4	656.7	474.3	3.8	3.9	0.00	0.0021	2.391	2.603	0.214	2.604	0.2097	0.0083	73.2	0.07315	301.6	0.0386	0.047	0.169
13:00:00	29.7	36.4	650.3	480.9	4.1	4.2	0.00	0.0023	2.391	2.603	0.216	2.607	0.2097	0.0083	88.2	0.08821	302.7	0.0412	0.053	0.192
14:00:00	30.1	36.7	648.0	483.2	4.2	4.3	0.00	0.0023	2.391	2.603	0.217	2.607	0.2097	0.0083	94.2	0.09424	303.1	0.0422	0.056	0.200
15:00:00	30.7	37.2	644.8	486.5	4.3	4.4	0.00	0.0024	2.391	2.603	0.218	2.609	0.2097	0.0083	103.5	0.10353	303.7	0.0436	0.059	0.213
16:00:00	30.1	36.8	647.9	483.3	4.2	4.3	0.00	0.0023	2.391	2.603	0.217	2.607	0.2097	0.0083	94.5	0.09454	303.1	0.0422	0.056	0.201
17:00:00	29.3	36.1	652.5	478.6	4.0	4.1	0.00	0.0022	2.391	2.603	0.215	2.606	0.2097	0.0083	82.7	0.08270	302.3	0.0403	0.051	0.183
18:00:00	27.7	34.7	661.5	469.4	3.6	3.7	0.00	0.0020	2.391	2.603	0.212	2.603	0.2097	0.0083	63.6	0.06358	300.7	0.0367	0.043	0.154

APPENDIX E – ET MODEL CALCULATIONS

Common Model Inputs

Elevation [mamsl]	1500	
Reference Height [m]	2	
Wind Speed @ Ref [m/s]	1.6	
Atmospheric Pressure [kPa]	12.1	P_a

S-W Model Inputs

Specific Heat Moist Air [MJ/kg/°C]	1.01E-03	C_p
Soil surface resistance	500	r_s^s [s/m]
Extinction coefficient for net radiation	0.5	C_r
Cloudiness (tenth)	0.6	C

Field Model

R_a Scaling Factor	3.80
Effective Leaf Area (m^2/m^2)	4.80

Land Cover

Site-Specific

α_m	0.20
LAI_{max}	7
LAI_{eff}	3.5
h_c [m]	7.2
w_{max} [m]	0.01
F_{cl}	0
$r_{ST\ min}$ [s/m]	150
$NDVI_{98\%}$	0.611
d_{rz} [m]	2.5
z_{0g} [m]	0.02

Month	Temperature T_{xd} (°C)	T_{mxd} (°C)	T_{mnd} (°C)	Act. Vapour e_d (kPa)	Sat. Vapour e_a (kPa)	Radiation R_a (MJ/m2/d)
Jan	22.3	28.6	16.1	1.6	2.70	25.0
Feb	22.4	29.5	15.3	1.6	2.71	22.6
Mar	20.8	27.1	14.5	1.5	2.46	20.7
Apr	18.1	24.8	11.5	1.1	2.08	17.8
May	17.0	25.4	8.5	0.8	1.93	15.6
Jun	11.5	19.0	4.0	0.7	1.36	14.4
Jul	12.4	19.9	4.9	0.6	1.44	14.4
Aug	16.4	25.2	7.6	0.6	1.87	16.9
Sep	16.9	24.0	9.8	0.8	1.93	19.9
Oct	22.2	30.3	14.1	1.0	2.68	21.8
Nov	21.3	29.6	13.0	1.2	2.53	24.5
Dec	24.4	31.7	17.1	1.4	3.06	25.5

FAO Penman-Monteith

Month	ET	Temp	Vapour	Atmosphere	Radiation Parameters				Constants	
	E_{rpm} (mm/d)	T_{ra} (°C)	Δ	γ (kPa/°C)	R_n (MJ/m²/d)	R_{sn} (MJ/m²/d)	R_{iw} (MJ/m²/d)	R_s (MJ/m²/d)	b	c
Jan	3.694	13.9	0.126	0.00006	9.054	12.076	6.629	15.683	0.0116	1.9204
Feb	2.987	13.4	0.127	0.00006	7.321	10.602	6.447	13.768	0.0102	1.9666
Mar	2.560	13.8	0.116	0.00006	6.273	10.008	6.725	12.998	0.0106	1.9611
Apr	1.583	15.3	0.100	0.00006	3.878	8.912	7.697	11.575	0.0109	1.9152
May	0.736	17.3	0.094	0.00006	1.797	8.229	8.890	10.687	0.0149	1.7906
Jun	0.477	17.8	0.069	0.00006	1.162	7.608	8.718	9.880	0.0523	1.3391
Jul	0.357	18.5	0.072	0.00006	0.867	7.529	8.911	9.779	0.0408	1.3914
Aug	0.844	18.8	0.091	0.00006	2.062	8.935	9.541	11.603	0.0215	1.6180
Sep	1.880	17.9	0.094	0.00006	4.603	10.149	8.577	13.181	0.0271	1.5165
Oct	2.268	16.0	0.126	0.00006	5.554	10.568	8.171	13.725	0.0089	1.9218
Nov	3.232	15.1	0.120	0.00006	7.920	11.919	7.560	15.480	0.0163	1.7438
Dec	3.575	14.3	0.141	0.00006	8.760	12.410	7.357	16.118	0.0076	2.0669

Shuttleworth-Wallace ET Model

Month	ET [mm/d]	Model Parameters						
		ET_c [mm/d]	ET_s [mm/d]	C_c	C_s	R_a	R_c	R_s
Jan	5.036	12.3463	0.4659	0.9941	0.1198	2.90	0.4	55.54
Feb	4.643	11.3857	0.4134	0.9941	0.1195	2.91	0.4	55.68
Mar	4.066	9.9796	0.4188	0.9937	0.1273	2.68	0.4	51.71
Apr	3.484	8.5772	0.3227	0.9931	0.1419	2.34	0.4	45.53
May	3.494	8.6068	0.3560	0.9928	0.1488	2.20	0.4	43.08
Jun	2.527	6.2674	0.2075	0.9912	0.1857	1.65	0.4	33.25
Jul	2.527	6.2940	0.0362	0.9915	0.1789	1.73	0.4	34.73
Aug	3.661	9.0627	0.1191	0.9926	0.1520	2.14	0.4	42.02
Sep	3.837	9.4945	0.1219	0.9928	0.1491	2.19	0.4	42.98
Oct	4.923	12.0965	0.2543	0.9940	0.1203	2.88	0.4	55.26
Nov	5.218	12.8241	0.3455	0.9938	0.1248	2.75	0.4	52.93
Dec	5.691	13.9328	0.4459	0.9945	0.1103	3.22	0.4	61.22

	Climate								
Month	λ [MJ/kg]	e_s [kPa]	$e^0(T_{xd})$ [kPa]	$e^0(T_{mxd})$ [kPa]	$e^0(T_{mnd})$ [kPa]	Δ [kPa/°C]	ρ [kg/m^3]	γ	T_{kv} [K]
Jan	2.45	2.87	2.70	3.90	1.83	0.16	0.14	0.008	298.3
Feb	2.45	2.93	2.71	4.11	1.74	0.16	0.14	0.008	298.3
Mar	2.45	2.62	2.46	3.58	1.66	0.15	0.14	0.008	296.8
Apr	2.46	2.24	2.08	3.13	1.35	0.13	0.14	0.008	294.0
May	2.46	2.18	1.93	3.25	1.11	0.12	0.14	0.008	292.9
Jun	2.47	1.50	1.36	2.19	0.81	0.09	0.15	0.008	287.3
Jul	2.47	1.60	1.44	2.32	0.87	0.09	0.15	0.008	288.3
Aug	2.46	2.13	1.87	3.21	1.05	0.12	0.14	0.008	292.3
Sep	2.46	2.10	1.93	2.99	1.21	0.12	0.14	0.008	292.8
Oct	2.45	2.97	2.68	4.32	1.61	0.16	0.14	0.008	298.2
Nov	2.45	2.83	2.53	4.16	1.49	0.16	0.14	0.008	297.2
Dec	2.44	3.31	3.06	4.66	1.96	0.18	0.14	0.008	300.4

	Aerodynamic										
Month	r_a^s [s/m]	r_a^a [s/m]	Z_0 [m]	d_p [m]	K_h [m^2/s]	u_* [m/s]	d_0 [m]	z_0 [m]	z_{0c} [m]	c_d	n
Jan	299.6	16.9	0.9	4.5	0.2	0.3	5.4	0.5	0.5	0.23	3.70
Feb	299.6	16.9	0.9	4.5	0.2	0.3	5.4	0.5	0.5	0.23	3.70
Mar	299.6	16.9	0.9	4.5	0.2	0.3	5.4	0.5	0.5	0.23	3.70
Apr	299.6	16.9	0.9	4.5	0.2	0.3	5.4	0.5	0.5	0.23	3.70
May	299.6	16.9	0.9	4.5	0.2	0.3	5.4	0.5	0.5	0.23	3.70
Jun	299.6	16.9	0.9	4.5	0.2	0.3	5.4	0.5	0.5	0.23	3.70
Jul	299.6	16.9	0.9	4.5	0.2	0.3	5.4	0.5	0.5	0.23	3.70
Aug	299.6	16.9	0.9	4.5	0.2	0.3	5.4	0.5	0.5	0.23	3.70
Sep	299.6	16.9	0.9	4.5	0.2	0.3	5.4	0.5	0.5	0.23	3.70
Oct	299.6	16.9	0.9	4.5	0.2	0.3	5.4	0.5	0.5	0.23	3.70
Nov	299.6	16.9	0.9	4.5	0.2	0.3	5.4	0.5	0.5	0.23	3.70
Dec	299.6	16.9	0.9	4.5	0.2	0.3	5.4	0.5	0.5	0.23	3.70

	Bulk Stomatal and Boundary Layer Resistances			Radiation over Vegitation Canopy						Appendix A		
Month	r_s^c [s/m]	r_a^c [s/m]	r_s^s [s/m]	R_n [MJ/m^2/d]	R_{ns} [MJ/m^2/d]	R_{nl} [MJ/m^2/d]	R_n^s [MJ/m^2/d]	G	α	R_a (MJ/m^2)	R_{solar}	R^0_{solar}
Jan	42.9	0.18	500.0	8.7419	13.9654	5.224	0.2640	-0.1414	0.19802	25.0	17.41	19.50
Feb	42.9	0.18	500.0	7.4012	12.6247	5.224	0.2235	-0.1059	0.19802	22.6	15.74	17.63
Mar	42.9	0.18	500.0	6.1596	11.5634	5.404	0.1860	-0.2982	0.19802	20.7	14.42	16.15
Apr	42.9	0.18	500.0	3.7498	9.9434	6.194	0.1132	-0.2700	0.19802	17.8	12.40	13.88
May	42.9	0.18	500.0	1.8279	8.7144	6.887	0.0552	-0.4641	0.19802	15.6	10.87	12.17
Jun	42.9	0.18	500.0	0.7616	8.0441	7.282	0.0230	-0.3178	0.19802	14.4	10.03	11.23
Jul	42.9	0.18	500.0	0.6196	8.0441	7.424	0.0187	0.3460	0.19802	14.4	10.03	11.23
Aug	42.9	0.18	500.0	2.0162	9.4406	7.424	0.0609	0.3146	0.19802	16.9	11.77	13.18
Sep	42.9	0.18	500.0	4.2299	11.1165	6.887	0.1277	0.4051	0.19802	19.9	13.86	15.52
Oct	42.9	0.18	500.0	5.7652	12.1779	6.413	0.1741	0.3077	0.19802	21.8	15.18	17.00
Nov	42.9	0.18	500.0	7.7019	13.6861	5.984	0.2326	0.1527	0.19802	24.5	17.07	19.11
Dec	42.9	0.18	500.0	8.6545	14.2447	5.590	0.2613	0.0715	0.19802	25.5	17.76	19.89

APPENDIX F – SVF WATER BALANCE CALCULATIONS

Initial Water Balance

	STUDY AREA			RECHARGE		INFLOWS					OUTFLOWS			SIMULATION	
Date	Observed G1111 (mamsl)	Study Area (km^2)	Specific Yield	Monthly Rainfall (mm/month)	Effective Recharge (Ml/d)	Zuurbekom Inflows (Ml/d)	Gemsbok East (Ml/d)	Leeuspruit Leakage (Ml/d)	Rietspruit Leakage (Ml/d)	Dolomite Storage (Ml/d)	Ezulwini Pumping (Ml/d)	Cooke 3 Pumping (Ml/d)	Gemsbok Eye (Ml/d)	Water Level (mamsl)	ΔH (m)
Jan-14	1531	161000000	0.0043	107	41	9.2	6.1	7.6	5.1	28.0	58.2	9.0	0.0	1532.3	29.1
Feb-14	1532	161000000	0.0043	97	37	8.8	5.9	7.3	4.9	28.0	58.4	9.0	0.0	1533.3	28.0
Mar-14	1534	161000000	0.0043	158	60	8.2	5.5	6.8	4.6	28.0	58.7	9.0	0.0	1535.3	26.0
Apr-14	1535	161000000	0.0043	19	7	8.3	5.6	6.9	4.6	28.0	62.1	9.0	0.0	1534.8	26.5
May-14	1535	161000000	0.0043	0	0	8.6	5.7	7.1	4.8	28.0	63.5	9.0	0.0	1534.1	27.3
Jun-14	1535	161000000	0.0043	0	0	8.9	5.9	7.3	4.9	28.0	65.7	9.0	0.0	1533.2	28.1
Jul-14	1535	161000000	0.0043	0	0	9.1	6.1	7.5	5.1	28.0	63.8	9.0	0.0	1532.5	28.9
Aug-14	1533	161000000	0.0043	2	1	9.5	6.3	7.8	5.3	28.0	75.0	9.0	0.0	1531.3	30.0
Sep-14	1532	161000000	0.0043	10	4	9.7	6.5	8.0	5.4	28.0	72.1	9.0	0.0	1530.5	30.9
Oct-14	1531	161000000	0.0043	47	18	9.8	6.5	8.1	5.5	28.0	73.2	9.0	0.0	1530.2	31.2
Nov-14	1530	161000000	0.0043	187	71	9.2	6.1	7.6	5.1	28.0	72.9	9.0	0.0	1532.2	29.2
Dec-14	1531	161000000	0.0043	72	27	9.2	6.1	7.6	5.1	28.0	72.4	9.0	0.0	1532.2	29.1
Jan-15	1533	161000000	0.0043	140	53	8.8	5.9	7.3	4.9	28.0	74.1	9.0	0.0	1533.3	28.0
Feb-15	1533	161000000	0.0043	9	3	9.2	6.1	7.6	5.1	28.0	75.2	9.0	0.0	1532.2	29.1
Mar-15	1532	161000000	0.0043	74	28	9.2	6.1	7.6	5.1	28.0	75.6	9.0	0.0	1532.2	29.1
Average	*1533*	*161000000*	*0.0*	*61.4*	*23.4*	*9.0*	*6.0*	*7.5*	*5.0*	*28.0*	*68.1*	*9.0*	*0.0*	*1532.6*	*28.7*

ET Modified Water Balance

	STUDY AREA			RECHARGE					INFLOWS					OUTFLOWS				SIMULATION	
Date	Observed G1111 (mamsl)	Study Area (km^2)	Specific Yield	Monthly Rainfall (mm/month)	Effective Recharge (Ml/d)	Evapo-Transpiration (mm/month)	Evapo-Transpiration Ml/d	Reduced Recharge Ml/d	Zuurbekom Inflows (Ml/d)	Gemsbok East (Ml/d)	Leeuspruit Leakage (Ml/d)	Rietspruit Leakage (Ml/d)	Dolomite Storage (Ml/d)	Ezulwini Pumping (Ml/d)	Reduced Ezulwini (Ml/d)	Cooke 3 Pumping (Ml/d)	Gemsbok Eye (Ml/d)	Water Level (mamsl)	ΔH (m)
Jan-14	1531	161000000	0.0043	107	41	187	30	11	9.4	6.3	7.8	5.2	28.0	58.2	47.2	9.0	0.0	1531.5	29.9
Feb-14	1532	161000000	0.0043	97	37	168	27	10	9.3	6.2	7.7	5.2	28.0	58.4	47.4	9.0	0.0	1531.9	29.4
Mar-14	1534	161000000	0.0043	158	60	111	18	42	8.7	5.8	7.2	4.8	28.0	58.7	47.7	9.0	0.0	1533.7	27.7
Apr-14	1535	161000000	0.0043	19	7	64	10	0	8.8	5.9	7.3	4.9	28.0	62.1	51.1	9.0	0.0	1533.4	27.9
May-14	1535	161000000	0.0043	0	0	55	9	0	8.9	5.9	7.3	4.9	28.0	63.5	52.5	9.0	0.0	1533.1	28.2
Jun-14	1535	161000000	0.0043	0	0	24	4	0	9.0	6.0	7.4	5.0	28.0	65.7	54.7	9.0	0.0	1532.8	28.6
Jul-14	1535	161000000	0.0043	0	0	26	4	0	9.1	6.1	7.5	5.0	28.0	63.8	52.8	9.0	0.0	1532.5	28.8
Aug-14	1533	161000000	0.0043	2	1	61	10	0	9.3	6.2	7.7	5.2	28.0	75.0	64.0	9.0	0.0	1531.8	29.5
Sep-14	1532	161000000	0.0043	10	4	91	15	0	9.5	6.3	7.8	5.3	28.0	72.1	61.1	9.0	0.0	1531.2	30.1
Oct-14	1531	161000000	0.0043	47	18	171	27	0	9.7	6.4	8.0	5.4	28.0	73.2	62.2	9.0	0.0	1530.6	30.7
Nov-14	1530	161000000	0.0043	187	71	202	32	39	9.3	6.2	7.7	5.2	28.0	72.9	61.9	9.0	0.0	1531.7	29.7
Dec-14	1531	161000000	0.0043	72	27	276	44	0	9.5	6.3	7.9	5.3	28.0	72.4	61.4	9.0	0.0	1531.1	30.2
Jan-15	1533	161000000	0.0043	140	53	187	30	23	9.4	6.3	7.8	5.2	28.0	74.1	63.1	9.0	0.0	1531.4	29.9
Feb-15	1533	161000000	0.0043	9	3	168	27	0	9.6	6.4	8.0	5.4	28.0	75.2	64.2	9.0	0.0	1530.8	30.6
Mar-15	1532	161000000	0.0043	74	28	111	18	10	9.7	6.5	8.0	5.4	28.0	75.6	64.6	9.0	0.0	1530.5	30.8
Average	*1533*	*161000000*	*0.0*	*61.4*	*23.4*	*126.7*	*20.3*	*9.0*	*9.3*	*6.2*	*7.7*	*5.2*	*28.0*	*68.1*	*57.1*	*9.0*	*0.0*	*1531.9*	*29.5*